THESIS FOR THE DEGREE OF DOCTOR OF PHILOSOPHY (PHD)

Ethanol accelerates vascular calcification in human aortic smooth muscle cells
Quantitative Trait Locus mapping reveals alcohol consumption genes

by
Melinda Oros

Consulent: Prof. Dr. László Nagy
Prof. Dr. Csaba Vadász

UNIVERSITY OF DEBRECEN
DOCTORAL SCHOOL OF MOLECULAR CELL AND IMMUNE BIOLOGY

DEBRECEN, 2015

TABLE OF CONTENTS

1. ABBREVIATIONS

AC – alcohol consumption
AC34GKD – alcohol consumption database
ADH1 - alcohol dehydrogenase 1
ALP - alkaline phosphatase
Cbfa-1 - Core binding factor alpha-1
CKD - chronic kidney disease
CIM – composite interval mapping
CNs - coding-nonsynonymous SNPs
CT - computed tomography
D1Mit167 – marker name
DBA/2J – mouse strain name
DMEM - Dulbecco's Modified Eagle Medium
DMSO - dimethyl-sulfoxide
Eac - Ethyl alcohol consumption
EDTA – ethylenediaminetetraacetic acid
ESRD - End Stage Renal Disease
FBS – fetal bovine serum

GAPDH - glyceraldehyde 3-phosphate dehydrogenase

GM – growth medium

Grm7 – glutamate receptor metabotropic 7

GO – Gene Ontology

HBSS - Hank's Balanced Salt Solution

HCl – hydrochloric acid

HRP - horseradish peroxidase

HUVECs - primary human umbilical vein endothelial cells

I5B25A – alcohol-preferring mouse strain name

IBD - identical-by-descent region

IgG - Immunoglobulin G

LOD – likelihood ratio

LSD – least significant difference

MGI – Mouse Genome Informatics database

MIM – multiple interval mapping

MTT - 3-[4,5-Dimethylthiazol-2-yl]-2,5-diphenyl-tetrazolium bromide

mRNA - messenger RNA

NaCl – sodium chloride

NaOH – sodium hydroxide

OB – osteoblast

PAGE - polyacrylamide gel electrophoresis

PBS - phosphate buffered saline

P_i – inorganic phosphate

Pit-1, Pit-2, Pit 3 - sodium-dependent phosphate co-transporters

QTLs – Quantitative Trait Loci

QTG – Quantitative Trait Gene

RI – Recombinant Introgression

RNA – ribonucleic acid

ROS – reactive oxygen species

RQI – Recombinant QTL Introgression

RQIgbase – RQI database

Runx2/*Cbfa-1* - Core binding factor alpha-1

SD – Standard Deviation

SDS - sodium dodecyl sulfate

SEM – Standard Error of the Mean

siRNA - small interfering RNA

SMC - smooth muscle cells

SNP – single nucleotide polymorphism

TFBS - transcription factor binding site

Vmap – The Mouse Genetic Variation mapping

B6 – C57BL/6ByJ, background strain

C – BALB/cJ, donor strain

I – CXBI/By, donor strain

B6.C – introgression strain set, BALB/cJ donor segments are distributed on B6 background

B6.I – introgression strain set, CXBI donor segments are distributed on B6 background

b_5i_7 – strain developed by 5 backcrosses and 7 intercrosses

C5B3 – the abbreviated name of B6.Cb_5i_7-β3/Vad, the first letter C (or I) stands for the donor strain name, 5 (or 4) designates the backcross-intercross series b_5i_7 (or b_4i_5), B (or A) indicates the replicate line β (or α), and the last character, 3, is the identification number of the strain (the numbers range from 1 to 34 in each replicate line).

2. INTRODUCTION

2.1. Vascular calcification

Epidemiological studies suggested in early nineties that moderate consumption of alcohol in France (20-30 g alcohol intake per day) can reduce risk of coronary heart disease by at least 40% [1] Since then studies from several countries confirmed this finding demonstrating a 20–40% lower incidence for cardiovascular disease among drinkers of alcoholic beverages as compared to non-drinkers [2-3]. The epidemiological consensus currently is that frequent moderate consumption of alcohol is associated with the lowest risk for coronary artery disease and mortality. Although a recent study is in accordance with these observations, namely moderate alcohol use has an apparent protective association with coronary heart disease, the authors found no evidence of such a protective association of alcohol consumption and coronary artery calcification [4-5]. In fact, they reported evidence that heavy alcohol consumption, in particular hard liquor, is associated with greater calcification in coronary arteries. Accordingly, binge or heavy episodic drinking in short periods of time, defined as 5 or more drinks, was shown to be associated with increased cardiovascular disease and subsequent mortality [6-8]. Moreover, calciphylaxis, known to almost exclusively develop in patients with Stage 5 chronic kidney disease, was also reported to occur in heavy drinkers with physiological renal function [9-12]. While we are gradually deciphering how alcohol might exert beneficial effects on atherosclerosis leading to prevention of cardiovascular and cerebrovascular disease [13], the molecular basis of the dichotomous effects of alcohol on vascular calcification have not been explored.

Vascular calcification is a common complication of conventional risk factors for cardiovascular morbidity, and the extent is predictive of subsequent mortality beyond the established conventional disease states. Calcification develops in two main distinct sites within arteries.

2.2. Intima calcification

Intima calcification of atherosclerosis occurs focally. As a result of dyslipidemia and hypercholesterolemia the lipid accumulation, foam cell formation and inflammation are accompanied with vascular mineralization. The cells are going through oxidative stress which can lead to apoptosis, and complicated plaque formation[14].

A

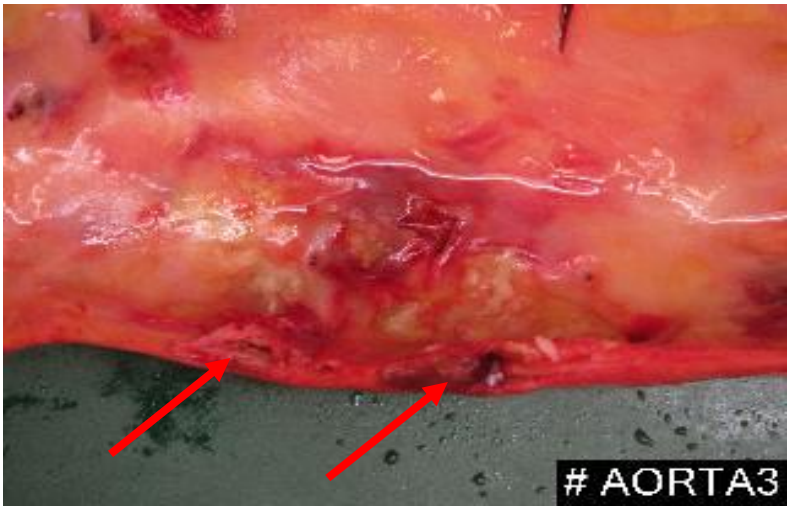

B

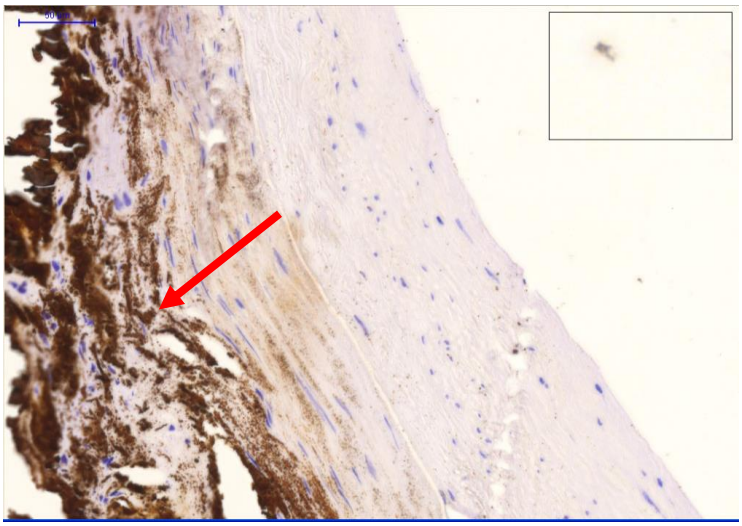

Figure 1. Intima calcification in atherosclerosis

(A) Cross-section of human aorta reveals atherosclerotic plaques. Red arrow indicates the distinct focal atherosclerotic lesions of the vessel. (B) Von Kossa staining demonstrates severe vascular mineralization of the intima. Red arrow points out dark brown staying signifying accumulation of calcium (calcium hydroxyapatite) within the intima of aorta. Patients were treated at the Department of

Nephrology, University of Debrecen. Histology was performed by the Department of Pathology, University of Debrecen.

2.3. Media calcification

While in atherosclerosis the intima is affected focally at predisposed areas of vessels (Figure 1), in medial sclerosis the media layers of the large- and medium-sized arterial wall are mineralized in a diffuse generalized fashion (Figure 2) [15].

A

B

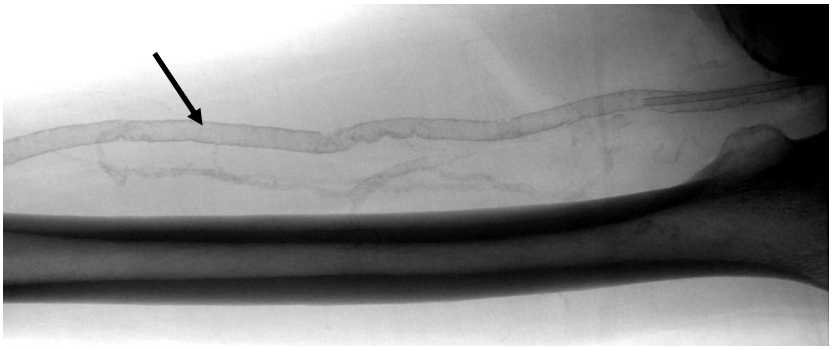

C

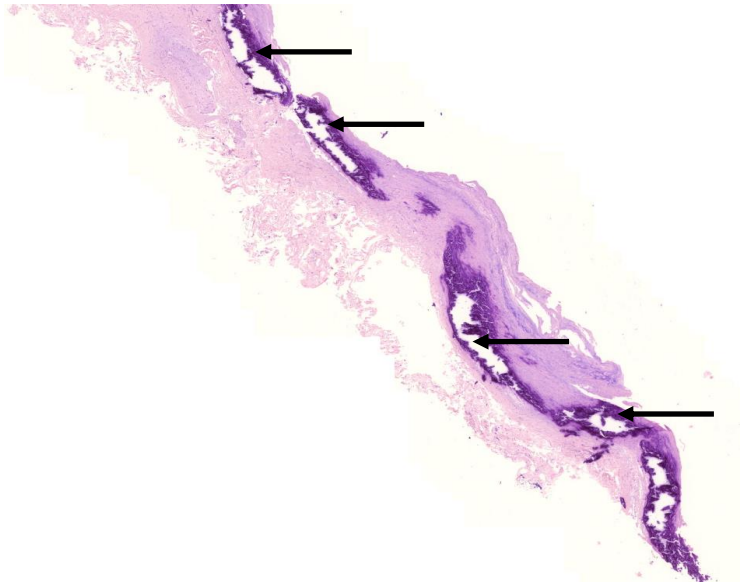

D

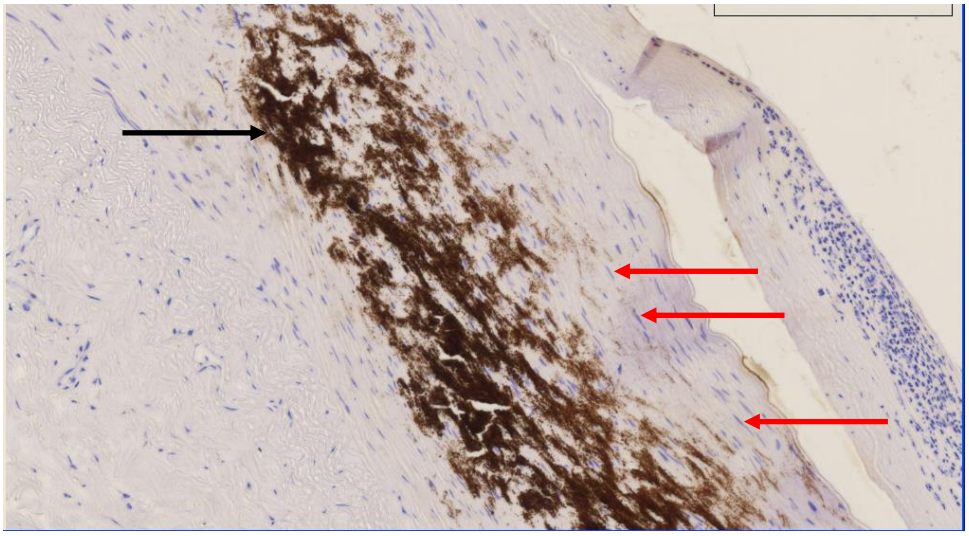

Figure 2. Media calcification

(A) Computer tomography scan identifies calcification of abdominal aorta in a patient diagnosed with chronic kidney disease. Black arrow indicates a concentric increase in density of the artery that approaches bone density. (B) Digital substraction angiography of a calcified femoral artery in the same patient (no contrast agent is used). Black arrow points to the continuously mineralized vessel. Note small branches are also calcified. (C) Histopathology of a calcified artery demonstrates severe remodelling/destruction of the media (hematoxylin/eosin staining). Extensive media mineralization appears in the purple streak labeled by black arrows. (D) Substantial deposition of hydroxyapatite associated with extracellular matrix is detected by von Kossa staining (black arrows). Some of the

smooth muscle cells of the media are labeled by red arrows. Patients were treated at the Department of Nephrology, University of Debrecen. CT-Scan, X-Ray were taken at the Department of Radiology, University of Debrecen and histology was performed by the Department of Pathology, University of Debrecen.

Media calcification (arteriosclerosis or Mönkeberg's sclerosis) is an active, generalized process which is induced by many factors such as high serum phosphate levels, calcium and parathyroid hormone levels. Other risk factors are ageing, diabetes, renal failure, osteoporosis and hypertension. The vascular smooth muscle cells trans-differentiate into bone-like cells and hydroxiapatite accumulates in the extracellular matrix which leads to arterial stiffening and increased pulse pressure and pulse wave velocity [14].

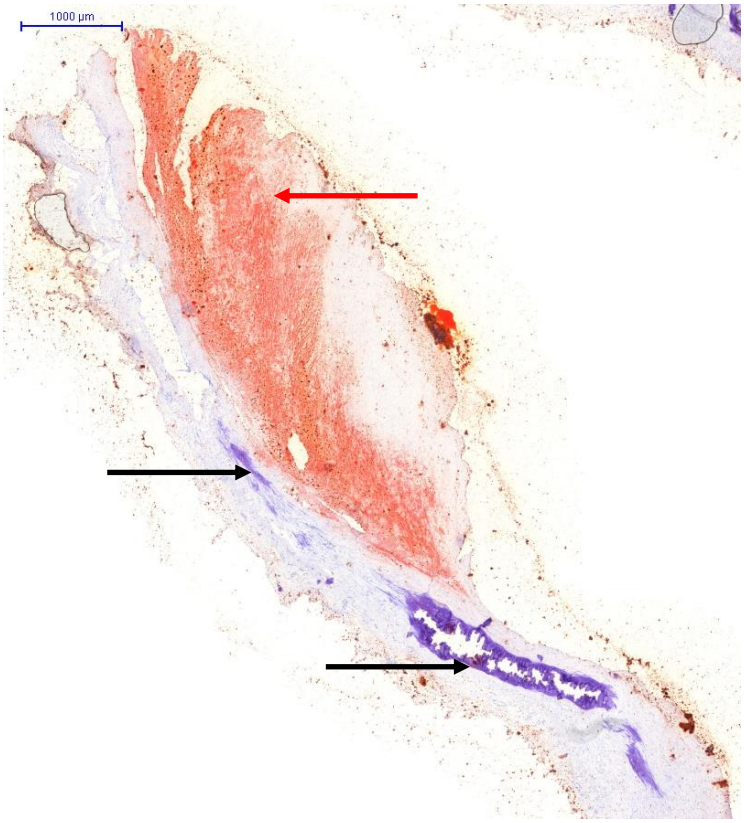

Figure 3. Atherosclerosis and media calcification coexist in pathologies

Extracellular intimal fat accumulation is demonstrated by oil red O staining in atheroma (red arrow) and mineralization of the media occurs under and next to the fatty plaque (black arrows). Patients were treated at the Department of Nephrology, University of Debrecen. Histology was performed by the Department of Pathology, University of Debrecen.

Intimal calcification in atherosclerosis is frequently accompanied by medial calcification and vice versa (Figure 3). They are strongly associated with aging, arterial remodeling including intimal-medial thickening and changes of the geometry and function of valves of the heart. Such calcifications have devastating clinical consequences related to an increased risk of cardiovascular morbidities and complications such as atherosclerotic plaque burden [16-18], myocardial infarction [19-20], coronary and cerebrovascular artery disease [21-22], postangioplasty dissection [23], and increased ischemic episodes in peripheral vascular disease [24]. Medial artery calcification was revealed to be a strong independent predictor of total, cardiovascular, and coronary heart disease mortality, and it is also a significant predictor of future coronary heart disease events (fatal or nonfatal myocardial infarction), stroke, and amputation in patients diagnosed with non-insulin-dependent diabetes mellitus [21]. Both the Framingham risk index and coronary calcification have been demonstrated to predict future cardiovascular events [25]. Studies also indicated that coronary calcification may be predictive of, or strongly associated with, sudden cardiac death [25-26]. The principal pathologic effects of vascular calcification are the abnormal perfusion of organs and stiffening of the vessels leading to increased left ventricular afterload.

2.4. Calciphylaxis

In calciphylaxis, the small cutaneous arterioles are affected (Figure 4). The main feature of calciphylaxis is the mineralization of vessels almost exclusively occurring in patients diagnosed with advanced chronic kidney disease (CKD) [27]. After medial calcification by smooth muscle cells, the endothelium acquires a procoagulant phenotype resulting in occlusion of small arterioles. The clinical picture is typically characterized by very painful skin necrosis that is life-threatening due to sepsis and concomitant cardio- and cerebrovascular diseases. The disease state was first described and studied by the famous Hungarian scientist, Hans Selye [28].

A

B

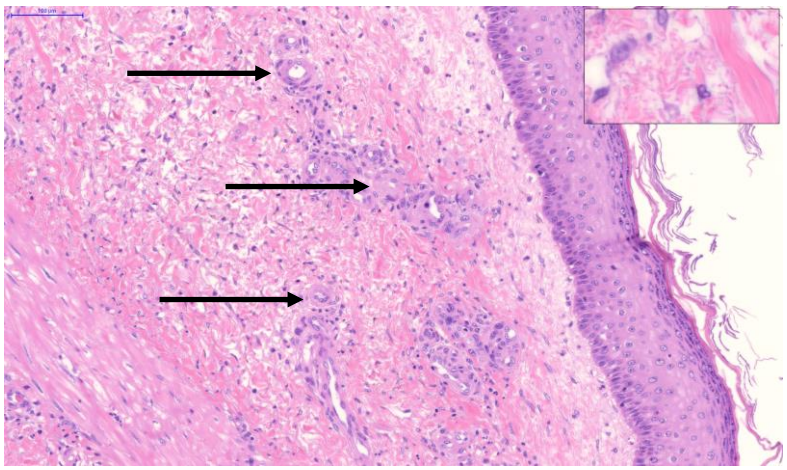

C

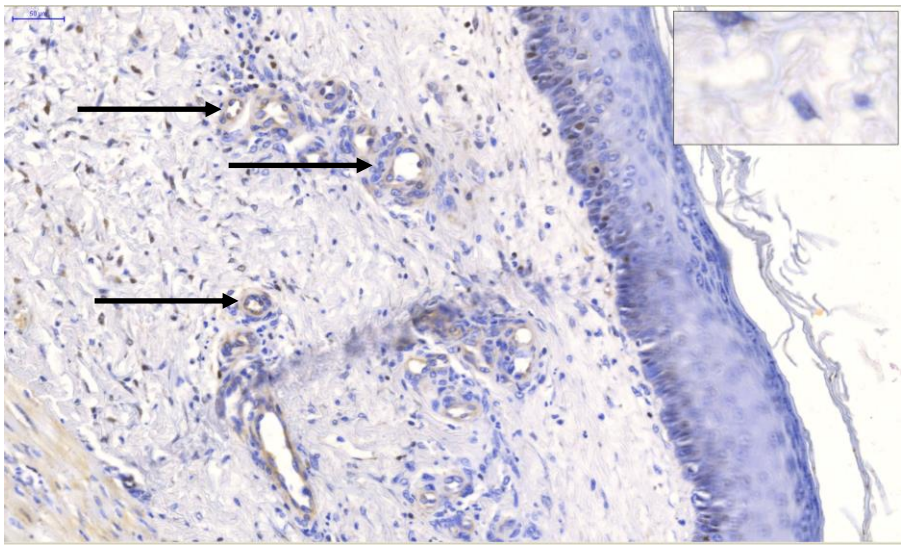

D

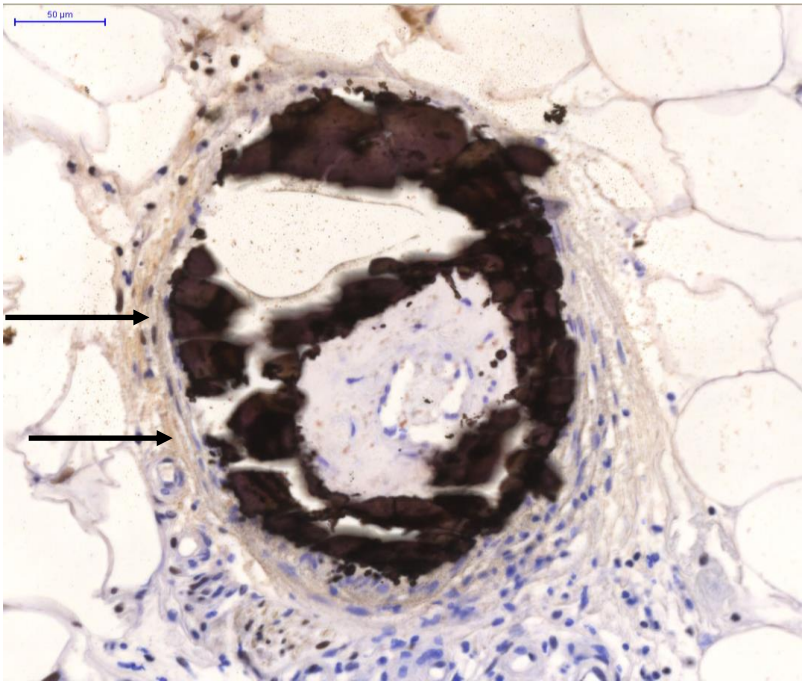

E

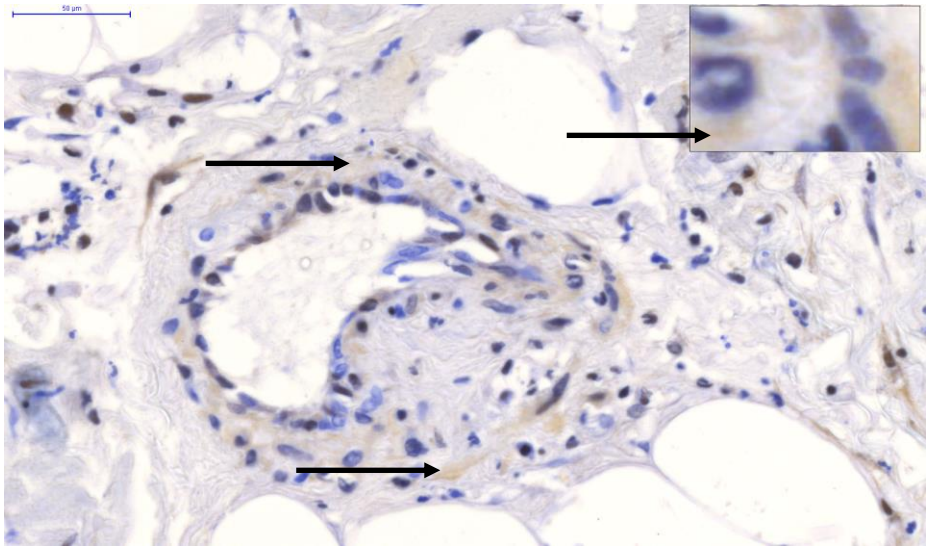

Figure 4. Calciphylaxis occurs in small cutaneous arterioles

(A) Painful skin necrosis resulted in a deep and extended ulcer of a limb in chronic kidney disease. (B) Histopathology of the skin lesion reveals excess material within the thickened wall of small cutaneous arterioles labeled by black arrows (hematoxylin/eosin staining). (C) Calcium deposition (arrows) in the wall of arterioles is detected by von Kossa staining. (D) Obliterated then revascularized subcutaneous arteriole with calcium deposits. (E) Obliterated subcutaneous arteriole with calcium deposits – close-up demonstrates fine staining. Patients were treated at the Department of Nephrology, University of Debrecen. Histology was performed by Department of Pathology, University of Debrecen.

Hyperphosphatemia has been demonstrated to act as a nontraditional risk factor for cardiovascular disease and found to increase mineralization [5, 29-32]. The physiological range of P_i is 0.8 mmol/L to 1.5 mmol/L. Serum levels of phosphorus are significantly related to the presence of coronary artery calcification [33]. Hyperphosphatemia is commonly observed in chronic kidney patients (the P_i level can readily increase to 3 mmol/L or above), and there is a strong association of serum phosphate level with mortality risk in chronic hemodialysis patients [34]. Tight associations between arterial calcification and stiffness, pulse pressure, or mortality have also been found to contribute to the high rates of cardiac and peripheral ischemic disease and left ventricular hypertrophy in this population [35-37]. Moreover, the phosphate level was also found to be independently related to aortic calcification in healthy individuals with physiological renal function [38]. In those healthy individuals who are drinking soft drinks regularly P_i can reach the level of 3 mmol/L.

2.5. Proteins and enzymes involved in vascular calcification

It is well established that inorganic phosphate is an important regulator of vascular calcification [39]. Although the precise mechanisms of vascular calcification are not completely understood, abnormalities in mineral metabolism are considered important risk factors. In this regard, we should mention that acute ethanol ingestion has been shown to increase serum phosphate [40]. It is thought to be an actively regulated multistep process in which interchangeable cellular phenotypes under certain pathological conditions are the driving force. One of the main contributors is the trans-differentiation of smooth muscle cells into osteoblast-like cells. After osteoblastic differentiation these cells lack characteristics of smooth muscle cells, and develop osteoblast features. Jono et al. revealed that human smooth muscle cells cultured in media containing physiological serum phosphate levels do not mineralize, but these cells can be induced to mineralize by elevating phosphate level in culture medium to that typically observed in hyperphosphatemic individuals (Figure 5) [31]. Granular deposits associated with the extracellular matrix developed in a time- and dose-dependent fashion. Exposure of human smooth muscle cells to elevated phosphate was shown to provoke substantial phenotypic transition towards osteoblasts [41]. At physiological phosphate levels, cells express smooth muscle lineage markers, including SM 22α and SM α-actin. After exposure to elevated phosphate, a dramatic loss of the markers for smooth muscle cell lineage occurs and simultaneously a gain of osteogenic markers such as alkaline phosphatase, osteocalcin and core-binding factor alpha-1 (*Cbfa-1*) develops.

2.5.1. Phosphate co-transporter, Pit-1 and Core-binding factor-α-1, *Cbfa-1*

Cellular uptake of P_i occurs through a sodium-dependent phosphate co-transporter, Pit-1, which is essential for vascular smooth muscle cell calcification and phenotypic modulation in response to elevated phosphate [42]. Three types of phosphate co-transporters have been identified based on structure and regulation. While types I and II transporters are restricted to the kidney and intestine, type III transporters are present in many tissues including kidney, heart, lung, and bone. Pit-1 and Pit-2 represent type III transporters. Of the known transporters, Pit-1 was found to be expressed in human smooth muscle cells as well as human aorta [39]. Vascular calcification during which smooth muscle cells gain an osteoblastic phenotype is accompanied by increased expression of *Cbfa-1* in cells exposed to high phosphate or platelet-derived growth factor. *Cbfa-1* is a transcription factor that acts as

an essential regulator of osteoblast differentiation and fulfills a dominant function for other gene products [43-44]. *Cbfa-1* is also crucial for chondrocyte differentiation [45]. In *Cbfa-1* null mice the intramembranous and endochondral ossification are completely blocked, owing to the maturational arrest of osteoblasts [46] demonstrating that this transcription factor is essential for osteoblast differentiation, bone matrix gene expression and, consequently, bone mineralization [47] (Figure 5).

2.5.2. Alkaline phosphatase (ALP)

Alkaline phosphatase is one of the phenotypic markers of osteoblasts. The expression of alkaline phosphatase occurs in type IV atherosclerotic lesions, areas of medial calcification, and valves of the heart. Alkaline phosphatase is expressed on the cell surface contributes to vascular calcification through cleaving organic phosphate compounds and releasing inorganic phosphate. The enzyme activity is indispensable in early osteogenesis. Inflammatory cytokines and vitamin D upregulate alkaline phosphatase activity and mineralization [48-49]. Several *in vitro* studies suggested that vascular calcifying cells express high levels of alkaline phosphatase, and the capacity for mineralization of these cells is dependent on their alkaline phosphatase activity. Therefore, it is most likely that the induction of alkaline phosphatase in vascular cells accelerates the development of vascular calcification.

2.5.3. Osteocalcin

Osteocalcin, a skeletal member of the family of extracellular mineral binding Gla proteins, is the major noncollagenous protein in bone matrix [50]. It is synthesized by the osteoblast and it is secreted into the bone matrix at the time of bone mineralization [51]. The calcium binding properties of osteocalcin and its pattern of expression in bone suggests an important function during bone mineralization. Osteocalcin is a gamma-carboxyglutamic acid containing protein present in calcified atherosclerotic lesions and mineralized heart valves at high concentration. [52-53]. Upregulation of osteocalcin was shown to occur in vascular cells in response to elevated phosphate [39].

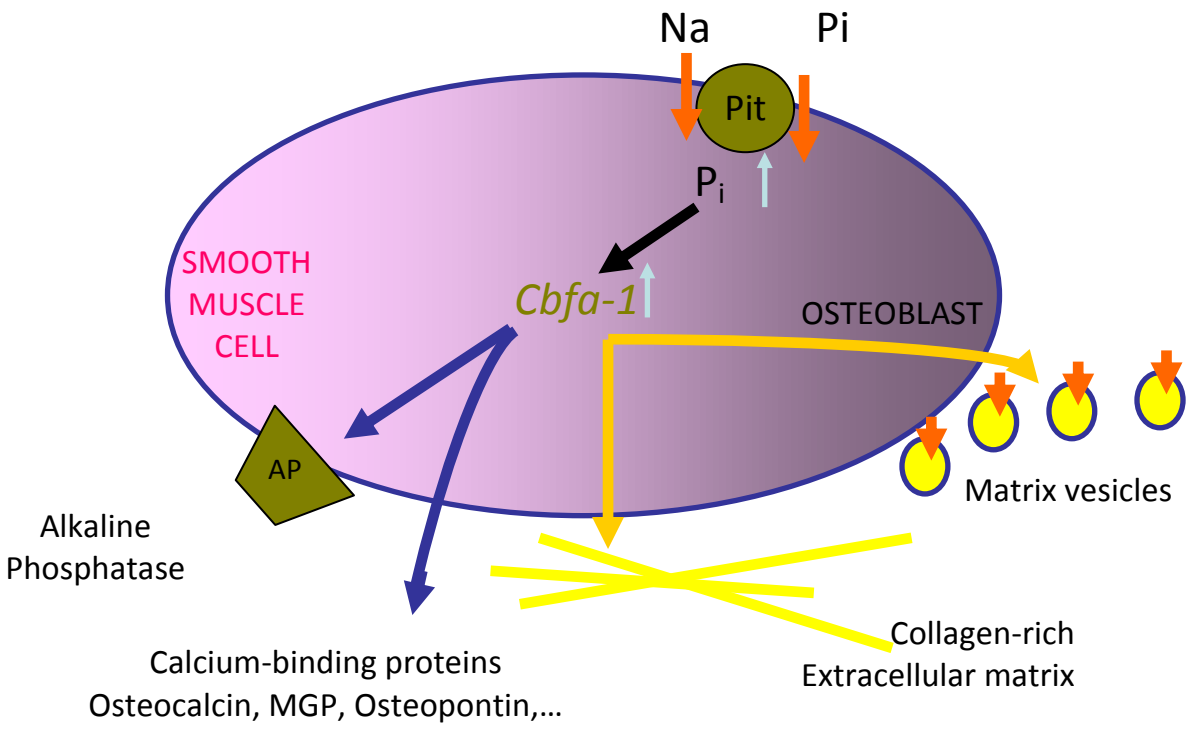

Figure 5. Regulation of human smooth muscle cell mineralization by inorganic phosphate – transition of vascular smooth muscle cells into osteoblast like cells

Vascular calcification is highly correlated with elevated serum phosphate levels in chronic kidney disease patients. Vascular smooth muscle cells cultured in media containing phosphate levels comparable to those seen in hyperphosphatemic individuals (>1.4 mmol/L), exhibit dose-dependent increases in cell culture calcium deposition in the extracellular matrix. Studies demonstrated that elevated phosphate levels also enhance the expression of the osteogenic markers, alkaline phosphatase, calcium binding proteins (osteocalcin, osteopontin) and *Cbfa-1* (transcription factor that acts as an essential regulator of osteoblast differentiation). The effects of elevated phosphate level are mediated by a sodium-dependent phosphate cotransporter (Pit-1) via enhancing intracellular phosphate level. Osteogenic transformation of vascular smooth muscle cells occurs in vivo resulting in mineralization of arteries in atherosclerosis and media calcification as well as in calciphylaxis.

Reprinted from Giachelli CM, Jono S, Shioi A, Nishizawa Y, Mori K, Morii H: Vascular calcification and inorganic phosphate. *Am J Kidney Dis* 38: S34–S37, 2001, with permission from the National Kidney Foundation.

2.6. ROS generation in alcohol metabolism

It has been well established that three major enzymatic pathways are involved in ethanol metabolism: alcohol dehydrogeanse, microsomal ethanol oxidation system (MEOS) and catalase. Each of these reactions could generate free radicals ([54-56] Das et al., 2005).

Ethanol metabolism directly promotes not only the formation of ROS production, but also enables the environment favourable to oxidative stress including hypoxia, endotoxaemia and cytokine release [57].

1, In moderate ethanol consumption ethanol is classically metabolized by alcohol dehydrogenases in the liver to form acetaldehyde leading to the formation of free radicals. Hydride ion is transferred from ethanol to NAD^+ [58].

2, The 3 isoforms of cytochrome P450 [59] take place in ethanol oxidation varying in their capacities to oxidize ethanol. In acute and chronic ethanol consumption the microsomal cytochrome P450 2E1 isoform is enhanced [60]. In ethanol consumers the 2E1 isoenzyme acts as a catalyst for increased formation of ROS, increased generation of superoxide anion radical, H_2O_2 and hydroxyl radicals.

3, In heavy ethanol consumers peroxisomal activity also participates in ethanol oxidation in the liver. In the peroxisomes alcohol is degraded by catalase to form acetaldehyde. Oxidized fatty acids are accumulated in the liver due to increased peroxisomal oxidation of fatty acids.

During the next metabolic step acetaldehyde also oxidized by mitochondrial aldehyde dehydrogenases (ALDH) to form acetate (Das et al., 2007).

At the last step of the metabolism acetate is activated to acetyl-CoA by acetyl-CoA synthetize.

In the course of ethanol oxidation there is a significant increase in the $NADH/NAD^+$ ratio both in the mitochondria and in the cytoplasm favoring oxidative damage [58].

Finally, ethanol reduces the activity of antioxidant system [57]. ROS production and oxidative stress in liver cells contribute to the development of alcoholic liver disease (Das et al., 2007).

2.7. QTL mapping of alcohol self-administration

Recent studies revealed that there is a dichotomy in vascular diseases and alcohol consumption - namely although moderate alcohol intake provides protection against cardiovascular disease, heavy alcohol use is associated with severe calcification in arteries. Importantly, heavy episodic drinking in short periods of time was shown to be associated with increased cardiovascular disease and subsequent mortality [6-8]. In an *in vitro* study the

calcification effect of ethanol was proved by intracoronary injection of ethyl alcohol in a porcine model of ischemic heart failure [61].

Nerves containing glutamate located close to bone cells exhibit functional glutamate receptor. It was revealed that glutamate alters bone resorption *in vitro* via a mechanically sensitive glutamate/aspartate transporter protein suggesting a function for glutamate in mechanical load and bone remodelling. Metabotropic glutamate receptor type 7 (*Grm7*) gene was also shown to serve a promising candidate that might be implicated in altered alcohol preference. The association of heavy alcohol consumption, alcoholism with hard liquor use, and arterial calcification prompted us to study the genetic background that might be connected to vascular diseases. In the central nervous system, the excitatory amino acid glutamate serves as a potent neurotransmitter exerting its effects via various membrane glutamate receptors [62].

We studied the genetic background of alcoholism. Alcoholism has been shown to be a complex disorder determined by genetic background of several genes. Our interest was to expand genome scanning of 5 chromosomes (1, 2, 3, 9 and 15) to cover all autosomal chromosomes and find ethanol consumption locus/loci (QTLs) and Quantitative Trait Genes (QTGs) involved in alcoholism. Neurochemical processes underlying alcoholism and drug addiction are not well explored. One strategy to identify neurochemical mechanisms of addiction is to map the relevant genes. Strong evidence in quantitative genetics suggests that most traits and alcoholism are significantly affected by genetic factors. Genetic variation in alcohol drinking was revealed by McClearn and Rodgers half a century ago via comparing well established inbred mouse strains [63-64]. In spite of intensive effort the biological basis of oral alcohol self-administration is not well revealed. New genetic tools, including high throughput SNP genotyping and gene expression microarrays, provide hope that genes responsible for alcoholism can be identified. This is substantial because effective therapy can be obtained if the molecular relation between the genetic basis and the biochemical pathways involved are understood.

Alcohol preference in rodents serves as an important model for hedonic aspects of alcoholism. Since the early 1990s a substantial number of Quantitative Trait Loci (QTLs) have been mapped in genetic studies for alcohol preference, consumption, and acceptance. Many excellent studies detected numerous QTLs employing C57BL/6J and DBA/2J based genetic designs, but only very few QTLs have been considered as consistently confirmed on chrs. 2, 3, 4, and 9 [65]. Retinaldehyde binding protein 1 (*Rlbp1*) and syntaxin 12 (*Stx12*) [66-67], and syntaxin binding protein 1 (*Stxbp1*) [68] were identified to be good candidate genes

for alcohol preference drinking. These previous studies relied on the "gene pool" of two inbred strains, C57BL/6J and DBA/2J. In a recent study Dubose et al. proved some previously identified significant QTLs for EtOH-induced locomotor activation on chromosomes 2 and 5 and one novel significant QTL for EtOH-induced motor incoordination on chromosome 7 at BXD RI mouse strains [69]. Wang et al. found that a promoter polymorphism in the Per3 gene was associated with circadian rhythm, alcohol, stress response and schizophrenia also in the BXD family of mouse strains [70].

Since in the species a lot of gene variants might segregate which are not represented by these two strains, a tendency to carry out most studies only on two strains and their descendants will limit our understanding at the species level, and we will be able to identify fewer genes in animal models for testing alcoholism in human. Accordingly, there is a need to identify the most representative genes at species level. Only a few laboratories worked on strains other than C57BL/6J and DBA/2J in mapping QTLs for alcohol consumption and preference (e.g., A/J [71-72] and 129P3/J [73]). HAP/LAP selection lines were established [74] from HS/Ibg mice and employed in mapping QTLs for alcohol preference [75]. The HS/Ibg mice were derived from eight inbred strains, including A, BALB/c, C57BL/6, DBA/2 [76]. In an other study of HS/Ibg mice 3 provisional QTLs were found on chromosomes 1, 3 and 9 in alcohol preference behaviour [77].

Alcohol drinking behavioral phenotypes of C57BL/6ByJ, BALB/cJ, CXBI/ByJ, progenitors and RQI strains have been described previously [78-80]. There was a novel trait gene mapping strategy Recombinant QTL Introgression, (Vadasz, C, 1990) [81-84] which was applied to map QTLs on five chromosomes for alcohol preference and consumption in 80 RQI strains of the b_5i_7 series [78]. In that study five mouse chromosomes (1, 2, 3, 9, and 15) with polymorphic microsatellite markers for Quantitative Trait Loci (QTLs) for alcohol consumption were scanned. 44 B6.C and 36 B6.I inbred congenic Recombinant QTL Introgression (RQI) mouse strains of the b_5i_7 series carrying genes of BALB/cJ or CXBI origin on C57BL/6ByJ genetic background were used. In the B6.C set of strains, multiple regression analysis resulted a model with three microsatellite markers, which explained 32% of the genetic variance. The two markers with the highest significance levels in the model, D1Mit167 and D2Mit74, have been mapped to chromosome regions close to the gene opioid receptor kappa 1 (chr. 1) and opioid receptor kappa 3 (chr. 2), respectively. The results of this gene-mapping research indicated that genetic polymorphisms in kappa opioid receptors might contribute to genetic predisposition to voluntary alcohol-drinking behavior. The follow-up

studies on opioid receptor kappa 1 knock-out mice suggested that complete constitutional dysfunction of the *Oprk1* gene can decrease alcohol consumption [85], however chromosome position of microsatellite marker “D1Mit167” in the MIT database was assigned incorrectly, and the proposed chr. 1 region was not associated with genetic variation in alcohol consumption [86].

3. AIMS OF THE STUDY

Calcification of soft tissues develops under pathological conditions and has detrimental consequences, particularly when it occurs within vessel walls such as arteries, arterioles and heart valves. Calcification plays a crucial role in the pathogenesis of atherosclerosis and medial sclerosis, both leading to cardiovascular morbidity and mortality. It is also essence of a rare disease, calciphylaxis with very high mortality.

Epidemiologic studies suggest a complex association between alcohol consumption and cardiovascular disease.

Identification of processes involved in the complex interaction between alcohol consumption and vascular calcification should enable prediction of susceptibility to the disease and give potential targets to establish new preventive measures and effective therapies.

Alcohol preference in rodents serves as an important model for hedonic aspects of alcoholism, and alcoholism shown to be a complex disorder determined by genetic background factors.

<u>The objectives of our studies</u>

1. To determine whether ethanol alters the mineralization of vascular smooth muscle cells and accumulation of calcium in extracellular matrix.
2. To determine whether ethanol affects the transition of vascular smooth muscle cells into osteoblast-like phenotype.
3. To determine the mechanism by which the osteoblastic transition of vascular smooth muscle cell occurs.
4. To expand genome scanning from 5 chromosomes (1, 2, 3, 9 and 15) to cover all autosomal chromosomes, and increased sample sizes in alcohol drinking preference tests of b_5i_7 RQI mouse strains. To analyze the combined data with composite interval mapping (CIM) and by multiple interval mapping (MIM).
5. To identify loci and genes that play a role in alcohol preference and drinking behavior.

4. MATERIALS AND METHODS

4.1. Cell culture and reagents

Human aortic smooth muscle cells were purchased from Cell Applications Inc. (San Diego, CA, USA) and fetal bovine serum (FBS) from Gibco (Paisley, UK). Unless otherwise mentioned, all other reagents were obtained from Sigma-Aldrich (Steinheim, Germany). Cell cultures were maintained in growth medium DMEM (GM) containing 15% FBS, 60 U/mL penicillin, 60 μg/mL streptomycin, 120 μg/mL neomycin, and 1 mM of sodium pyruvate. Cells were grown to confluence and used from passages 3 to 7 [87]. Primary human umbilical vein endothelial cells (HUVECs) were removed from human umbilical veins by exposure to dispase and cultured in medium 199 containing 15% FBS, antibiotics, L-glutamine, sodium pyruvate and endothelial cell growth factor [88]. HepG2 cells were maintained in DMEM containing 10% FBS, 100 U/mL penicillin, and 100 μg/mL streptomycin.

4.2. Histopathologic examination

For histopathologic examination, tissues and vessels were fixed in 10% formalin and embedded in paraffin. Five-micrometer sections were deparaffined with xylol for 8 minutes and rehydrated in a descending series of isopropyl-alcohol. Hematoxylin/eosin staining was performed (hematoxylin for 6 minutes, followed by a wash in distilled water for 8 minutes, staining with eosin for 2 minutes, dehydrating, and mounting on a coverslip). After rehydration, von Kossa staining was also performed - tissues in 5% silver-nitrate solution in front of a 60-watt lamp were incubated for one hour then rinsed in distilled water, exposed to 5% sodium thiosulfate for 5 minutes, stained with hemalaun solution, dehydrated and finally mounted on a coverslip. For lipid staining fresh frozen sections were used (at 8 to 10 micrometer) after drying the section to the slides. Formalin fixation, a brief wash with tap water (1-10 mins) and rinse with 60% isopropanol were followed by staining with freshly prepared Oil Red-O working solution (15 mins). Tissues were rinsed with 60% isopropanol and then stained for nuclei with hemalaun solution. Stained slides were scanned with a Mirax Midi scanner (3D Histech, Budapest, Hungary) for digital documentation.

4.3. Induction of calcification

At confluence, cells were maintained in calcification medium which was prepared by adding 1 to 4 mmol/L of inorganic phosphate (P_i) to the growth medium. Both growth medium and calcification medium were changed every 2 days. The enhancement of P_i-provoked calcification by ethanol was most pronounced at a P_i concentration of 3 mmol/L. Therefore, we used 3 mmol/L P_i for inducing calcification in our experiments.

4.4. Quantification of calcium deposition

Cells grown on 48 well-plates were washed twice with PBS and decalcified with 0.6 N HCl for 30 minutes. Calcium content of the supernatants was determined by the QuantiChrome Calcium Assay Kit (Gentaur, Paris, France) as described by the protocol. After decalcification, cells were washed twice with PBS and solubilized with NaOH (0.1 mol/L) and SDS (0.1%), and the protein content of samples was measured with a BCA protein assay kit (Thermo Scientific, Rockford, IL, USA). Calcium content of the cells was normalized to protein content and expressed as μg/mg protein. For time-course experiment cells were treated for 5, 7, 10, 12 days before solubilizing. Mineral deposition in the extracellular matrix was also assessed by Alizarin Red staining [87]. After staining, cells were washed twice with distilled water and once with 70% ethanol. To solubilize the stained extracellular matrix granules we incubated the cells with 100 mmol/L cetylpyridinium chloride for 1 hour, followed by measuring the absorbance of the dissolved dye at 570 nm.

4.5 Inorganic phosphate measurement

P_i content of cell lysates was determined by the QuantiChrome Phosphate Assay Kit (Gentaur, Paris, France). After the ethanol treatment, cells were washed twice with PBS, solubilized with 1 % Triton X-100 and the cell lysates were assayed for P_i. Phosphate content of the cells was normalized to protein content and expressed as mmol/mg cell protein [87].

4.6. Alkaline phosphatase (ALP) activity assay

Cells grown on 6-well plates were washed with HBSS twice, cellular proteins were solubilized with 1% Triton X-100 in 0.9% NaCl and were assayed for ALP activity. Briefly, 130 μl of Alkaline Phosphatase Yellow Liquid Substrate (Sigma-Aldrich, Steinheim,

Germany) was combined with 50 μg of protein samples. Kinetics of p-nitrophenol formation was followed for 30 minutes at 405 nm during incubation at 37°C. Maximum slope of the kinetic curves was used for calculation [87].

4.7. Western Blot and Osteocalcin assay

To detect osteocalcin expression, cells grown on 6-well plates were treated for 7 days. Extracellular matrix was dissolved in 200 μL of EDTA (0.5 mol/L, pH 6.9) for osteocalcin and then cell lysate was obtained for glyceraldehyde-3-phosphate dehydrogenase assay. Equal loading of 30 μl EDTA solubilized sample was electrophoresed on a 16.5 % Tris-Tricine Peptide gel (Bio-Rad, Hercules, CA, USA) and blotted onto nitrocellulose membranes (Hybond-ECL, Amersham Biosciences, Buckinghamshire, UK). After blocking, the membranes were incubated with polyclonal anti-osteocalcin antibody at 1:200 dilution (Santa Cruz, Santa Cruz, CA, USA), followed by a peroxidase labeled anti-rabbit IgG antibody (Amersham Biosciences, Buckinghamshire, UK). For glyceraldehyde-3-phosphate dehydrogenase (GAPDH), 30 μL of cell lysate was electrophoresed on a 12.5% SDS-PAGE then blotted onto a nitrocellulose membrane. The membrane was incubated with mouse monoclonal anti-GAPDH (Novus Biologicals, Inc., Cambridge, UK) followed by a peroxidase labeled anti-mouse IgG antibody (Amersham Biosciences, Buckinghamshire, UK). For alcohol dehydrogenase 1 expression, cell lysate was electrophoresed on a 12.5% SDS-PAGE and blotted onto a nitrocellulose membrane. After blocking, the membrane was incubated with rabbit monoclonal anti-alcohol dehydrogenase 1 antibody at 1:1000 dilution (Abcam, Cambridge, UK), followed by a peroxidase labeled anti-rabbit IgG antibody. After quantification, the membrane was reprobed for glyceraldehyde-3-phosphate dehydrogenase. Antigen-antibody complex was visualized with a horseradish peroxidase chemiluminescence system according to the manufacturer's instructions (Amersham Biosciences, Buckinghamshire, UK). Quantification of proteins was performed using computer-assisted video densitometry (Alpha DigiDoc RT, Alpha Innotech, San Leandro, CA, USA). Osteocalcin content of the same EDTA solubilized extracellular matrix samples were quantified by an enzyme-linked immunoabsorbent assay (Bender MedSystems, Vienna, Austria) according to the manufacturer's instructions.

4.8. Quantitative reverse transcription-polymerase chain reaction

Total RNA was isolated, reverse transcribed and *Cbfa-1* mRNA was determined as described previously [28,29]. Briefly, for *Cbfa-1* mRNA levels the 25 µl reaction mixture contained 5 µl of reverse transcribed sample, 0.3 nmol/L of forward (5'-ATGGCGGGTAACGATGAAAAT-3') and reverse primers (5'-ACGGCGGGGAAGACTGTGC-3') and 12.5 µl of iQ SYBR Green Supermix (Bio-Rad, Hercules, CA, USA). PCRs were carried out using the iCycler iQ Real Time PCR System (Bio-Rad, Hercules, CA, USA). Results were normalized by Cyclophilin mRNA levels.

4.9. Cell viability assays

After treatment of cells with 20 to 80 mmol/L of ethanol in the presence or absence of calcification medium for 7 days. Following this, the monolayers were washed twice with HBSS and the test solutions were replaced with 550 µl of 3-[4,5-Dimethylthiazol-2-yl]-2,5-diphenyl-tetrazolium bromide (MTT) (0.5 mg/mL) solution in HBSS after which the cells were incubated for an additional 6 hours. After the MTT solution was removed, 550 µl of dimethyl-sulfoxide (DMSO) was added to the wells, and the optical density at 570 nm was measured.

4.10. Measurement of ROS generation

ROS production was determined by measuring the change in fluorescence intensity of 5-chloromethyl-2,7-dichlorodihydrofluorescein diacetate (CM-H_2DCFDA) converting to the fluorescent DCF, (Molecular Probes, Eugene, OR, USA).

Cells were seeded in 96-well plates then treated with growth or calcification medium in the presence or absence of ethanol for 2 days. Next 10 µM CM-H_2DCFDA in HBSS was added to the cells for 30 min in the dark. After cells were washed 2 times with HBSS. The change in fluorescence intensity was measured in HBSS by BioTek Synergy 4 Fluorometer with 488 nm, as excitation and 530 nm, as emission wavelengths.

4.11. Statistics

Data are shown as mean ± SD. At Figure 10, 13 and 20 data are shown as mean ± SEM. Statistical analysis was performed by one-way ANOVA test followed by a Newmann-Keuls test for multiple comparisons and two-way ANOVA test for Figure 6. A value of $p < 0.05$ was considered significant and marked with *, and $p < 0.01$ was considered highly significant and marked with ** and $p < 0.001$ marked with ***.

4.12. Recombinant QTL Introgression strains

Recombinant QTL Introgression was employed for the genetic analysis of complex quantitative straits. During this method we used short-term phenotypic selection, congenicity, recombination and inbreeding [83]. For phenotype we selected a mesotelencephalic dopamine system related trait, since it plays an important role in the control of motor activity, learning, emotion, motivation, and importantly addiction. QTLs from BALB/cJ and CXBI donor strains that are determining continuous variation of mesencephalic tyrosine hydroxylase (TH/MES) enzyme activity were introgressed onto B6 background strain from BALB/cJ and CXBI donor strains. CXBI is a recombinant inbred strain carrying B6 and BALB/cBy genes [89]. We developed two types of F2s [78, 81, 90] (B6XC and B6XI) and in each type replicate lines (α and β) were produced by equal division of each F2 litter. For the phenotype we tested at least 45 F2 males in each of the four lines and selected 15 for the first backcross to B6 females. We examined ≥ 45 backcross1 (b_1i_0) male offspring and 15 males were chosen then intercrossed with nonlittermate females resulting in b_1i_1 generation. Via backcross-intercross cycles QTL transfer was carried out in two directions with concomitant selection for the extreme high and low expressions of TH/MES enzyme activity in replicates leading to four QTL introgression lines. From these lines we selected the top and the bottom one third of each generation considering the expression of TH/MES enzyme activity. These steps were repeated for four (b_4i_5 series) or five (b_5i_7 series) cycles. The QTL introgression phase was followed by initiation of brother sister (bxs) mating for at least 30 generations in closed lines. RQI strains of the $b4i_5$ and b_5i_7 series carry <5% and <3% of the donor BALB/cJ genome, respectively, on the background B6 genome.

In order to ensure independent derivation of strains from the population of the last backcross-intercsross cycles eight sublines of the b_5i_7 series were excluded from the analysis.

Average of donor genome contribution in carrier strains was calculated as Q%=Ncc/(Ncc+NBB)*100±SD, where Ncc=number of markers with CC (donor) genotype; NBB=number of markers with BB (background) genotype. Estimates of donor genome contribution were based on RQIgbase, release November 20, 2004 (http://rqigenetics.org/).

4.13. Development of congenic strain B6By.C6

The alcohol-nonpreferring quasi-congenic RQI strain B6.Cb_5i_7-Alpha3 (C5A3) was developed by five backcross-intercross cycles using the alcohol-avoiding C strain as donor and the alcohol-preferring B6By strain as background. Using C5A3 as a progenitor, the congenic B6.C6 strain was developed by an additional five backcrosses to B6By with concomitant selection for C alleles of Chr.6 microsatellite markers (e.g., D6Mit105). Other relevant markers were selected from the genome-wide genotype database of RQI strain (http://rqigenetics.org/). Congenic status was tested by a genome scan with a mouse SNP panel of 402 markers (service provided by Genetics Division, Brigham and Women's Hospital, Harvard Medical School). Only the expected single chr.6 donor segment was detected as of C origin.

4.14. Phenotype definition of alcohol consumption (AC)

AC34GKD represents alcohol consumption in $g \cdot BW_{kg}^{-1} \cdot day^{-1}$. Consumption of 12% alcohol was averaged over trials 3 and 4 for individual, and mean value of a strain was calculated across individuals. For the b_4i_5 series of B6.C RQI strains we assayed only trials 3 and 4 systematically. Trial 5 does not exhibited AC34GKD phenotype. For the b_5i_7 series of B6.C and B6.I RQI strains data for trials 3, 4, and 5 were available. Accordingly, for AC345GKD consumption of 12% alcohol was averaged over trials 3, 4 and 5 for an individual, then mean for a strain was obtained across individuals, and expressed as $g \cdot BW_{kg}^{-1} \cdot day^{-1}$. AC34GKD and AC345GKD data are presented in Tables 1-2.

4.15. Behavioral tests

Adult (11±2-week-old) male mice of C57BL/6By, BALB/cJ, CXBI, and RQI strains were utilized and had been kept in the study room for ≥ one week prior to the behavioral assessment. Testing system provided a high capacity allowing us to perform ethanol-

preference tests in batches of ≥ 70 subjects. In each batch 3 littermate males of available RQI strains were tested, along with 3 males of each of the progenitor strains. In order to assess inter-assay variability the latter served as standard reference throughout the phenotyping. We employed a "two-bottle choice" paradigm with enhancing ethanol concentration. The test consisted of five 3-day trial periods, in which mice were allowed to choose between ethanol solution and tap water. To adapt the animals to the taste of ethanol, ethanol solutions were offered in increasing concentrations as follows: a 3% solution for trial 1 (day 1-3) was elevated to 6% in trial 2 (day 3-6), and further enhanced to 12% for trials 3 (day 6-9), 4 (day 9-12), and 5 (day 12-15). This arrangement provided us to perform triplicate measurements of ethanol preference at concentration of 12% (v/v).

We did not carry out experiments for 3% and 6% of ethanol consumption in duplicate since ethanol solutions of 3% and 6% provided an acclimation period for animals to 12% ethanol solution. Our data analysis was focused on the consumption of 12% ethanol solution measured in triplicate (i.e., three subsequent 3-day trial periods), and the values used for analysis were 3-day access ones. The solutions were provided in custom-made drinking tubes consisting of centrifuge tubes fitted with single-hole rubber stopper into which stainless steel sippers were inserted. In order to prevent chewing and playing with the drinking tubes stainless-steel washers were glued to the bottom region of the rubber stoppers. To fasten the tubes firmly to the top of the cage covers stainless steel springs were used. Two empty cages with alcohol and tap water drinking tubes were inserted into the racks for control to measure the leakage and evaporation of solution. In order to avoid the position effect the place of ethanol solution and tap water on the cage cover were alternated in each 3-day preference trial. The weights of the drinking tubes were measured before and after a 3-day trial by an A&D electronic analytical balance connected to a computer. Data were entered automatically employing A&D COLLECT software and QUATTRO spreadsheets. Previously collected ethanol consumption data for RQI strains and new data obtained in our study using the same methods were coanalyzed.

4.16. DNA extraction, polymerase chain reaction, capillary gel electrophoresis

DNA was isolated from tail tips of mice derived from each RQI strain using the method of Miller et al. [91]. We selected PCR primers as markers polymorphic for B6 and C strains with information from the Mouse Genome Database (Mouse Genom Informatics, The Jackson Laboratory). For QTL mapping 396 microsatellite markers were employed. To

analyze PCR products using our ABI Prism 310 Genetic Analyzer, dye (FAM, TET or HEX)-labeled microsatellite markers were custom-synthesized, fluorescently labeled and, purified by Integrated DNA Technologies, Inc., Coralville, IA. Employing a 310 Genetic Analyzer one base size difference could be detected. Therefore the reproducibility of the size identification was good. Since there are fluctuations, standard DNA products (PCR products from C57BL/6 and BALB/c DNA) were included.

4.17. QTL mapping

For mapping we used M-estimators, robust alternatives to sample mean and median for estimating the center of locations. The original phenotypic data were processed in the Explorer function of SPSS ver.13 to receive Tukey's biweight M-Estimators.

QTL position and effect size was judged by CIM using Windows QTL Cartographer version 2.5. We employed the standard model Zmapqtl 6 in the CIM procedure with a 10 cM window size and a 2 cM walking speed, forward and backward method of regression with probability of into or out of 0.1. Threshold values of significance for QTLs was determined by permutation analysis [92]. This involved reassining the phenotypic data to RQI lines at random and redoing the likelyhood ratio Test Statistic analysis. This procedure was repeated 1000 times, for each repetition the global maximum was recorded. Values were ranked in increasing order of significance. The 950th, 900th, 800th LRS values gave the LRS values for the p=0.005, p=0.1, and P=0.2 levels of significance. Tests were performed for AC345GKD in each population of b_5i_7 RQI strains. Significant QTLs exceeded the 0.05 genomwide adjusted threshold. QTLs exceeding the 0.2 threshold were considered suggestive.

Strain sets were also analysed by the MIM option for QTL Cartographer version 2.5. The MIM method combines QTL mapping analysis with the analysis of genetic architecture of quantitave traits. It utilizes multiple marker intervals to construct multiple putative QTLs [93]. The MIM model is based on Cockerham's model for interpreting genetic parameters and the method of maximum likelihood for estimating genetic parameters. This method fits all QTLs into the model altogether and has the ability for analyzing QTL epistasis and associated statistical issues. Through a search algorithm, the method can obtain information about the QTL simultaniously such as number, positions effects and interaction of the significant QTLs. The search strategy of MIM method is to select the "best" genetic model in the parameter space. Model selection is critically important in data analysis and interpretation. It is well known that the appropriate criteria or stopping rules used for model selection are difficult to

decide. In the Windows QTL Cartographer program we used Bayesian Information Criteria (BIC) to control the type I and type II errors at a reasonable level for QTL mapping situation [94]. BIC was defined as: BIC=n*ln(Q*Q)+p*c(n), where n=sample size, Q*Q=residual variance of model, p=regression (marker) number, c(n) is a penalty function, which can take different forms. Criteria of MIM model selection was based on BIC-M0, where c(n)=ln(n). MIM search walk speed was 1 cM. The model was created by MIM forward search method.

4.18. Data analysis of QTL mapping

Descriptive statistics, eta-squared, Post Hoc Test LSD 0.05 (least significant difference at 0.05 probability level) for alcohol consumption data in RQI strains were analyzed using GLM Univariate ANOVA procedure of SPSS software ver.13. (Table 2).

4.19. Bioinformatics

Chromosome segments carrying significant and suggestive QTL peaks were investigated for relevant QTLs and genes using http://informatics.jax.org and http://omicspace.riken.jp [95]. Range of QTL peak was approximated by inspecting marker genotype patterns in all strains, identifying all donor segments which contained the peak position (cM), and recording rough approximation gives an estimate of minimum range of donor segments because positions of segment-limiting donor-type markers were used.

5. RESULTS

5.1. Ethanol fosters human vascular smooth muscle cell calcification in a dose- and time-response fashion enhanced by increased inorganic phosphate

Since studies have shown the paramount importance of high extracellular inorganic phosphate to induce vascular calcification in humans, we established an *in vitro* model for vascular calcification by culturing human vascular smooth muscle cells in growth medium containing increased concentration of P_i (hereafter designated calcification medium). Calcification medium was prepared using 1 to 4 mmol/L of P_i growth medium (GM) consisting of DMEM containing 15% FBS, 60 U/mL penicillin, 60 μg/mL streptomycin and 120 μg/mL neomycin, and supplemented with 1 mM of sodium pyruvate. We maintained human vascular smooth muscle cells for 7 days and measured the calcium accumulation in the extracellular matrix in the presence or absence of ethanol (Figure 6).

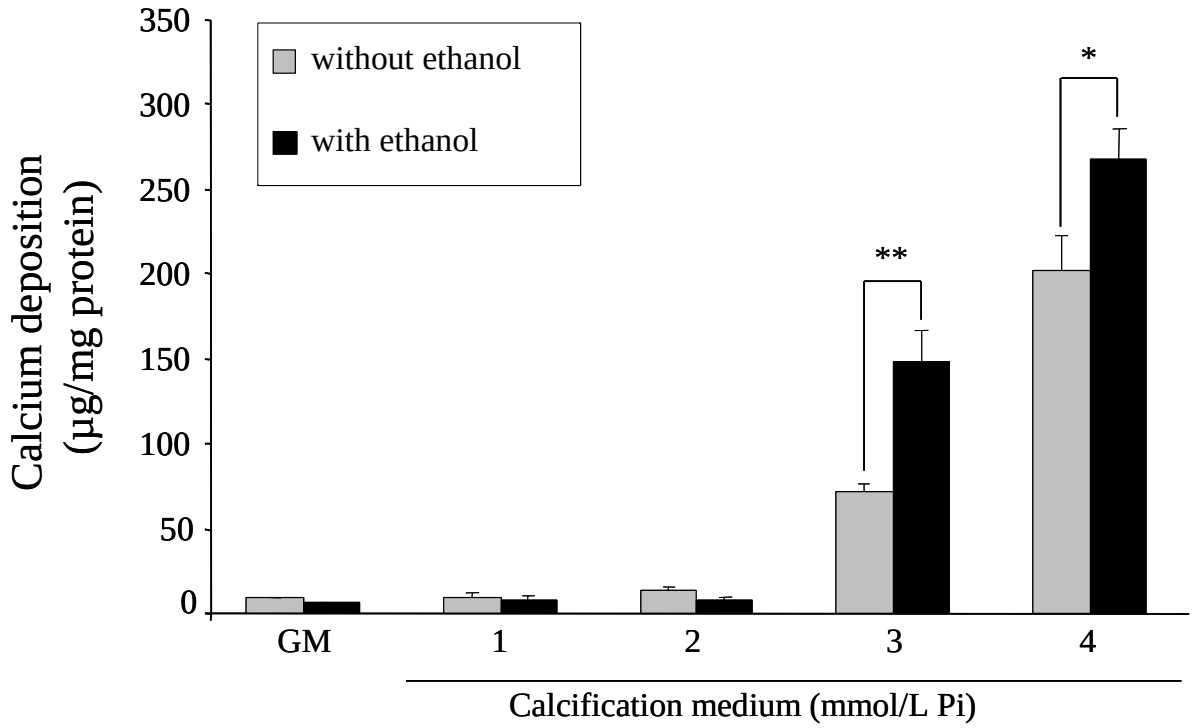

Figure 6. Ethanol promotes human vascular smooth muscle cell calcification provoked by increased phosphate.

Human vascular smooth muscle cells were cultured in GM alone or in calcification medium containing 1 to 4 mmol/L of phosphate. Media were supplemented with 60 mmol/L of ethanol. Calcium content of cells was measured after 7 days of culture as described in Methods, and was normalized by protein content. Data are presented as the mean ± SD of 3 independent experiments performed in duplicates. *$P < 0.05$, **$P < 0.01$.

As expected, phosphate induced mineralization in a dose-response fashion. Significant calcium accumulation was observed at ≥ 3 mmol/L of P_i. To our surprise, treatment of human vascular smooth muscle cells with ethanol promoted deposition of calcium provoked by P_i. Exposure of cells to 60 mmol/L of ethanol (a concentration occasionally observed in very heavy drinkers' blood) resulted in a further enhancement in calcium accumulation (100%). We suspected that ethanol alone might alter the calcification of human vascular smooth muscle cells over a longer period of time. However, cells maintained for up to 14 days in growth medium supplemented with ethanol failed to develop mineralization (Figure 7).

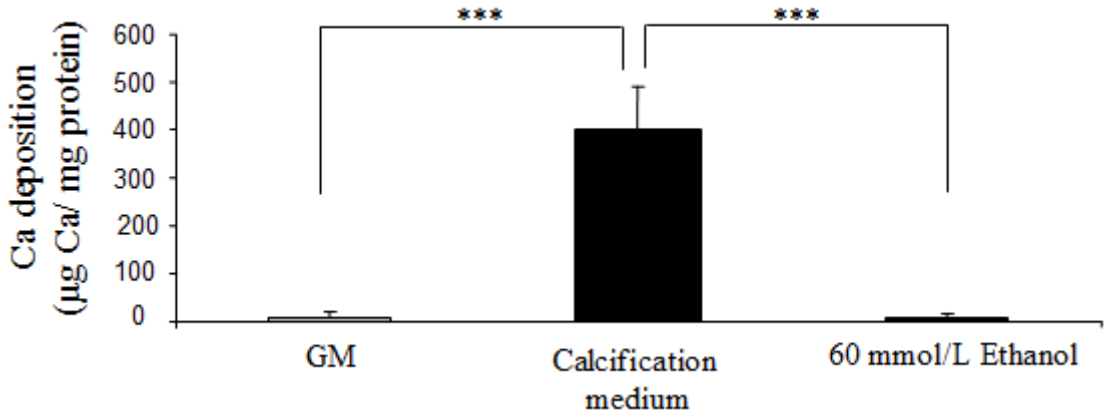

Figure 7. Prolonged (14 day) exposure of smooth muscle cells to ethanol alone does not provoke calcification.

Human vascular smooth muscle cells were cultured in GM or in calcification medium in the absence or presence of 60 mmol/L of ethanol for 14 days extracellular calcium measurements were carried out using QuantiChrome Calcium Assay. Data are presented as mean ± SD of 2 independent experiments performed in quadriplicates. *$P < 0.05$, **$P < 0.01$.

In order to confirm the additional accumulation of calcium provoked by ethanol in the extracellular matrix of human vascular smooth muscle cells we performed Alizarin Red

staining of cells cultured in calcification medium in the presence or absence of ethanol (Figure 8).

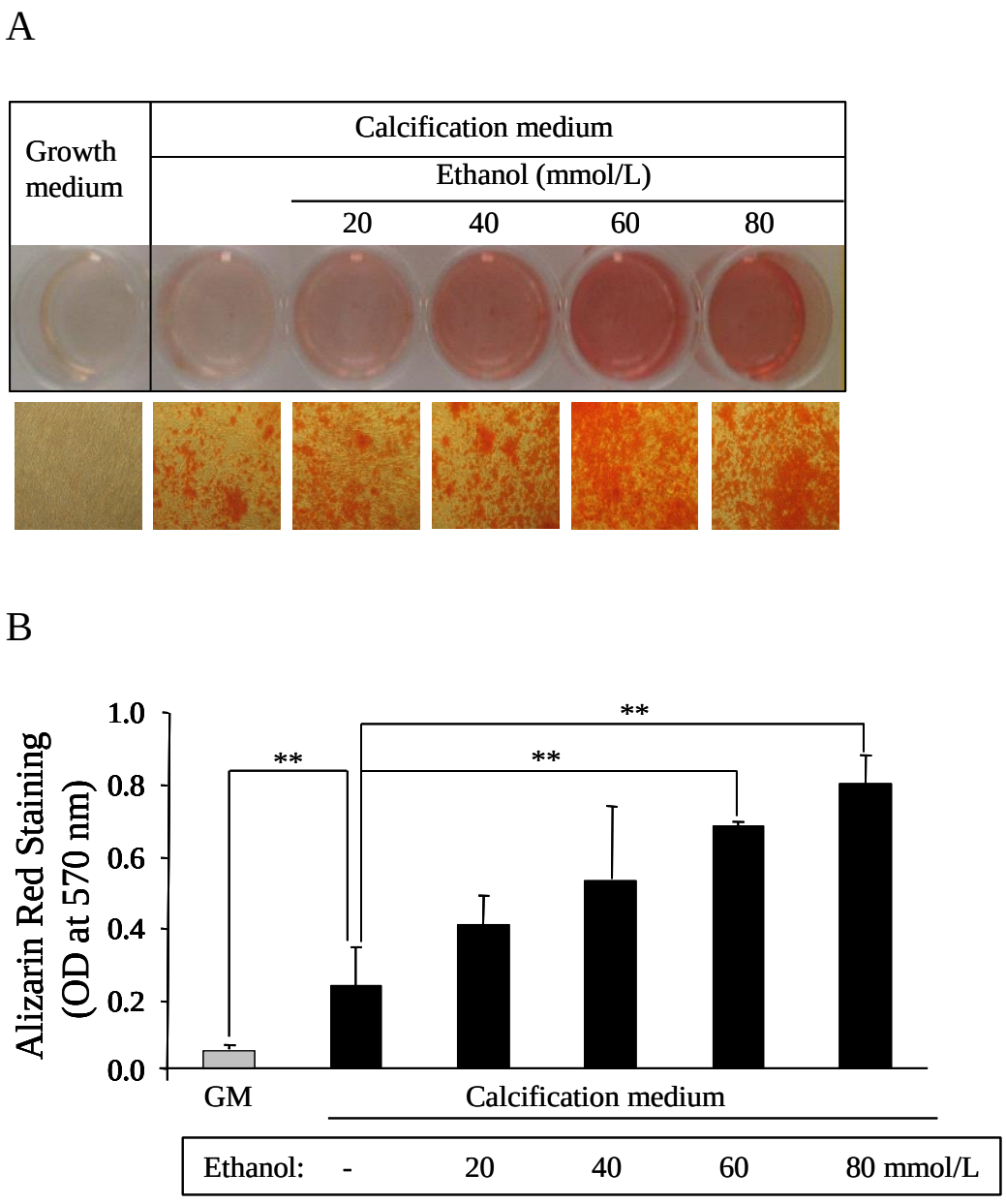

Figure 8. Dose dependent effect of ethanol on human smooth muscle cell calcification.

(A) Human vascular smooth muscle cells were cultured in GM or in calcification medium in the absence or presence of increasing concentration of ethanol for 7 days then Alizarin Red staining was performed. Representative images of stained plates (upper) and microscopic views (x100, lower) from 3 independent experiments are shown. (B) Quantification of Alizarin Red staining after solubilization of granular deposits with cetylpyridinium chloride as described in Methods. Data are presented as mean ± SD of 3 independent experiments performed in duplicates. *$P < 0.05$, **$P < 0.01$.

Importantly, after exposure of vascular smooth muscle cells to ethanol for 7 days, more granular deposits developed throughout the cell cultures as compared to vascular smooth muscle cells maintained in ethanol free calcification medium (Figure 8A). On the contrary, in cells cultured in growth medium without P_i and ethanol, no calcification occurred.

We next tested whether ethanol dose-dependently enhanced phosphate-provoked mineralization. Calcium content of extracellular matrix was measured in smooth muscle cell monolayers after exposing them to increasing concentrations of ethanol (20 to 80 mmol/L) for 7 days. Phosphate induced calcification at concentrations of 3 mmol/L and above, whereas cells maintained in growth medium failed to accumulate calcium. As shown in Figure 9, ethanol further increased calcium accumulation, reaching significance at ≥ 60 mmol/L concentration.

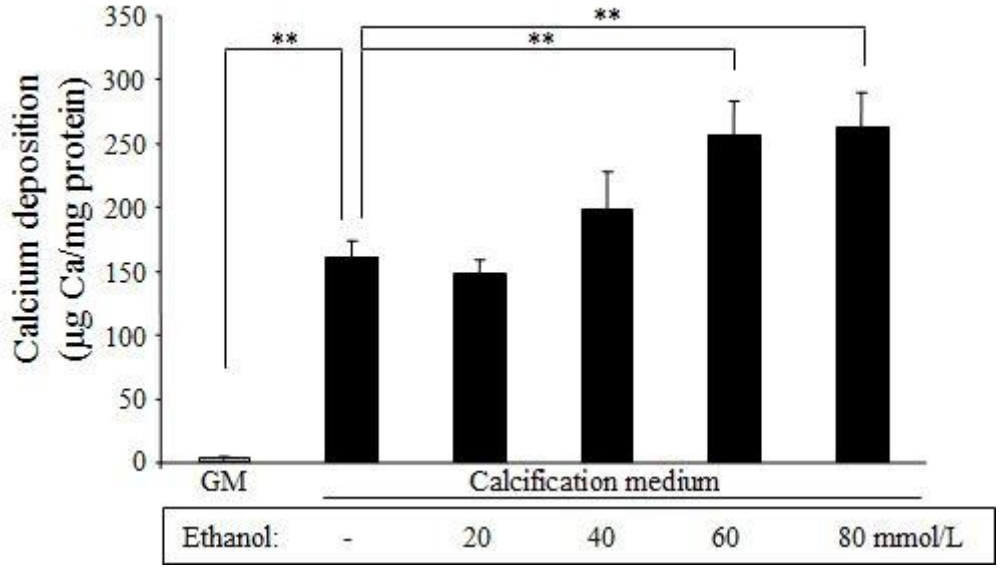

Figure 9. Dose-dependent effect of ethanol on human smooth muscle cell calcification.
In the same experiments as in Figure 6 extracellular calcium measurements were carried out using QuantiChrome Calcium Assay. Data are presented as mean ± SD of 3 independent experiments performed in duplicates. *$P < 0.05$, **$P < 0.01$.

Next we performed the time-course experiment of ethanol enhancing phosphate-provoked mineralization. Calcium content of extracellular matrix was measured in smooth muscle cell monolayers after exposing them to increasing concentrations of ethanol (20 to 80

mmol/L) for 5, 7, 10 and 12 days. Phosphate induced calcification at concentrations of 2.1 mmol/L and above, whereas cells maintained in growth medium failed to accumulate calcium. As shown in Figure 10, ethanol further increased calcium accumulation, reaching significance at ≥ 60 mmol/L concentration (only data of 60 mmol/L ethanol concentration is shown).

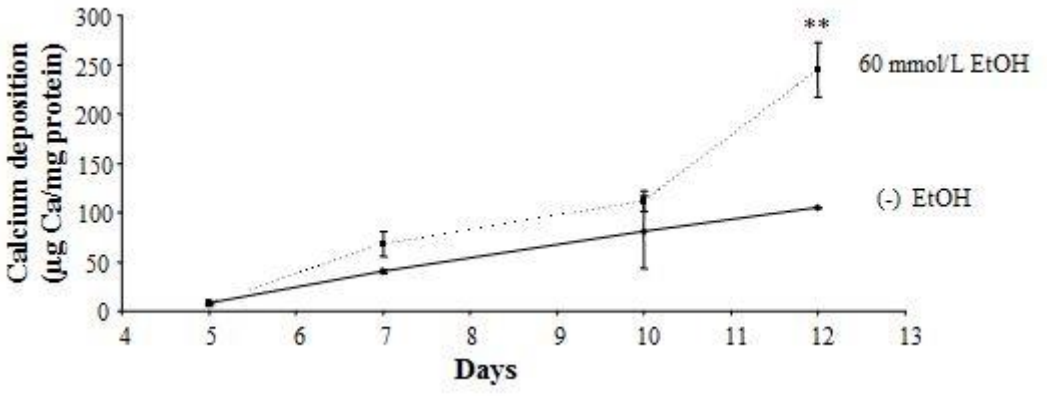

Figure 10. Time-course experiment of ethanol on human aortic smooth muscle cell calcification.

In the same experiments as in Figure 6 extracellular calcium measurements were carried out using QuantiChrome Calcium Assay. Data are presented as representative mean ± SEM of 3 independent experiments performed in duplicates. **P* < 0.05, ***P* < 0.01.

5.2. Ethanol promotes the expression of alkaline phosphatase activity in human vascular smooth muscle cells cultured in calcification medium

We sought to determine whether the enhancing effects of ethanol on calcium deposition were just limited to calcium deposition or whether this involved up-regulation of genes responsible for osteoblastic transformation of vascular smooth muscle cells. Expression of alkaline phosphatase is important in early osteogenesis. This enzyme liberates P_i for mineralization and is a characteristic feature of vascular calcification *in vivo* that parallels bone mineralization. We therefore tested whether ethanol increases alkaline phosphatase activity in human vascular smooth muscle cells. While cells maintained in medium supplemented with 3 mM P_i resulted in a 1.61-fold increase in alkaline phosphatase activity, exposure of human vascular smooth muscle cells this concentrations of P_i and 60 and 80

mmol/L of ethanol led to a significant further enhancement of 2.17- and 2.12-fold, respectively (Figure 11).

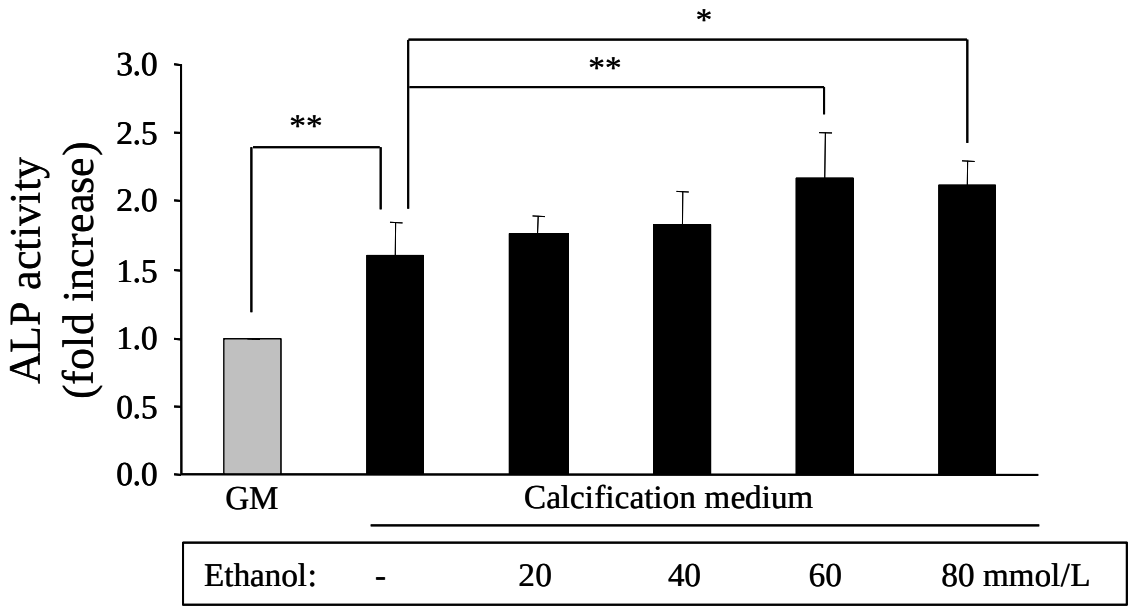

Figure 11. Ethanol enhances the expression of alkaline phosphatase activity in human vascular smooth muscle cells cultured in calcification medium.

Human vascular smooth muscle cells were cultured in GM or in calcification medium in the absence or presence of increasing concentration of ethanol for 7 days. Alkaline phosphatase activity of cells was measured as described in Methods. Data are expressed as the means ± SD of 6 independent experiments each performed in duplicate. *$P < 0.05$, **$P < 0.01$.

In contrast, ethanol failed to alter the expression of alkaline phosphatase activity in human vascular smooth muscle cells cultured in normal growth medium (Figure 12).

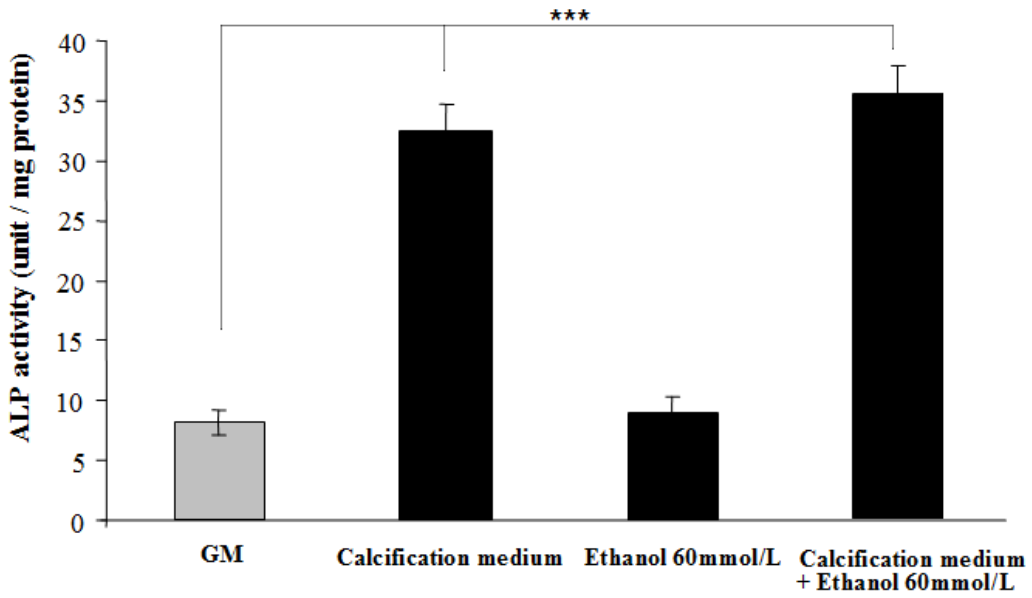

Figure 12. Prolonged (7 day) exposure of smooth muscle cells to ethanol alone does not increase alkaline phoshatase activity.

Human vascular smooth muscle cells were cultured in GM or in calcification medium in the absence or presence of 60 mmol/L of ethanol for 7 days. Alkaline phosphatase activity of cells was measured as described in Methods. Data are presented as mean ± SD of experiment of 6 parallel samples. *P < 0.05, **P < 0.01, ***P < 0.001.

5.3. Ethanol increases the synthesis of osteocalcin, a calcium binding protein in human vascular smooth muscle cells cultured in calcification medium

Osteocalcin is the major noncollagenous protein in bone matrix that regulates mineralization via binding calcium in the extracellular matrix. Accumulation of osteocalcin in vessels was shown to occur during vascular calcification in humans. Therefore we assessed the expression of osteocalcin in human vascular smooth muscle cells exposed to ethanol for 7 days (Figure 13).

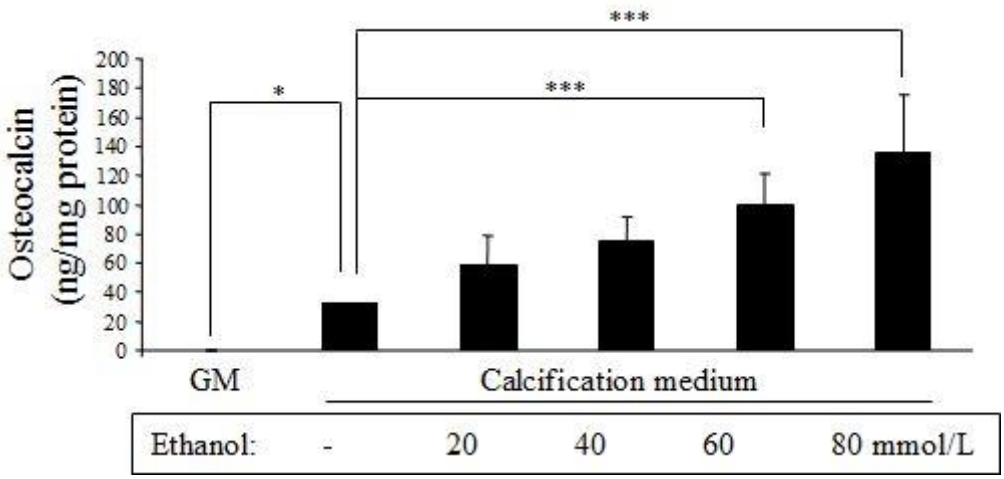

Figure 13. Ethanol increases the synthesis of osteocalcin in human vascular smooth muscle cells cultured in calcification medium.

(A) After 7 days exposure of human vascular smooth muscle cells to GM or calcification medium alone or supplemented with 20, 40, 60 and 80 mmol/L ethanol, the extracellular matrix was dissolved and osteocalcin deposition was quantified as described in Methods. Data are expressed as the means ± SEM of 3 independent experiments. **P* < 0.05, ***P* < 0.01, ****P* < 0.001.

Osteocalcin was not detectable in the solubilized extracellular matrix derived from monolayers of cells maintained in normal growth medium. As expected, the extracellular matrix of human vascular smooth muscle cells cultured in high phosphate medium exhibited a marked accumulation of osteocalcin. Importantly, exposure of cells to ethanol at concentrations of ≥60 mmol/L resulted in a more pronounced increase in osteocalcin content of extracellular matrix. In order to confirm that ethanol fosters phosphate-induced transition of human vascular smooth muscle cells into osteoblast-like cells we performed Western blot analysis for osteocalcin. As demonstrated in Figure 14, the expression of osteocalcin was higher after vascular smooth muscle cells were maintained in ethanol containing calcification medium (lane 5 and 6) compared to cells cultured in ethanol free calcification medium (lane 2).

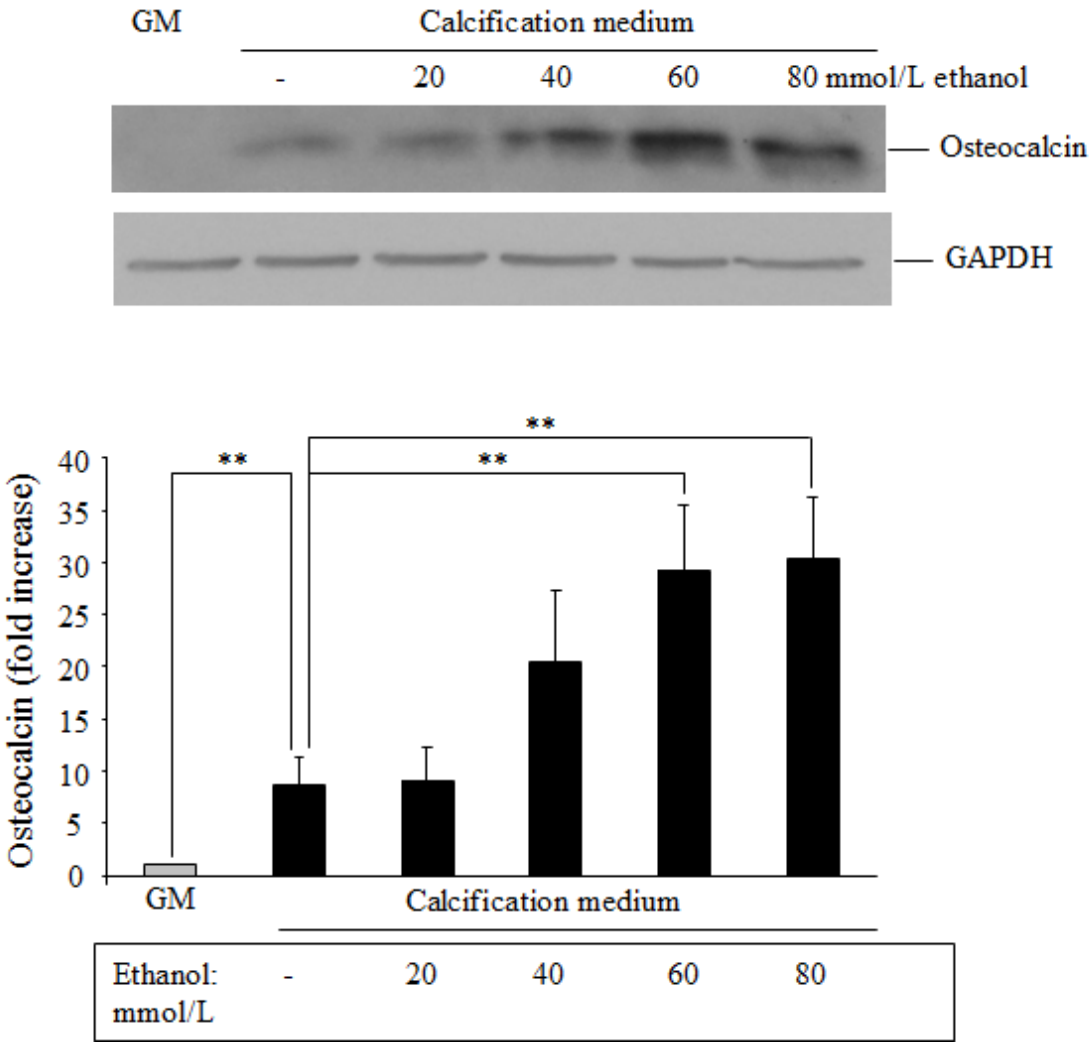

Figure 14. Ethanol increases the synthesis of osteocalcin in human vascular smooth muscle cells cultured in calcification medium.

(A) After 7 days exposure of human vascular smooth muscle cells to GM or calcification medium alone or supplemented with 20, 40, 60 and 80 mmol/L ethanol Western blot analysis was performed and densitometric measurement of the band intensities for osteocalcin and the corresponding GAPDH from cell monolayer were determined as described in Methods. Data are expressed as the means ± SD of 4 independent experiments. *$P < 0.05$, **$P < 0.01$

Treatment of vascular smooth muscle cells with ethanol in normal growth medium had no effect on osteocalcin synthesis (Figure 15).

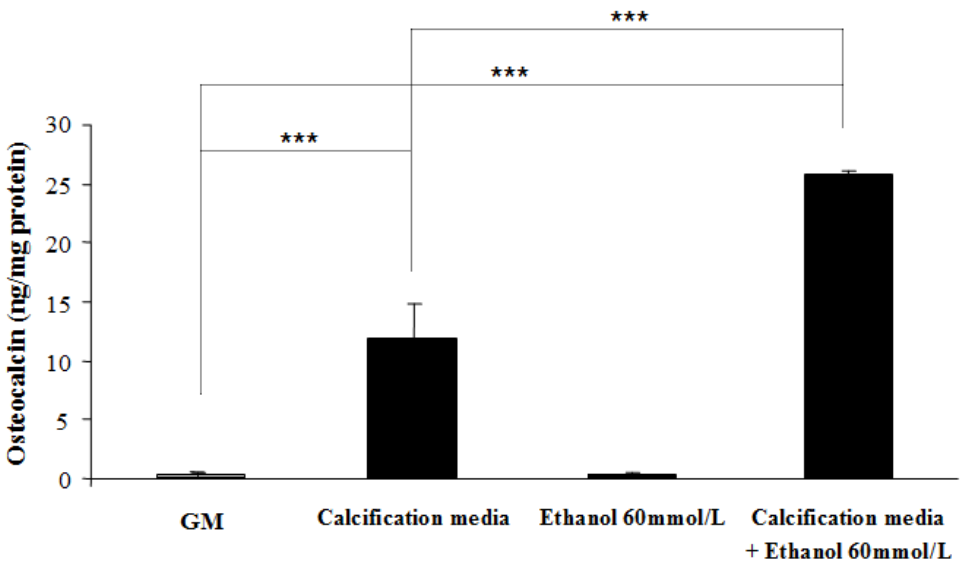

Figure 15. Exposure of ethanol for 7 days does not increase the synthesis of osteocalcin in human vascular smooth muscle cells.

After 7 days exposure of human vascular smooth muscle cells to GM or calcification medium alone or supplemented with 60 mmol/L ethanol, the extracellular matrix was dissolved and osteocalcin deposition was quantified as described in Methods. Data are expressed as the means ± SD of 2 independent experiments performed in triplicates. **P* < 0.05, ***P* < 0.01, ****P* < 0.001.

5.4. Ethanol enhances the expression of osteoblast specific transcription factor, *Cbfa-1* provoked by high inorganic phosphate

The essential regulator of osteoblast differentiation is the core binding factor alpha-1 (*Cbfa-1*), a transcription factor that controls the expression of matrix genes and, consequently, bone mineralization. Because transcription factor *Cbfa-1* has been also implicated in the transition of vascular smooth muscle cells into osteoblast-like cells provoked by high phosphate, we examined whether ethanol might affect the expression of *Cbfa-1* in human vascular smooth muscle cells cultured in calcification medium possibly providing an explanation for the phenotypic transition. As shown in Figure 16, maintaining human vascular smooth muscle cells in high phosphate containing medium for 24 hours led to a 1.62-fold increase in *Cbfa-1* mRNA level compared to cells cultured in a normal growth medium.

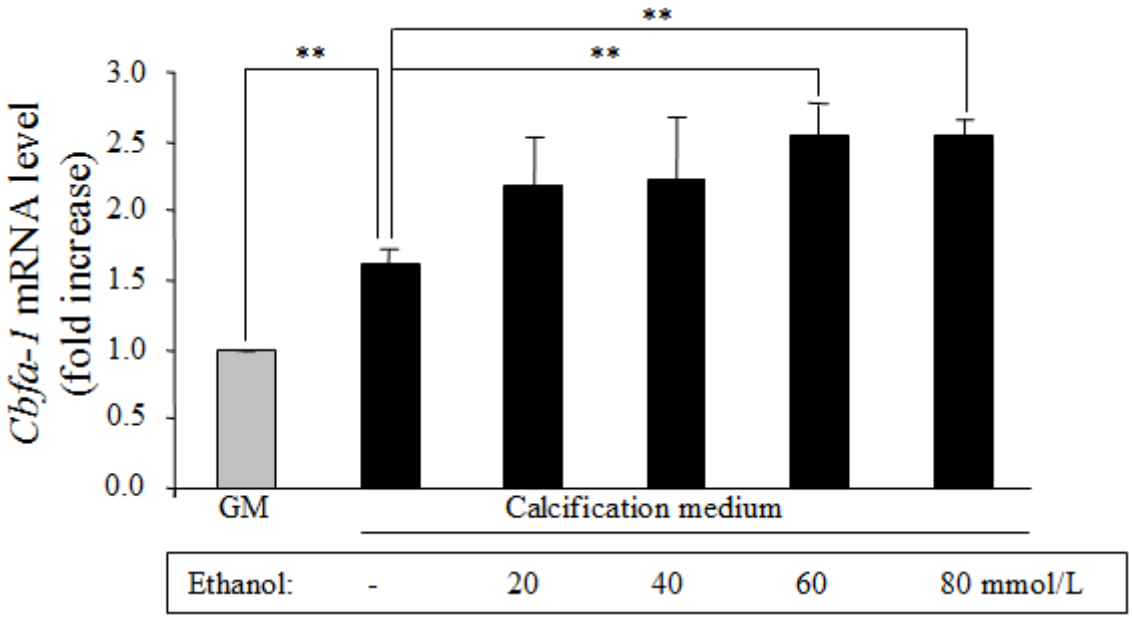

Figure 16. Ethanol enhances the expression of osteoblast specific transcription factor *Cbfa-1* in human vascular smooth muscle cells provoked by high phosphate.

Human vascular smooth muscle cells were cultured in GM or in calcification medium alone or in the presence of ethanol (20, 40, 60 and 100 mmol/L) for 24 hours. *Cbfa-1* mRNA levels were determined by quantitative RT-PCR as described in Methods. Results are presented as the mean ± SD of 3 independent experiments performed in triplicates. **P* < 0.05, ***P* < 0.01.

While ethanol in a normal growth medium failed to alter *Cbfa-1* expression (data not shown), treatment of cells with ethanol in calcification medium at concentrations of 60 mmol/L and above further enhanced the *Cbfa-1* mRNA level compared to those grown in calcification medium alone (Figure 16).

5.5. Ethanol does not alter intracellular phosphate levels in human vascular smooth muscle cells exposed to elevated extracellular phosphate concentrations

Sodium-dependent phosphate co-transporter (Pit-1) facilitates entry of P_i into vascular smooth muscle cells to render a signal for *Cbfa-1*. Because evidence suggests that vascular calcification caused by hyperphosphatemia might be mediated in part by the function of Pit-1 we investigated whether ethanol could alter intracellular phosphate levels in human vascular smooth muscle cells cultured in calcification medium which might further promote the transition of smooth muscle cells into osteoblast-like cells. After 24 hours incubation we measured the phosphate content of smooth muscle cells maintained in calcification medium in

the presence or absence of ethanol. As demonstrated in Figure 17, ethanol did not affect the intracellular phosphate levels in human vascular smooth muscle cells exposed to high extracellular phosphate concentrations.

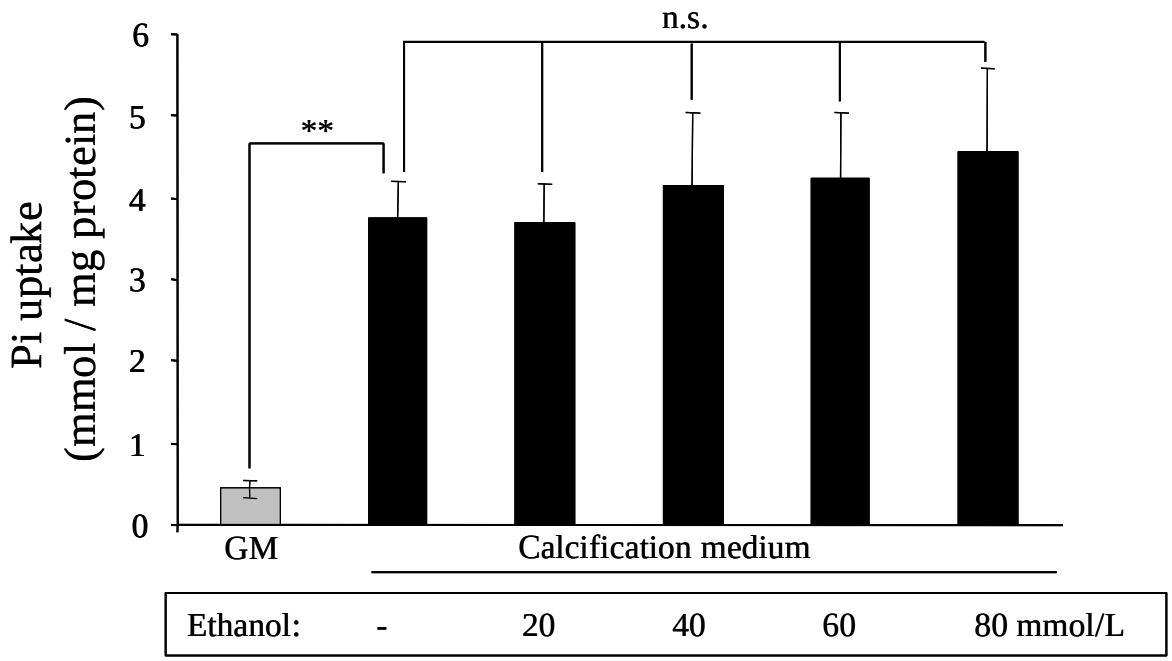

Figure 17. Ethanol does not alter phosphate entry into human vascular smooth muscle cells exposed to elevated extracellular phosphate concentrations.

Human vascular smooth muscle cells were cultured in GM or calcification medium alone or supplemented with ethanol (20, 40, 60, 80 mmol/L) for 24 hours. Cell lysate was used to measure P_i levels as described in Methods. Data are the means ± SD of 4 separate experiments in duplicates. *P < 0.05, **P < 0.01.

5.6. The effect of ethanol on the viability of human vascular smooth muscle cells in calcification medium

Studies suggest that apoptosis of vascular smooth muscle cells may contribute to calcification in vessels in atherosclerosis and medial sclerosis in patients diagnosed with chronic kidney disease. Apoptotic cells might serve as a nidus for mineralization and generation of hydroxyapatite. Hence, by performing MTT assay we assessed the viability of cells challenged with ethanol in calcification medium. As demonstrated in Figure 18, the viability of human vascular smooth muscle cells cultured in calcification medium for 7 days dropped significantly only at 80 mmol/L. Importantly, vascular

smooth muscle cells challenged with 20 to 60 mmol/L of ethanol in a calcification medium for 7 days did not exhibit a decline in cell viability.

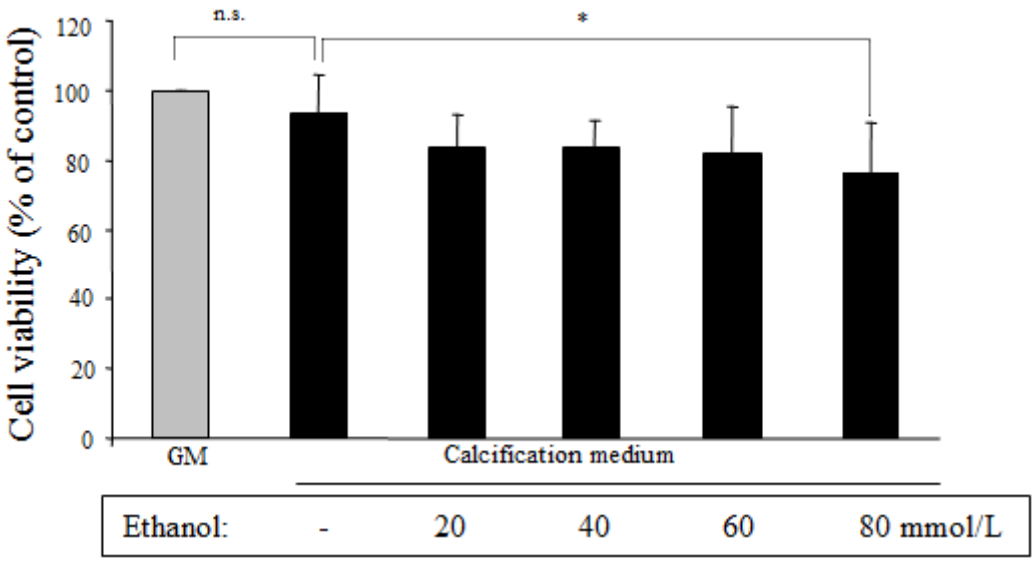

Figure 18. Effect of ethanol on the viability of human vascular smooth muscle cells in calcification medium.

Human vascular smooth muscle cells were cultured in GM or calcification medium alone or supplemented with ethanol (20, 40, 60, 80 mmol/L) for 7 days. To determine whether ethanol causes toxicity MTT assay was performed. Data are the means ± SD of 4 separate experiments in duplicates. *$P < 0.05$.

5.7. Alcohol dehydrogenase 1 is not expressed in human vascular smooth muscle cells

Ethanol is catabolized by alcohol dehydrogenase 1 in hepatocytes, producing acetaldehyde. If this was also to occur in vascular smooth muscle cells, acetaldehyde might be a contributing factor to mineralization and osteoblastic phenotype transition. We therefore measured the expression of alcohol dehydrogenase 1 in human vascular smooth muscle cells using Western blot analysis. As shown in Figure 19, there was a marked protein expression in a human-derived hepatoma cell line (HepG2 cells, used as positive control).

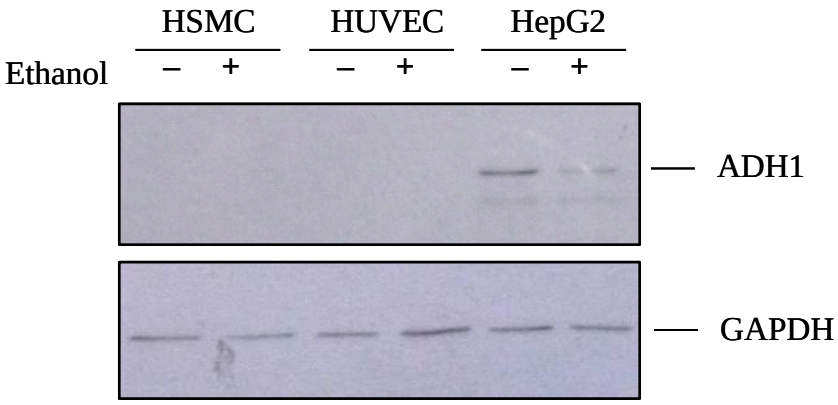

Figure 19. Alcohol dehydrogenase 1 is not detectable in human vascular smooth muscle cells.

After 7 days exposure of human vascular smooth muscle cells, HUVEC (as negative control) and HepG2 (positive control) cells to medium alone or medium supplemented with 60 mmol/L ethanol, Western blot analysis was performed for alcohol dehydrogenase 1 (ADH1). Membranes were reprobed for GAPDH as described in Methods.

As previously reported, human umbilical vein endothelial cells lack alcohol dehydrogenase 1 (used as negative control) and we found no expression of this enzyme whether the HUVECs were exposed to ethanol or not. Similar to human endothelium, alcohol dehydrogenase 1 was not detectable by Western blot analysis in human vascular smooth muscle cells.

5.8. Ethanol increases ROS production during calcification of smooth muscle cells

We hypothesized that ethanol treatment increases ROS production in smooth muscle cells in the presence of calcification medium promoting the mineralization. Therefore we examined the ROS production of cultured smooth muscle cells in calcification medium. We used 80 mmol/L ethanol concentration in our investigation system with growth or calcification medium in the presence or absence of ethanol for 2 days, followed by CM-H_2DCFDA treatment for 30 min in the dark. The change in fluorescence intensity was measured at 488 nm, as excitation and 530 nm, as emission wavelengths. We found that ethanol alone doesn't enhance ROS production in growth medium, but when cells were challenged with ethanol in calcification medium ROS production was fostered (Figure 20).

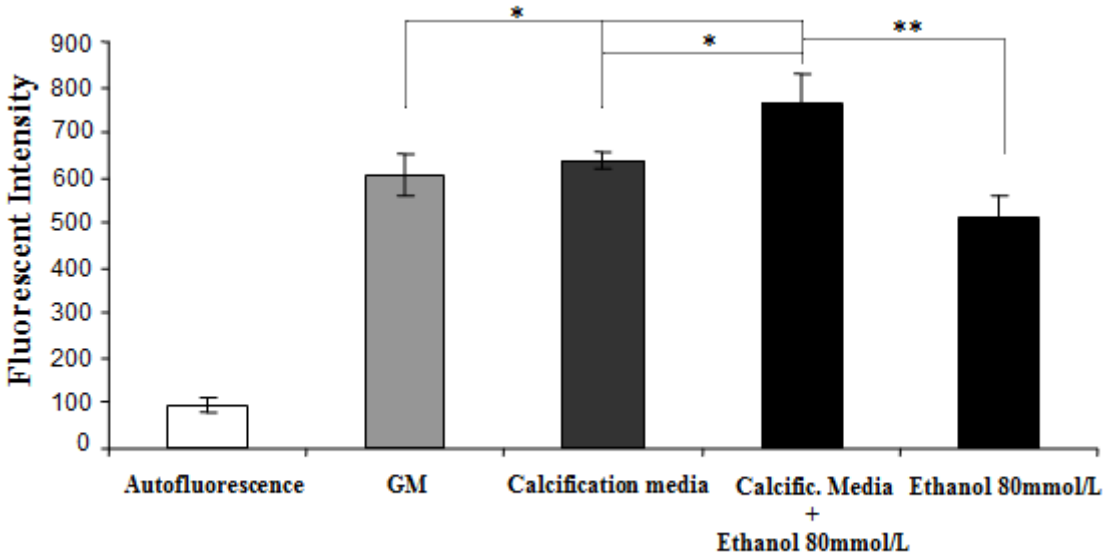

Figure 20. Ethanol increases ROS production during calcification of smooth muscle cells

ROS production was determined by measuring the change in fluorescence intensity of 5-chloromethyl-2,7-dichlorodihydrofluorescein diacetate (CM-H_2DCFDA) converting to the fluorescent DCF.

Cells were seeded in 96-well plates then treated with growth or calcification medium in the presence or absence of ethanol for 2 days. Next 10 μM CM-H_2DCFDA in HBSS was added to the cells for 30 min in the dark. The change in fluorescence intensity was measured in HBSS by BioTek Synergy 4 Fluorometer with 488 nm, as excitation and 530 nm, as emission wavelengths. Data are presented as mean ± SEM of representative of 3 independent experiments performed in quadriplicates. *$P < 0.05$, **$P < 0.01$.

5.9. Quasi-congenic nature of the B6.C and B6.I RQI strains

Since the harmful effect of ethanol on arteries strongly depends upon its concentration that reflects the extent of alcohol consumption and heavy episodic drinking that might possess common genetic background of several genes, our interest was to expand genome mapping from 5 chromosomes (1, 2, 3, 9 and 15) to all autosomal chromosomes. Genome-wide genotyping resulted in a more precise estimate of the donor genome content of each strain. The average donor genome content in RQI strains varied as a function of the number of backcross-intercross cycles, and the BALB/cJ genome content of the donor strain. B6.Cb_4i_5, B6.Cb_5i_7-α, B6.Cb_5i_7-β, B6.Ib_5i_7-α, and B6.Ib_5i_7-β strains had 4.4±1.3%, 2.3±1.6%, 2.4±1.5%, 1.4±1.4%, and 0.99±0.86% of the BALB/cJ genome, respectively. The B6.Cb_4i_5 (13 strains), B6.Cb_5i_7 (47 strains), and B6.Ib_5i_7 (39 strains) mice contained 32.5%, 43.12%, and 20.11% of

the BALB/cJ genome, respectively (RQIgbase, release November 20, 2004, www.RQIgenetics.org). 107 RQI strains of RQIgbase carried more than half of the BALB/cJ genome (65.34% of all microsatellite markers have been observed as BALB/ cJ-type alleles). B6.Ib$_5$i$_7$ mice contained about half as many CC markers as B6.Cb$_5$i$_7$ mice since the CXBI donor strain, being a recombinant inbred (RI) strain with C57BL/6ByJ and BALB/cByJ progenitors, is carried only 50% of the BALB/cByJ genome. The present study demonstrates that in the CXBI strain 39.95% of the microsatellite markers contained BALB/cJ genotype. The small genomic difference between BALB/cJ and its subline BALB/cByJ could be responsible for the lower proportion of CC markers in CXBI and its B6.I-type descendants.

5.10. Genetic variation in oral alcohol self-administration in quasi-congenic B6.Cb$_5$i$_7$ and B6.Ib$_5$i$_7$ RQI strain sets and their progenitors

The new and combined ethanol consumption for RQI strains and for the progenitors is shown in Table 1. Descriptive statistics for strain sets is presented in Table 2. New data (strain means for 59 strains) was found to be highly significant correlation with old data (Pearson $r=0.73$ $p<0.001$, two-tailed). Alcohol consumption among the progenitors were significantly different ($F_{2,312}=369.65$, $p<0.001$). Pairwise comparisons with Bonferroni adjustments revealed differences (B6 vs. BALB/cJ, $p<0.001$; B6 vs. CXBI (aka CXB-5/ByJ), $p<0.001$; BALB/cJ vs. CXBI, $p=0.001$). Our data are in accordance with previous reports namely BALB/cJ and CXBI are alcohol avoiding strains, while C57BL/6ByJ exhibits remarkable oral alcohol self-administration [63, 78, 96]. Across RQI strains genetic (between-strain) variation of alcohol consumption was highly significant for both the B6.Cb$_5$i$_7$ ($F_{42,969}=5.59$, $p<0.001$) and B6.Ib$_5$i$_7$ ($F_{34,729}=7.37$, $p<0.001$) inbred strain sets. Two-bottle choice test data for B6.Cb$_4$i$_5$ mice were previously analyzed as alcohol preference phenotype [80]. In order to establish better comparability, these data were recalculated as alcohol consumption ($g \cdot BW_{kg}^{-1} \cdot day^{-1}$) (Tables 1-2).

Table 1. Alcohol consumption ($g \cdot BW_{kg}^{-1} \cdot day^{-1}$) in B6.C and B6.I quasi-congenic RQI strains

	Published*			New			Combined		
STRAIN	Mean	SD	N	Mean	SD	N	Mean	SD	N
B6	7.82 ±	3.7	85	9.84 ±	3.33	33	8.39	3.7	118
C	0.12 ±	0.2	75	0.09 ±	0.05	20	0.1	0.1	95
C5A1	8.02 ±	4.1	16	6.52 ±	2.83	4	7.72 ±	3.90	20
C5A12	9.8 ±	3.2	18	6.96 ±	6.90	2	9.11 ±	3.91	21
C5A13	5.78 ±	3.6	17				5.78 ±	3.6	17

C5A15	5.2 ± 2 19		5.2 ± 2 19
C5A16	4.51 ± 2.8 13	4.08 ± 2.91 10	4.32 ± 2.79 23
C5A17	5.68 ± 2.9 17	4.32 ± 1.15 3	5.48 ± 2.71 20
C5A18	5.59 ± 4 17	4.92 ± 0.32 3	5.49 ± 3.66 20
C5A19	6.11 ± 3.8 14	3.87 ± 2.76 9	5.24 ± 3.53 23
C5A24	7.21 ± 3.8 11	6.84 ± 3.06 8	7.06 ± 3.44 19
C5A26	6.51 ± 3.6 16	5.88 ± 2.98 5	6.36 ± 3.50 21
C5A26A		4.99 ± 3.37 20	4.99 ± 3.37 20
C5A3	2.89 ± 3 20	2.25 ± 2.39 20	2.57 ± 2.71 40
C5A32	8.7 ± 4.6 20		8.70 ± 4.58 20
C5A32A	7.54 ± 3.4 17	4.34 ± 1.28 4	6.93 ± 3.32 21
C5A34	5.74 ± 4.7 17	5.54 ± 2.29 3	5.71 ± 4.35 20
C5A35	6.02 ± 3 21	5.19 ± 2.48 2	5.95 ± 2.94 23
C5A3A		4.21 ± 3.22 20	4.21 ± 3.22 20
C5A4	7.91 ± 3.5 14	8.99 ± 3.93 11	8.39 ± 3.66 25
C5A5	7.11 ± 3.9 23		7.11 ± 3.87 23
C5A6	7.89 ± 3.8 17	9.77 ± 3.48 4	8.25 ± 3.75 21
C5A7	9.78 ± 4.4 17	9.75 ± 1.36 3	9.77 ± 4.07 20
C5A8	9.27 ± 3.7 24		9.27 ± 3.72 24
C5A9	6.73 ± 4.4 11	4.91 ± 3.46 20	5.55 ± 3.86 31
C5B1	5.88 ± 2.4 16	8.19 ± 2.15 10	6.77 ± 2.58 26
C5B10	8.93 ± 3.4 13	7.45 ± 3.56 9	8.33 ± 3.45 22
C5B12	7.21 ± 4.1 20		7.21 ± 4.08 20
C5B13	7.37 ± 3.6 17	5.90 ± 4.08 3	7.15 ± 3.61 20
C5B15	3.95 ± 2.5 20		3.95 ± 2.50 20
C5B16	5.4 ± 4.4 20		5.40 ± 4.36 20
C5B19	5 ± 2.7 15	4.78 ± 3.14 7	4.93 ± 2.74 22
C5B19A		8.95 ± 4.25 6	8.95 ± 4.25 6
C5B2	3.98 ± 2.3 18	3.31 ± 2.09 2	3.92 ± 2.25 20
C5B20	8.42 ± 3.8 18	7.46 ± 1.29 2	8.32 ± 3.58 20
C5B23	4.88 ± 3.7 24		4.88 ± 3.66 24
C5B25	5.2 ± 3.1 16	3.72 ± 1.76 6	4.79 ± 2.84 22
C5B26	8.11 ± 3 20		8.11 ± 2.95 20
C5B27	5.62 ± 2.7 24		5.62 ± 2.72 24
C5B28	8.89 ± 3.8 17		8.89 ± 3.8 17
C5B3	2.7 ± 1.7 14	2.73 ± 2.00 26	2.72 ± 2.11 40
C5B30	6.51 ± 3.7 16	6.44 ± 2.40 4	6.50 ± 3.41 20
C5B31	7.79 ± 3.6 17	4.73 ± 4.92 4	7.20 ± 3.90 21
C5B33	6.83 ± 3.2 14	5.78 ± 3.58 10	6.39 ± 3.35 24
C5B34	8.2 ± 4.2 17	6.80 ± 1.72 3	7.99 ± 3.95 20
C5B4	8.96 ± 4.8 12	7.23 ± 4.05 10	8.17 ± 4.45 22
C5B5	5.25 ± 3 18	6.99 ± 3.47 5	5.63 ± 3.14 23
C5B5A		6.14 ± 3.63 14	6.14 ± 3.63 14
C5B6	8.5 ± 3.6 16	6.43 ± 4.73 6	7.94 ± 3.93 22
C5B9	4.49 ± 3.5 8	3.37 ± 2.39 15	3.76 ± 2.80 23
I	1.2 ± 1.3 74	0.9 ± 1 20	1.1 ± 1.3 94
I5A10	5.59 ± 4.4 13		5.59 ± 4.4 13
I5A11	5.21 ± 3.7 24		5.21 ± 3.65 24
I5A12	7.24 ± 2.2 16	5.67 ± 1.90 4	6.93 ± 2.18 20
I5A14	8.63 ± 3.4 10	7.30 ± 3.11 10	7.96 ± 3.26 20
I5A15	8.61 ± 3.4 22		8.61 ± 3.39 22
I5A16	6.47 ± 3.5 16	7.18 ± 2.65 5	6.64 ± 3.60 21
I5A16at	7.2 ± 3.9 24		7.20 ± 3.90 24
I5A19	4.93 ± 3 17	6.33 ± 2.24 3	5.14 ± 2.88 20
I5A22	7.31 ± 2.6 18	5.81 ± 1.54 4	7.04 ± 2.47 22

I5A23	5.33 ± 3.94 26	5.33 ± 3.94 26	
I5A25	4.85 ± 2.5 20	4.85 ± 2.53 20	
I5A26A	6.22 ± 2.9 15	8.24 ± 3.01 9	6.98 ± 3.04 24
I5A27	8.09 ± 3.9 20	8.09 ± 3.87 20	
I5A31	5.23 ± 2.2 17	6.02 ± 3.21 17	
I5A33	7.68 ± 4.7 16	5.50 ± 2.94 6	7.09 ± 4.34 22
I5A4	5.33 ± 3.3 21	5.33 ± 3.29 21	
I5A4G	6.03 ± 3.62 16	6.03 ± 3.62 16	
I5A5	6.44 ± 2.5 11	5.26 ± 2.47 9	5.91 ± 2.47 20
I5A8	7.28 ± 2.4 17	3.81 ± 1.47 3	6.76 ± 2.62 20
I5A9	6.39 ± 3.1 17	4.72 ± 1.15 5	6.01 ± 2.82 22
I5B1	5.93 ± 4.1 16	3.60 ± 2.27 6	5.29 ± 3.76 22
I5B11	4.88 ± 2.9 17	7.14 ± 2.14 4	5.31 ± 2.87 21
I5B12	5.12 ± 3.5 22	5.12 ± 3.50 22	
I5B14	4.01 ± 1.8 17	5.90 ± 3.59 3	4.29 ± 2.12 20
I5B15	5.77 ± 2.9 13	4.14 ± 2.77 11	5.02 ± 2.54 24
I5B16	7.56 ± 4.4 20	5.97 ± 5.03 3	7.35 ± 4.42 23
I5B19	7.05 ± 3.7 13	6.57 ± 1.82 3	6.96 ± 3.36 16
I5B1A	6.89 ± 3.8 17	3.60 ± 2.32 3	6.40 ± 3.77 20
I5B22	9.16 ± 2.8 24	9.16 ± 2.82 24	
I5B23	6.83 ± 3.8 19	5.82 ± . 1	6.78 ± 3.70 20
I5B24	5.54 ± 3.5 17	6.84 ± 2.35 3	5.73 ± 3.35 20
I5B25	9.43 ± 3.38 20	9.43 ± 3.38 20	
I5B25A	11.89 ± 2.3 22	9.63 ± 3.18 18	10.87 ± 2.94 40
I5B27	5.11 ± 2.5 16	2.53 ± 1.62 4	4.59 ± 2.55 20
I5B31	9.07 ± 3.5 21	9.07 ± 3.50 21	
I5B33	6.1 ± 3.2 16	8.20 ± 2.56 4	6.52 ± 3.18 20
I5B34	4.59 ± 2.8 20	4.59 ± 2.78 20	
I5B6	9.47 ± 3.2 16	7.59 ± 5.95 6	8.96 ± 4.07 22
I5B7A	7.18 ± 2.9 17	8.09 ± 2.13 4	7.36 ± 2.73 21
C4A10**	4.37 ± 3.46 28		
C4A11**	4.12 ± 3.29 34		
C4A12**	7.13 ± 3.40 30		
C4A12A**	5.94 ± 3.29 24		
C4A13**	4.26 ± 3.20 22		
C4A4**	6.55 ± 4.12 23		
C4A6**	8.04 ± 4.23 26		
C4A8**	6.70 ± 3.51 28		
C4B10**	6.04 ± 3.93 26		
C4B13**	9.75 ± 4.93 23		
C4B13C**	11.93 ± 4.20 29		
C4B14**	12.56 ± 3.10 23		
C4B4A**	7.50 ± 4.92 21		
C4B9**	7.47 ± 3.66 36		
Total	1620	553	

*Alcohol (12% v/v) consumption data for RQI strains of the b_5i_7 series were reported in Vadasz et al., 2000b.
All b_5i_7 series data are based on three 3-day trials.
New and Combined data represent alcohol (12% v/v) consumption data for RQI strains of the b_5i_7 series averaged over three 3-day trials.
**Alcohol (12% v/v) preference data for RQI strains of the b_4i_5 series were reported in Vadasz et al., 2000a.
Here the same data are converted to alcohol consumption ($g \cdot BW_{kg}^{-1} \cdot day^{-1}$, based on two 3-day trials).

Table 2. Descriptive statistics for consumption of 12% (v/v) alcohol solution ($g \cdot BW_{kg}^{-1} \cdot day^{-1}$) averaged over two (B6.C introgression type, b_4i_5 series) or three (B6.C and B6.I introgression types, b_5i_7 series) alcohol preference test trials in quasi-congenic RQI strain populations derived from B6, C, and I

Population	n	Trait	Minimum	Maximum	Mean	Background	Donor	LSD 0.05	Eta-squared
RQI B6.C b4i5^	12	AC34GKD	4.12	12.56	7.16	7.82	0.12	2.18	0.32
RQI B6.C b5i7^^	43	AC345GKD	2.57	9.77	6.46	8.39	0.1	2.1	0.2
RQI B6.I b5i7^^	35	AC345GKD	4.29	10.87	6.51	8.39	1.1	1.98	0.26

Background: B6; Donors: C (for B6.C) and I (for B6.I); LSD: Least significant difference at the 0.05 probability level for the strain population.
The eta-squared statistic describes the proportion of total variability attributable to genotype (strain).
n: number of RQI strains
^Based on published data, Vadasz 2000a
^^Based on combined (published and new) data, see Table 1.

5.11. QTL mapping

Data of Composite Interval Mapping are shown in Table 3. QTLs are designated as *Eac1-6* (ethanol consumption 1-6). CIM with 43 B6.Cb_5i_7 RQI strains gave significant peaks on chr. 6 at 36.5 cM ($p<0.001$), 42.5 cM ($p<0.001$) 62.2 cM ($p<0.01$), and 73.5 cM ($p<0.001$), and on chr. 12 at 51 cM ($p<0.01$). Peaks were also found on chrs. 1, 5, 15, although these peaks did not reach the significant level. Only data on the chr. 15 peak are shown, since this QTL was included in the MIM model. In the B6.Ib_5i_7 set of 35 RQI strains two QTLs reached the significant level at LOD=2.0 (chr. 12: 21 cM, and chr. 19: 38 cM), but not at empirical threshold determined by 1000 permutations. CIM found several other nonsignificant peaks on chrs. 1, 3, 4, 12, 13, and 16 with LOD<2. Since this QTL was included in the MIM model only data for the chr. 12 peak are presented. In all QTLs indicated in Table 3 the B6 alleles enhanced alcohol consumption. CIM detected several QTLs where the donor allele was associated with increaser effect, but none of these reached the significant level as determined empirically by 1000 permutations. Markers next to the QTL peak were identified, and the number of strains containing the donor allele in homozygous condition were counted. As shown in Table 3 donor genome contribution (Q%) was evaluated for each carrier-strain.

Table 3. QTLs detected by CIM for alcohol consumption in RQI strains

Trait	Population	Chr.	Peak Position (cM)	LOD Score	Additive effect	R^2	Significance*	N	Q%±SD	Locus
AC345GKD	B6.Cb5i7	6	36.51	3.60	1.63	0.20	p<0.001	4	4.9±4.16	*Eac1*
AC345GKD	B6.Cb5i7	6	42.51	3.11	2.09	0.18	p<0.001	2	7.89	*Eac2*
AC345GKD	B6.Cb5i7	6	62.21	2.09	1.88	0.18	p<0.01	1	9.3	*Eac3*
AC345GKD	B6.Cb5i7	6	73.51	3.28	1.91	0.19	p<0.001	2	6.44	*Eac4*
AC345GKD	B6.Cb5i7	12	51.01	2.94	1.15	0.16	p<0.01	5	3.22±1.05	*Eac5*
AC345GKD	B6.Ib5i7	12	21.01	2.36	1.05	0.13	p<0.2	4	1.86±1.2	*Eac6*

*Empirical threshold determined by 1000 permutations
$R^{2:}$ Coefficient of genetic determination
N: Number of strains which carry the donor allele of the marker closest to the peak
Q%: Average of donor genome contribution in carrier strains $Q\%=N_{CC}/(N_{CC}+N_{BB})*100$
Eac: Ethyl alcohol consumption

Analysis of B6.Cb_5i_7 RQI strains with MIM employing the BIC-M0 relative criterion of QTL Cartographer, resulted in a model of three QTLs on chrs. 6, 12, and 15 (genetic R^2=0.47). According to tests for epistasis found no significant additive-additive interactions. MIM with the B6.Ib_5i_7 set of strains resulted in a model of three QTLs positioned on chrs. 8, 12, and 4 (genetic R^2=0.5). Similarly to B6.Cb_5i_7 strains, no epistatic effect was found in the B6.Ib_5i_7 set. Testing the MIM identified QTLs demonstrating that all QTLs were significant. Data of MIM are shown in Table 4.

Table 4. Estimates of QTL positions and effects by MIM for alcohol consumption

Population	Type	Chr.	Position	LOD	Effect	Effect (%)	Vp	Vg	Vr	R^2
B6.Cb$_5$i$_7$	A	6	43.5001	1.58	2.1052	23.5				
B6.Cb$_5$i$_7$	A	12	51.1001	1.24	1.1705	13.4				
B6.Cb$_5$i$_7$	A	15	35.2001	0.73	1.5099	10.4				
B6.Cb$_5$i$_7$							4.154	1.965	2.189	0.473
B6.Ib$_5$i$_7$	A	8	0.1001	1.25	-2.6021	22.7				
B6.Ib$_5$i$_7$	A	12	21.1001	1.16	1.2178	17.1				
B6.Ib$_5$i$_7$	A	4	64.2001	0.79	0.8175	10.4				
B6.Ib$_5$i$_7$							3.783	1.902	1.88	0.503

Positive effect indicates that the B6 allele increases mean alcohol consumption values.
R^2: coefficient of determination
A: additive
Vp: phenotypic variance
Vg: genetic variance
Vr: residual variance

CIM data (Table 3) and range of peaks were evaluated with comparison of microsatellite marker genotype patterns across quasi-congenic RQI strains. In the 43 B6.Cb$_5$i$_7$ RQI strains validity of QTLs on chrs. 1, 5, 6, 12, and 15 were judged. The nonsignificant chr. 1 QTL (7.5 cM) was excluded since it was associated with D1Mit167, which also mapped to chr. 5 and chr. 14. As in our earlier studies demonstrated, in the RQI strains D1Mit167 does not co-segregate with chr. 1 markers, however it does with proximal markers of chr. 5 (Saito et al., 2003). The nonsignificant chr. 5 QTL (59.01 cM) showed small negative additive effect (-1.29) in the B6.Cb$_5$i$_7$ population, therefore it was also excluded from further examination. As demonstrated in Table 5 QTLs on chrs. 6, 15, and 12 were retained for bioinformatic analysis. In the 35 B6.Ib$_5$i$_7$ RQI strains only QTLs on chrs. 12 and 19 were further studied ($p<0.2$). The chr. 12 QTL was retained for further evaluation since the donor allele of the peak marker was present in several strains (N=4) and the average donor genome content of these strains was low (1.86%), approaching congenic conditions (Table 5). The chr. 19 QTL was excluded from further consideration because no donor allele was found near the peak position in any of the strains, and the gap between the two markers flanking the peak was relatively large (7 cM).

Table 5. Some candidate genes and QTLs potentially relevant for alcohol consumption

Population	Locus name	Chr.	RQI Peak (cM)	RQI Donor Block Range^ (cM)	Candidates and QTLs	Description
B6.Cb$_5$i$_7$	*Eac1*	6	36.51	33.5-48.2	*Eila2* (36.5) QTL	ethanol induced
locomotor activity 2		[97]				
					Rear1 (36.5) QTL	rearing 1
					Bits2 (37) QTL	bitterness
sensitivity 2	[99]					
					D6Mit178 (38.5) Peak Marker	alcohol
preference	[72]					
					Vlrb2 (37)	vomeronasal 1,
receptor B2 (21 receptors in region)						
					Slc6a6 (38.2)	solute carrier
family 6 (neurotransmitter transporter, taurine), member 6						
					Taste5 (48.1) QTL	taste-saccharin
preference 5	[100]					
					Lrrtm1,4, (syntenic)	leucine rich
repeat transmembrane neuronal 1,4						
					Gpr73, 175, 27 (syntenic)	G protein-
coupled receptor 73, 175, 27						
					Lrrn1 (syntenic)	leucine rich
repeat protein 1, neuronal						
					Grm7 (syntenic)	glutamate
receptor, metabotropic 7						
					Grip2 (syntenic)	glutamate
receptor interacting protein 2						
					Chchd4 (syntenic)	coiled-coil-
helix-coiled-coil-helix domain containing 4						
B6.Cb$_5$i$_7$	*Eac2*	6	42.51	33.5-48.2	same as *Eac1*	
B6.Cb$_5$i$_7$	*Eac3*	6	62.21	(46-65.5)*	*Taste5* (48.1) QTL	taste-saccharin
preference 5	[100]					
					Camk1(48.7)	
	calcium/calmodulin-dependent protein kinase I					
					Taste8 (49.5) QTL	taste bitterness
sensitivity 8	[101]					
					Qui (50.5) QTL	quinine
sensitivity, taste	[102]					
					Aaj3 (52.5) QTL	anxiety in A/J 3
					Gnb3 (60.19)	guanine
nucleotide binding protein, beta 3						
					Tas2r104-7, 130 (62)	taste receptor,
type 2	[104]					
					Taste9 (63) QTL	taste bitterness
sensitivity 9	[101]					
					Btts (63.3) QTL	bitterness tasting
					Mop1 (63.3) QTL	morphine
preference 1	[105]					
					Soa (63.4) QTL	sucrose
octaacetate aversion (bitter taste locus)	[106]					
					Tas2r102,115,120, etc. (63.5)	taste receptor,
type 2	[104]					
					Etohcta6 (63.6) QTL	ethanol
conditioned taste aversion 6	[100]					
					Grin2b (64.5)	glutamate
receptor, ionotropic, NMDA2B (epsilon 2)						
B6.Cb$_5$i$_7$	*Eac4*	6	73.51	74 (SM)**	*Kcnj8* (70.0)	potassium
inwardly-rectifying channel, subfamily J, member 8						
B6.Cb$_5$i$_7$	*Eac5*	12	51.01	46-58	*Marq4* (47) QTL	
	methamphetamine response QTL 4			[107]		
					Calm1 (syntenic)	calmodulin 1
B6.Cb$_5$i$_7$		15	32.41	30.6-34.2	*Marq5* (29) QTL	
	methamphetamine response QTL 5			[107]		
					Dpm1 (32.5)	dopamine loss
B6.Ib$_5$i$_7$	*Eac6*	12	21.01	(16-29)*	*D12Mit37* (1) Peak Marker	alcohol
consumption	[72]					
					Rear2 (16) QTL	rearing 2
					Cocia 1 (23) QTL	cocaine induced
activation	[109]					
					Drb5 (25) QTL	dopamine
receptor binding 5	[110]					

				Aaq2 (27) QTL	alcohol
acceptance QTL 2, female specific		[111]			
				Prkchs-rs1 (29)	protein kinase
C, eta, related sequence 1					
				Stxbp6 (syntenic)	syntaxin binding
protein 6 (amisyn)					
B6.Ib$_5$i$_7$	4	64.20	57.6-77.5	*Stx12* (60)	syntaxin 12;
alcohol preference QTG	[66]				
				Oprd1 (64.8)	opioid receptor,
delta 1					
				Htr6 (64.9)	5-
hydroxytryptamine (serotonin) receptor 6					
				Htr1d (66)	5-
hydroxytryptamine (serotonin) receptor 1D					
B6.Ib$_5$i$_7$	8	0.10	1 (SM)**	*Adcy3* (syntenic)	adenylate
cyclase 3					

^Range considering all RQI strains (proximal and distal marker positions of donor segments, cM)
*Peak fell between identified donor segments in all strains. Proximal and distal limits of donor segments are shown.
**Single Marker

5.12. Alcohol consumption in a congenic strain

Using microsatellite marker-assisted selection and repeated backcrosses to the alcohol-preferring B6By background strain, we developed a new congenic strain, B6By.C.6.132.54 (B6By.C6). This congenic strain carries a BALB/cJ (C) donor chromosome segment on chr. 6 with proximal and distal background markers D6Mit275 (25.5 cM, 51.1 Mb, from UniSTS annotation of NCBI build 36) and D6Mit134 (57.5 cM, 125.3 Mb), respectively. The congenic strain in a two-bottle free-choice alcohol preference test demonstrated significantly lower consumption of 12% (v/v) alcohol in comparison to its background partner B6By, conforming a significant decreasing effect of the genetic factor(s) residing on the donor segment (Figure 21).

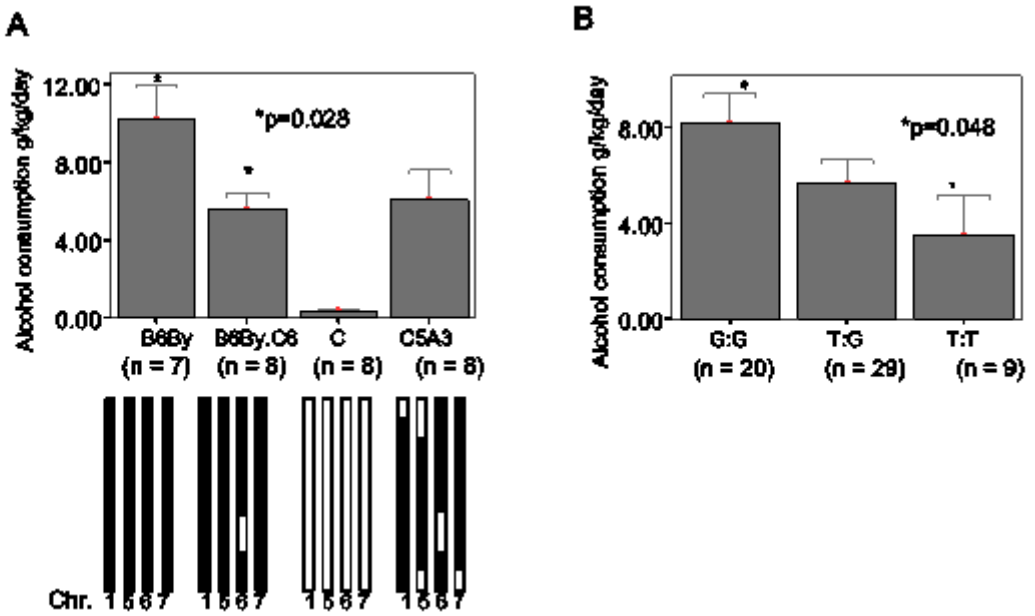

Figure 21. Alcohol consumption in inbred congenic mice and segregating quasi-congenic population. (A) Alcohol consumption (g/kg/day; mean±1 SE) and chromosome composition in C57BL/6ByJ (background strain, black chromosomes), BALB/cJ (donor strain, white chromosomes), C5A3 (quasi-congenic RQI strain carrying donor chromosome segments), and B6By.C.6.132.54, a congenic strain derived from C5A3). Only chromosomes 1, 5, 6, and 7 are shown because these were the only chromosomes that harbored differential donor segments in C5A3. In a preplanned comparison, alcohol consumption among the congenic B6By.C6 mice was significantly lower than that in the background C57BL/6ByJ ($F_{1,13}=6.21$, $p=0.028$). (B) SNP allelic effects on oral alcohol self-administration in a selectively genotyped reciprocal F2 population derived from respectively alcohol-preferring and alcohol-nonpreferring inbred strains I5B25A and C5B3. I5B25A and C5B3 are independently derived quasi-congenic strains on the B6By background. C5B3 carries a BALB/cJ-derived chromosome segment that overlaps with the Chr. 6 segments of C5A3 and B6.C6 (see details under Methods in the supporting information). F2 individuals with the G:G (B6By/B6By) genotype consumed significantly more alcohol than mice with the T:T (BALB/cJ/BALB/cJ) genotype (independent samples *t* test, $t_{27}=2.1$, $p=0.048$). SNP rs3723352 (Chr. 6: 111.318602 Mb; NCBI build 36) is in intron7 of *Grm7*. G:G has been detected in alcohol-preferring C57BL/6J and C57BL/6ByJ strains, while T:T has been detected in alcohol-nonpreferring BALB/cJ, BALB/cByJ, DBA/2J, and A/J (http://www.jax.org/phenome).

In an additional independent test, using a two-bottle free choice paradigm with intermittent access to alcohol, we found that consumption of 12% alcohol was significantly higher among B6By males (12.70±1.03, n=13) in comparison with B6By.C6 males [8.37±0.96 (g/kg/day, mean±SE), n=19, average of four 3-day trials, $t_{30}=3.00$, $p=0.005$, two-

tailed]. To test the hypothesis that other undetected chromosome segments are responsible for this effect, a genome scan with a mouse single-nucleotide polymorfism (SNP) panel of 402 markers was carried out. No additional donor segments were detected (Figure 22).

Because the genome scan showed flanking background markers at 75.9 Mb (rs4226008; NCBI mouse build 36/db SNP build 126) and 122.3 Mb (rs3023093), and limiting donor markers at 81.8 (rs4226024) and at 91.8 Mb (rs3712161), we concluded the segment size must be between 9.9 and 46.4 Mb.

An integrated genome and transcriptome analysis of the *Eac2* region on chr.6 suggests that a gene coding for metabotropic glutamate receptor subtype-7 (*Grm7*) is a candidate QTG for *Eac2*.

With the help of exclusion of identical-by-descent (IBD) regions we could reduce the number of candidate genes on the maximum segment length (46.4 Mb) to 212 genes. With analysis of structural polymorphism we found genes harboring a total of nine coding-nonsynonymous SNPs (CNs) in a non-IBD region, and two CNs in IBD regions. But the known function of these genes do not suggest the links to alcohol drinking preference or addiction. In the following step we searched for cis-regulated genes and found 7 which had genome-wide statistically significant LOD scores. The polymorphism of these genes was also determined. Next we had to find the gene expression differences in congenic and background strains and performed multistrain analysis to show the genotype - alcohol consumption correlation followed by GO annotation. The analysis of *Grm7* with promoter analysis the PromoterInspector program predicted 13 promoters and two regulated regions. MatInspector program detected a transcription factor binding site (TFBS) above a good match threshold: Sox5. The C57BL/6J carries the C allele showed lower transcript abundance of *Grm7* than strains with the T allele. The confirmatory analysis of cis-regulation of *Grm7* and linkage in reciprocal F2 populations also proved this finding.

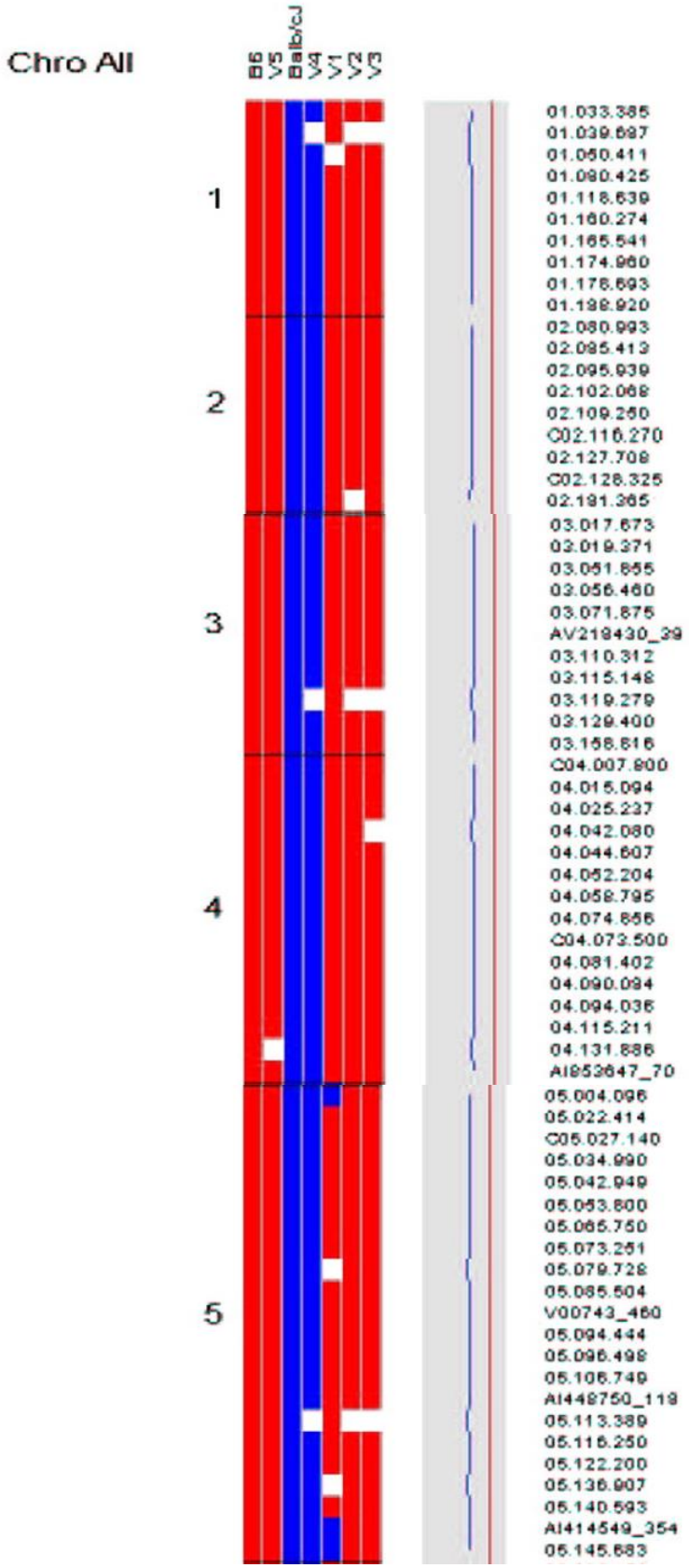
Chro All
B6
V5
Balb/cJ
V4
V1
V2
V3
1
2
3
4
5
01.033.385
01.039.697
01.050.411
01.090.425
01.118.639
01.160.274
01.165.541
01.174.960
01.176.693
01.198.920
02.080.993
02.085.413
02.095.939
02.102.068
02.109.250
C02.116.270
02.127.709
C02.128.325
02.191.365
03.017.673
03.019.371
03.051.855
03.056.460
03.071.875
AV219430_39
03.110.312
03.115.148
03.119.279
03.129.400
03.156.816
C04.007.900
04.015.094
04.025.237
04.042.080
04.044.607
04.052.204
04.058.795
04.074.856
C04.073.500
04.081.402
04.090.094
04.094.036
04.115.211
04.131.886
AI853647_70
05.004.096
05.022.414
C05.027.140
05.034.990
05.042.949
05.053.800
05.065.750
05.073.251
05.079.728
05.085.504
V00743_460
05.094.444
05.096.498
05.106.749
AI449750_119
05.113.389
05.116.250
05.122.200
05.136.907
05.140.593
AI414549_354
05.145.683

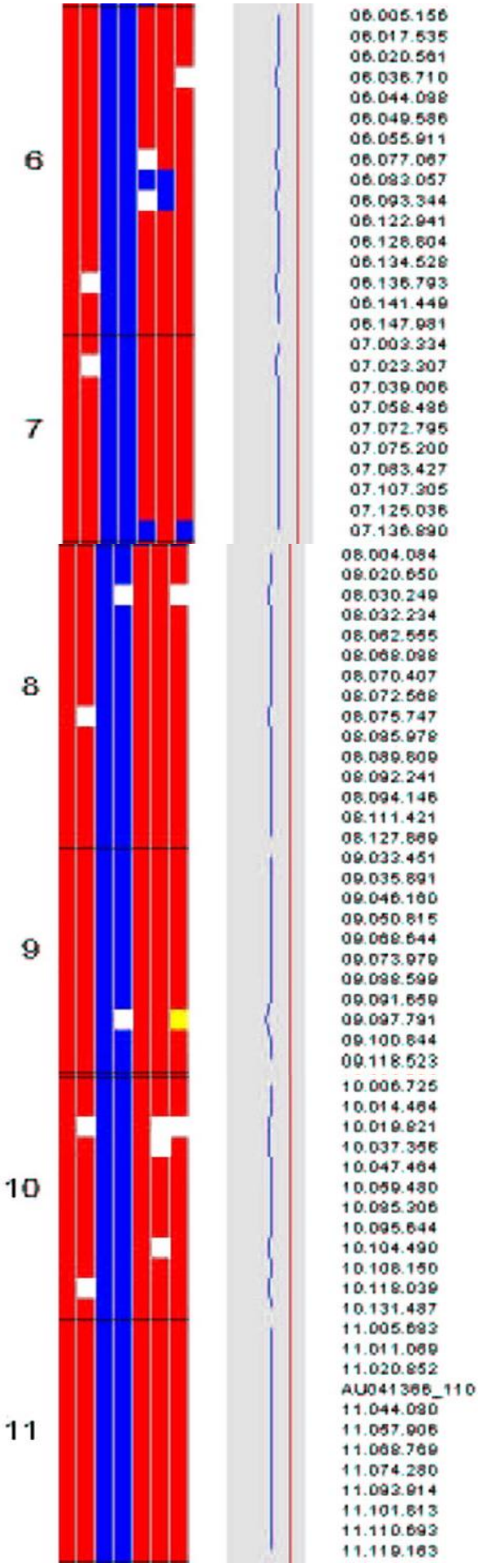
6
7
8
9
10
11
06.005.156
06.017.535
06.020.561
06.036.710
06.044.098
06.049.586
06.055.911
06.077.067
06.083.057
06.093.344
06.122.941
06.126.804
06.134.528
06.136.793
06.141.449
06.147.981
07.003.334
07.023.307
07.039.006
07.058.486
07.072.795
07.075.200
07.083.427
07.107.305
07.125.036
07.136.890
08.004.084
08.020.650
08.030.249
08.032.234
08.062.555
08.068.098
08.070.407
08.072.568
08.075.747
08.095.979
08.089.609
08.092.241
08.094.146
08.111.421
08.127.869
09.033.451
09.035.691
09.046.160
09.050.615
09.068.644
09.073.979
09.088.599
09.091.659
09.097.791
09.100.844
09.118.523
10.006.725
10.014.464
10.019.921
10.037.356
10.047.464
10.059.480
10.095.306
10.095.644
10.104.490
10.108.150
10.118.039
10.131.487
11.005.693
11.011.069
11.020.652
AU041366_110
11.044.090
11.057.906
11.068.769
11.074.280
11.092.914
11.101.613
11.110.693
11.119.163

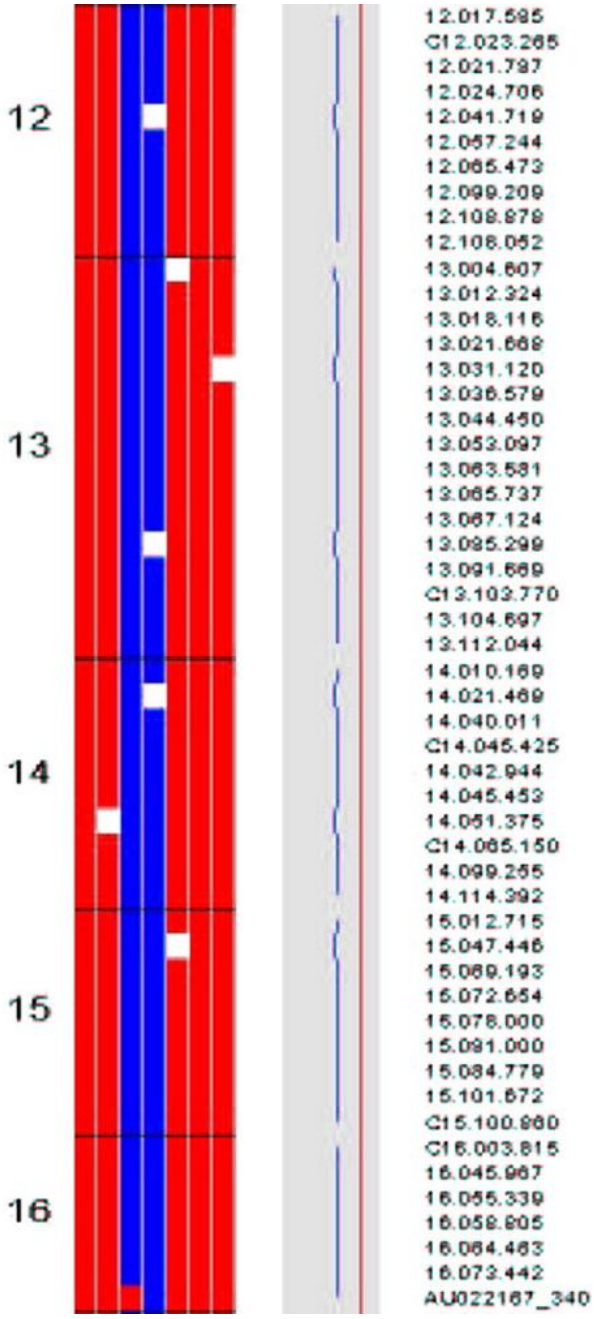
12
13
14
15
16
12.017.595
C12.023.265
12.021.797
12.024.706
12.041.719
12.057.244
12.065.473
12.099.209
12.108.879
12.108.052
13.004.607
13.012.324
13.018.116
13.021.668
13.031.120
13.036.579
13.044.450
13.053.097
13.063.581
13.065.737
13.067.124
13.085.299
13.091.669
C13.103.770
13.104.697
13.112.044
14.010.169
14.021.469
14.040.011
C14.045.425
14.042.944
14.045.453
14.051.375
C14.065.150
14.099.255
14.114.392
15.012.715
15.047.446
15.069.193
15.072.654
15.078.000
15.091.000
15.094.779
15.101.672
C15.100.960
C16.003.815
16.045.967
16.055.339
16.059.805
16.064.463
16.073.442
AU022167_340

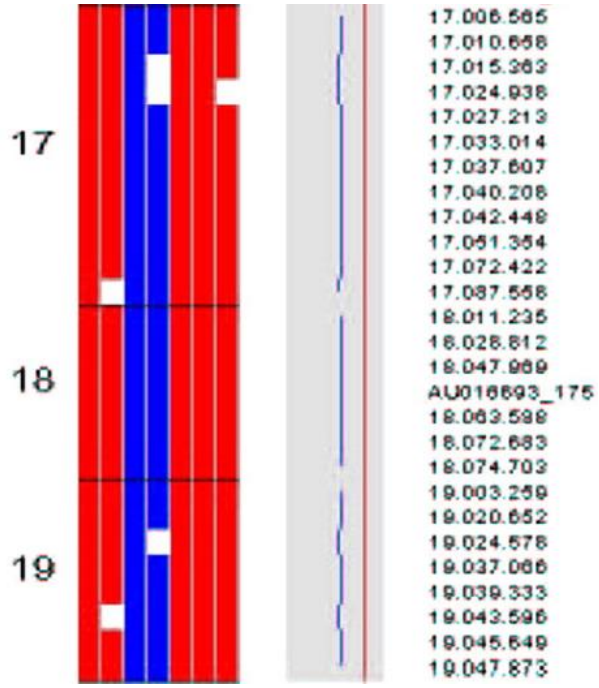

Figure 22. Results of a genome-wide SNP scan for testing the congenic status of B6.C6. Columns represent strains. Red and blue represent B6 and C alleles, yellow indicates heterozygotes. From left: B6 (Harvard Reference sample), V5 = B6By (Our test sample), BALB/cJ (Harvard Reference sample), V4 = BALB/cJ (Our test sample), V1 = C5A3 (Our quasi-congenic test sample), V2 = B6.C.6.132.54 (B6.C6; Our congenic test sample), V3 = B6.C.7.259 (B6.C7; Our congenic control test sample).

6. DISCUSSION

Mineralization in soft tissues occurs under pathological conditions and has detrimental consequences, particularly when it occurs within vascular walls and heart valves. Calcification develops in two main sites within arteries and medium-sized arterial walls. Intima calcification occurs in atherosclerosis and its progression parallels the growth of plaque. Arterial dysfunction results from narrowing of the arterial lumen leading to ischemia of tissues and organs. Plaque instability and infarction develop in coronary and cerebrovascular arteries as well as in the peripheral vasculature. The pathologic consequences are caused by instability of atherosclerotic plaques and the rupture of atheromatous lesions. This results from mechanical discontinuity between the inclusion of rigid material (calcium crystals) into distensible material (lipid core) resulting in plaque vulnerability and rupture. In contrast, in stable atherosclerotic lesions of type IVb the calcified plaque narrows the arterial lumen in a chronic way leading to ischemia [112-113].

Medial calcification is characterized by diffuse mineral accumulation within the smooth muscle cell layers of the arterial wall. While medial calcification is commonly observed in the elderly population, it is significantly more pronounced in disease states in the general population in patients diagnosed with metabolic disorders, such as the metabolic syndrome, diabetes or chronic kidney disease. Mineralization of the media is concentric, not extending into the intima and therefore the arterial lumen diameter is not affected. This mechanism represents the main cause of arterial stiffness (hardening of artery wall) [114]. The basic consequences of arterial stiffening are an altered arterial pressure wave (characterized by increased systolic and decreased diastolic pressures, leading to high pulse pressure) and enhanced aortic impedance [115] providing a substantial afterload for the heart and thereby promoting cardiovascular morbidity and mortality.

Calciphylaxis is a well defined but poorly understood disease with high morbidity and mortality (60–80%) for which there are no effective therapies [116]. In calciphylaxis the small and medium sized arterioles are calcified by diffuse mineralization within the smooth muscle cell layers of vessels. It almost exclusively develops in patients with chronic kidney disease [27]. Calcification of small vessels is associated with tissue ischemia, severe pain, infarction and ultimately secondary infection with high risk of septic death. It is still not clear, however, whether calcium acts as a primary trigger. As it was originally revealed by Selye et al. [28] in 1961, there is a two-step anaphylaxis-like process wherein there is an initial sensitization (e.g.

with phosphate, vitamin D, or parathyroid hormone) and then a systemic (e.g. glucocorticoids) or local (e.g. trauma) challenge that initiates dystrophic calcification.

Epidemiologic studies pointed to a dichotomous association between alcohol consumption and cardiovascular disease. Studies from several countries have revealed that light to moderate alcohol consumption is associated with reduced risk of multiple cardiovascular outcomes especially within the Mediterranean areas. But it remains to be established what levels of consumption are beneficial and whether drinking patterns alter the benefit. The current consensus is that moderate consumption of alcohol in the general population is associated with the lowest risk for cardiovascular disease morbidity and mortality compared to individuals who do not drink. [2-3]. For example, consuming up to 2 drinks a day is a negative risk factor for atheromatous diseases and the risk for myocardial infarction and ischemic stroke [117]. On the contrary, heavy episodic drinking - defined by 5 or more drinks a day - was shown to increase morbidity and mortality from cardiovascular disease [7-8]. Although it has been confirmed that moderate alcohol use has an apparent protective effect on the development of coronary heart disease [118-120], a recent study found no evidence of such a protective association of alcohol consumption and calcification of vessels [4]. What is more, the latter group reported firm evidence that heavy alcohol consumption, in particular hard liquors, is associated with greater calcification in coronary arteries. This finding has also been confirmed by Kim W. et al. demonstrating that intracoronary administration of ethanol provokes vascular calcification [61].

Moreover, alcohol consumption was found to dramatically increase the risk of calciphylaxis in individuals who have normal renal function and calcium-phosphate metabolism. Severe calcification, diffuse mineralization of small and medium sized vessels were reported to develop in patients diagnosed with alcoholic liver disease [9-11]. Calciphylaxis was also described in alcoholic cardiomyopathy in patients who did not have no liver and kidney disease nor any alteration in calcium-phosphate metabolism [12].

These studies prompted us to investigate whether ethanol promotes vascular smooth muscle cell mineralization and transition of smooth muscle cells into osteoblast like cells *in vitro*. Since phosphate levels have long been recognized to strongly correlate with vascular calcification both in patients with chronic kidney disease particularly above the physiological range [121-123] and in healthy individuals whose phosphate concentration is within the physiological range and have no sign of altered renal function and mineral metabolism [38]. We therefore employed elevations in exogenous phosphate to induce mineralization in our model. Evidence suggests that elevated phosphate can induce smooth muscle cell

calcification, as well as an osteochondrogenic phenotypic change *in vitro* [41]. Previous studies indicated a highly regulated cellular process where many different inducers and inhibitors of osteoblast differentiation have been recognized [124]. In such *in vitro* model vascular smooth muscle cells undergo mineralization, but also manifest upregulation of osteoblast markers [31, 42, 47]. These include *Cbfa-1*, the key regulatory transcription factor critical for differentiation of osteoblasts, and expression of downstream proteins such as alkaline phosphatase, a crucial enzyme in the context of bone and teeth formation, and osteocalcin, which is a very specific protein indicative of osteoblast activity. *Cbfa-1* knockout mice were reported to fail to form mineralized bone [46] and exhibit low alkaline phosphatase activity and osteocalcin expression.

Importantly, in our studies, exposure of cells to ethanol in calcification medium enhanced mineralization of the extracellular matrix of human vascular smooth muscle cells in a dose-response manner. Phosphate-induced calcification was further augmented providing significant additional extracellular calcium and phosphate deposition at concentrations of 60 mmol/L or above. Such concentrations can be found in heavy drinkers' blood. Since alkaline phosphatase is an important enzyme in the mineralization process and osteocalcin, a non-collagenous calcium binding protein, is specific for osteoblast phenotype, we also examined whether ethanol increases alkaline phosphatase activity and synthesis of osteocalcin in vascular smooth muscle cells. Ethanol caused a significant increase in the expression of alkaline phosphatase and osteocalcin. Furthermore, in cells challenged with ethanol the expression of *Cbfa-1*, a transcription factor involved in the regulation of osteoblastic transformation of smooth muscle cells, was also elevated.

Osteoblastic differentiation induced by hyperphosphatemia is mediated via a sodium-dependent co-transporter Pit-1 that facilitates entry of phosphate into vascular cells [42]. Therefore, we measured phosphate uptake. Our results demonstrate that the observed effects of ethanol are not due to alterations of phosphate uptake.

There are *in vitro* studies suggesting that apoptosis of human vascular smooth muscle cells can contribute to calcification of vessels. Apoptosis was reported to occur both in the intima of advanced lesions and in the media of arteries in chronic kidney disease. In fact, alcohol-induced apoptosis of vascular smooth muscle cells was recently demonstrated [125]. Apoptotic smooth muscle cells might act as a nidus for calcification, and thereby actively concentrate both calcium and phosphate to generate hydroxyapatite [126-128]. In our study we did not observe any decline in the viability of smooth muscle cells challenged with ethanol

up to 60 mmol/L concentration. Thus, apoptosis was not involved in the augmented mineralization provoked by ethanol.

Ethanol is catabolized mainly by the action of alcohol dehydrogenase 1 resulting in the generation of acetaldehyde in the liver. If acetaldehyde were produced by alcohol dehydrogenase 1 in smooth muscle cells, it might be a possible contributing factor to the mineralization in our model. Hence we measured the expression of alcohol dehydrogenase 1 in vascular smooth muscle cells by Western blot. Alcohol dehydrogenase 1 was not detectable in human vascular smooth muscle cells indicating that acetaldehyde did not promote the mineralization induced by ethanol. In our studies 3 mmol/L P_i or 60 mmol/L ethanol alone did not enhance ROS production in vascular smooth muscle cells. In contrast, in smooth muscle cells exposed to ethanol in the presence of P_i ROS production was significantly enhanced.

In an elegant study by Giachelli's group, osteoblastic differentiation of vascular smooth muscle cells was shown to be reversible [129]. They demonstrated that vascular cells with osteochondrogenic phenotype regain smooth muscle cell properties and downregulate osteochondrogenic gene expression in an environment that favors vascular smooth muscle cells. *Runx2/Cbfa-1* was found to be a decisive factor in the smooth muscle cell reprogramming. Thus, it remains possible that the enhanced mineralization of vascular smooth muscle cells provoked by ethanol might be reversible.

Our results strongly suggest that mineralization of human vascular smooth muscle cells and their transition into osteoblast-like cells induced by ethanol may contribute to the augmented vascular calcification observed in heavy alcohol consumption. It also offers an alternative mechanism by which calciphylaxis develops in heavy drinkers without kidney diseases or alterations in calcium-phosphate metabolism. This study may have relevance in chronic kidney diseases in which high alcohol consumption might promote vascular calcification.

The association of heavy alcohol consumption, alcoholism with hard liquor use, and arterial calcification prompted us to study the genetic background that might be connected to vascular diseases. Metabotropic glutamate receptor type 7 gene was shown to serve a promising candidate that might be implicated in altered alcohol preference. In the central nervous system, the excitatory amino acid glutamate serves as a potent neurotransmitter exerting its effects via various membrane glutamate receptors. Nerves containing glutamate located close to bone cells exhibit functional glutamate receptor. It was revealed that glutamate stimulates bone resorption *in vitro* via a mechanically sensitive glutamate/aspartate

transporter protein suggesting a function for glutamate in mechanical load and bone remodeling [62].

Alcoholism has been shown to be a complex disorder determined not only by genetic background of several genes, but also influenced via environmental factors. Mapping strategies provide ways to appoint the genes involved in alcoholism. For mapping the genes related to alcoholism we employed Quantitative Trait Loci (QTL) mapping of 43 B6.C and 35 B6.I quasi-congenic RQI mouse strains of the b_5i_7 series. During the congenic breeding we introgress BALB/cJ and CXBI/ByJ transgenes or targeted gene disruptions into C57BL/6ByJ genetic background. In these strains less than 3% of the donor genome was shown to be present on C57BL/6ByJ background. The B6.C genome carries BALB/cJ donor genes, while the B6.I strains carry CXBI/ByJ donor genes. C57BL/6ByJ, BALB/cJ and CXBI/ByJ animals exhibit different drinking behavior. Namely, BALB/cJ and CXBI/ByJ strains consume less alcohol compared to C57BL/6ByJ. We take advantage such a difference during our experiments. Here in this work we identified 6 *Eac* loci that play a role in alcohol preference and drinking behavior, one cis-regulated candidate gene of alcoholism, *Grm7*.

Study of marker haplotypes of B6.Cb_5i_7 strains showed that the minimum range for *Eac1* and *Eac2* across strains was identical, 33.5-48.2 cM. Since we used a limited number of markers, and the range was defined by the position of the donor marker alleles at the proximal and distal endings of the segments, the real sizes of the segments are not determined. According to the MGI database (NCBI build 34) at http://www.informatics.jax.org for relevant QTLs in this range *Eila2*, *Rear1*, *Bits2*, and *Taste5* are present ([97, 99-100]; see Table 5). Gill and Boyle [72] reported significant correlation between D6Mit178 and alcohol preference in a region containing A/J donor alleles on B6 background between 26.35 and 38.5 cM, although no chr.6 QTLs were found for alcohol preference in AcB RC and in the reciprocal AXB/BXA RI strains [72]. The region between the centromer and 33.5 cM contains Neuropeptide Y (*Npy*, 26 cM) and Ethanol induced locomotion 3 (*Etlm3*, 30 cM) suggesting to be as candidate gene and QTL for their QTL region of 26.35-38.5 cM [72]. In the RQI strains these candidates fell on a relatively large non-genotyped interval between the proximal donor allele (33.5 cM) and the flanking proximal background allele (25.5 cM) of our candidate region, therefore their involvement cannot be excluded.

The 33.5-48.2 cM region is also rich in candidate genes. Employing bioinformatic tools, such as the Genome-Phenome Superbrain computational system (GPS; http://omicspace.riken.jp/gps/full.jsp), genes above located in the interval were assessed.

Syntenic vomeronasal receptor genes are potential candidates since olfaction may influence alcohol preference. Other genes may also influence neurotransmission (Table 5). Importantly, the region contains *Grm7*, the metabotropic glutamate receptor type 7 gene. Since disturbances in glutamate function have been implicated in the pathophysiology of behavioral disorders, which may underlie some types of addiction (e.g., [130]), *Grm7* is a promising candidate to be studied.

In the range of *Eac3* (chr.6, 46-65.6 cM) additional important QTLs are located ([102-103, 105]; Table 5.). *Qui* coincides with the taste receptor, type 2 (*Tas2r*) on distal chromosome 6. Haplotypes at *Tas2r* locus vary with quinine taste sensitivity, C57BL/6 mice were shown to be quinine sensitive, while DBA/2J mice were quinine insensitive [131]. Haplotype variation suggests that BALB/cJ mice may carry *Tas2r* alleles associated with quinine insensitivity. *Taste8* and *Taste9* were mapped to 49.5 cM and 63 cM, respectively, suggesting a common polygenic basis for quinine and PROP avoidance in mice [101]. Ethanol conditioned taste aversion 6 [*Etohcta6* (63.6)] was found close to *Taste9* [100]. As Table 5 shows, within an approximately 1 cM region (63-64 cM) we can find three bitterness related loci, Tas2r taste receptor gene members, and an ethanol conditioned taste aversion locus. The accumulation of taste-related QTLs and taste receptor type 2 on a short chromosome region is tempting to hypothesize that *Eac3* detected effects of variations in members of *Tas2r*. *Eac5* on chr. 12 spans an interval of minimum 12 cM (46-58 cM) and has a peak at 51.01 cM. Gill and Boyle [72] described a QTL for alcohol intake on chr. 12 at 1.0 cM (range: 1.0-5.0 cM) which does not overlap the range of *Eac5*. *Marq4*, the locomotor stimulant effect of another psychostimulant (methamphetamine), was recently mapped to 47 cM on mouse Chromosome 12 which falls in the range of *Eac5* [107]. *Eac6*, a suggestive QTL which did not reach the significance threshold ($p<0.05$) by permutation, was mapped to 21 cM (6-29 cM) on chr. 12 in the B6.I set of strains. It is unlikely that the range of *Eac6* overlaps the range of the alcohol consumption QTL detected by Gill and Boyle [72] on chr. 12. Psychophysiological processes involved in exploratory behavior (*Rear2*, [98]), cocaine induced activation (*Cocia 1*, [109]), dopamine receptor binding (*Drb5*, [110], and alcohol acceptance (*Aaq2*, [111]) may be relevant to choice-based alcohol consumption (Table 5). Syntaxin binding protein 6 is involved in synaptic vesicle-mediated transport.

Similarly to *Stxbp1*, a candidate for an ethanol preference drinking locus on mouse chromosome 2 [68], *Stxbp6* may be a candidate gene for *Eac6*. Interestingly, MIM identified a locus on chr. 4 (64.2 cM), which was found near *Stx12* (60 cM), a potential contributor to ethanol preference in mice [66-67], and about 20 cM from *Ap3q* [73, 132-133]. Although his

locus is a weaker candidate for confirmation studies, because it was not significant in CIM after permutation ($p>0.2$). MIM data supported the CIM results, inasmuch the best model included chr. 6 and chr. 12 QTLs in addition to other QTLs.

Composite and multiple interval mapping of the whole genome of B6.C and B6.I sets of quasi-congenic RQI strains detected different sets of QTLs for alcohol consumption. This is not surprising, because the donor strains were different. BALB/cJ and CXBI provided donor material for B6.C and B6.I, respectively. BALB/cJ and CXBI strains are related because CXBI is one of the CXB recombinant inbred strains. CXBI is expected to carry about 50% BALB/cByJ and 50% C57BL/6By genome on the average. Another differentiating factor is directional selection, which was employed in the development of the B6.C and B6.I strain populations. B6.C mice were developed by five backcross-intercross cycles with 13 generations of concomitant selection for high expression of a brain dopamine-system related trait (mesencephalic tyrosine hydroxylase activity), while B6.I mice were subjected to the same gene introgression manipulation, but selected for extreme low expression of the same phenotype [84, 90, 134]. Therefore, selection pressure in the opposite directions favored the transfer of different sets of donor genes onto the B6 background. Transfer of alcohol preference- and consumption-related genes could be expected either because the mesotelencephalic dopamine system plays a critical role in addiction and alcohol selfadministration, or because both donor strains show very low alcohol preference in comparison to the background strain [63, 78, 96], and passenger genes for alcohol-related behaviors could be fixed in the RQI strains.

Recombinant QTL Introgression strain system, identified *Eac2* as a Quantitative Trait Locus (QTL) on mouse chromosome 6 which explained 18% of the variance with an effect size of 2.09g/kg/day alcohol consumption, and *Grm7* as a quantitative trait gene underlying *Eac2* (Neurochem Res, Genomics). *Grm7* knockout mice express increased alcohol consumption [135]. Sub-congenic, and congenic mice carrying a *Grm7* variant characterized by higher *Grm7* mRNA, drink less alcohol and show a tendency for higher circadian dark phase motor activity in a wheel running paradigm, respectively, and there are significant genetic differences in *Grm7* mRNA abundance in the mouse brain between congenic and the background mice identifying brain areas whose function is implicated in addiction related processes [136].

mGluR7-specific agonist AMN082 inhibited cocaine selfadministration, and reverse dialysis studies demonstrated that group III agonist L-AP4, possibly acting on mGluR7,

decreased *in vivo* extracellular glutamate in the nucleus accumbens by inhibiting nonvesicular glutamate release, and group III antagonist MSOP increased extracellular accumbal glutamate.

Significant downregulation of *Grm7* has recently been reported in mice lacking the subunit α1 of the GABA-A receptor (Gabra1). Because GABRA1 is associated with alcohol dependence, there is the possibility of signalling and genetic interaction between the two receptor.

In an ongoing human genetic study Melroy, W. E. et al. found that *GRM7* polymorphisms was suggestively associated with alcohol consumption and dependence in two independent longitudinal samples, the Colorado Center on Antisocial Drug Dependence (CADD) and the Genetics of Antisocial Drug Dependence (GADD). In Europen Americans (EA) rs3749380 was associated with alcohol consumption and dependence in the CADD sample. In subjects of Hispanic descent, rs1485175 was nominally associated with alcohol consumption in the GADD sample.

In an other relevant mammalian genetic study Guilfoyle D.N. et al. found that *Grm7* derived from BALB/cJ strain codes for higher abundance of mGluR7 mRNA in the hippocampus than the mGluR7 mRNA from C57BL/6By strain. With ^{1}H NMR spectroscopy using inbred C57BL/6By, BALB/cJ and congenic mice (B6By.C.6.132.54) carrying $Grm7^{BALB/cJ}$ on C57BL/6By genetic background, the authors found that the congenic mouse strain has significantly lower hippocampal glutamate level than that in the background C57BL/6By strain [137].

7. SUMMARY

The epidemiological consensus currently is that moderate consumption of alcohol is associated with the lowest risk for coronary artery disease and mortality. Although moderate alcohol use has an apparent protective association with coronary heart disease, heavy alcohol consumption, in particular hard liquor, is associated with greater calcification of arteries. Moreover, calciphylaxis, known to almost exclusively develop in patients with Stage 5 chronic kidney disease, was also reported to occur in heavy drinkers with physiological renal function. While we are gradually deciphering how alcohol might exert beneficial effects on atherosclerosis leading to prevention of cardiovascular and cerebrovascular disease, the molecular basis of the dichotomous effects of alcohol on vascular calcification have not been explored.

Abnormalities in mineral metabolism are considered as important risk factors of vascular calcification. It has been well established that it is an actively well regulated multistep process in which interchangeable cellular phenotypes under certain pathological conditions are the driving force. One of the main contributors is the trans-differentiation of smooth muscle cells into osteoblast-like cells. After osteoblastic differentiation these cells lack characteristics of smooth muscle cells, and develop osteoblast features. This process results in mineralization and involves increased activity of alkaline phosphatase, increased expression of core binding factor α-1 with the subsequent induction of osteocalcin.

We provide evidence that exposure of vascular human smooth muscle cells to ethanol at high concentration might contribute to vascular calcification. Accumulations of calcium and phosphate occurs forming hydroxyapatite in the extracellular matrix of smooth muscle cells as a response to exposure to ethanol. Phenotype change of the cells towards osteoblast is the main characteristic of such a transition. Mineralization is accompanied with enhancement of osteoblast specific gene products including alkaline phosphatase and a significant increase in the synthesis of osteocalcin occurs. Moreover, ethanol enhances the expression of *Cbfa-1*, a transcription factor involved in the regulation of osteoblastic transformation of human vascular smooth muscle cells. Our results may provoke clinical studies and preventive measures in the field of high alcohol consumption and vascular calcification.

Glutamate receptors are implicated in bone remodeling and are demonstrated to serve as candidates in altered alcohol preference. We present results of our animal study, in which we expanded genome scanning of 5 chromosomes (1, 2, 3, 9 and 15) to include all autosomal chromosomes, and increased sample sizes in alcohol preference tests of b_5i_7 RQI strains. The

combined data were analyzed by composite interval mapping (CIM) which shows a better performance than interval mapping in the case of multiple linked QTLs, and by multiple interval mapping (MIM). In our studies we identified new QTLs for alcohol consumption with genome-wide significance on chrs. 6 and 12. *Eac1* and *Eac6* overlap previously reported QTLs for alcohol preference and alcohol acceptance, respectively. Metabotropic glutamate receptor type 7 gene was shown to serve a promising candidate that might be implicated in altered alcohol preference. Future confirmation studies can take advantage of the quasi-congenic RQI strains by rapidly capturing candidate segments in congenic strains, or by creating segregating populations with low genetic background noise. QTG identification in B6.C RQI strains is now greatly aided by The Mouse Genetic Variation Mapping (Vmap) Initiative by sequencing the genomes in 15 mouse strains, making DNA sequence information available for both progenitors of the RQI strains.

ÖSSZEFOGLALÁS

Az epidemiológiai vizsgálatok eredményeként a közmegegyezés jelenleg az, hogy a mértékletes alkoholfogyasztás kapcsolatba hozható a kardiovaszkuláris megbetegedések és halálozás alacsony kockázatával. Habár a mértékletes alkoholfogyasztásnak látszólagos protektív hatása van, például a koszorúér megbetegedés vonatkozásában, a nagymértékű alkoholfogyasztás, különösen a szeszesitalok fogyasztása kapcsolatba hozható az artériák nagyobb mértékű kalcifikációjával. Ezen kívül a kalcifilaxisról - amely köztudottan és majdnem kizárólagosan a krónikus vesebetegekben fejlődik ki - szintén leírták, hogy a fiziológiás vesefunkciókkal rendelkező alkoholistákban is kifejlődik. Amíg az elmúlt évtizedek kutatásai arra vonatkozóan, hogy az alkohol hogyan hathat kedvezően az ateroszklerózisra, a kardiovaszkuláris és cerebrovaszkuláris megbetegedésekre, igen hangsúlyozott az irodalomban, a kettős hatás a vaszkuláris kalcifikáció tekintetében nem teljesen ismert.

A vaszkuláris mineralizáció fontos kockázati tényezőt jelent a kardiovaszkuláris halálozásban. Jól ismert, hogy egy aktívan és pontosan szabályozott többlépcsős folyamatról van szó, amelyben a hajtóerőt a patológiás folyamatok hátterében zajló sejtes transzdifferenciáció jelenti. Ebben a folyamatban a fő közreműködő sejt a simaizomsejt, és a meghatározó átmenet az oszteoblaszt irányban jelölhető meg. Ateroszklerózisban, media szklerózisban, és kalcifilaxisban az oszteoblasztokra jellemző tulajdonságok megjelenésével és a simaizomsejtekre jellemző tulajdonságok elvesztésével találkozunk. Ennek a folyamatnak az eredménye a mineralizáció, aminek letéteményese többek között az alkalikus foszfatáz, az oszteokalcin, és a *Cbfa-1* transzkripciós faktor.

Ebben a munkában bizonyítékot szolgáltattunk arra vonatkozóan, hogy az etanol magas koncentrációban hozzájárulhat a vaszkuláris simaizomsejtek oszteoblasztszerű sejtekké történő átalakulásához, és az extracelluláris mátrix kalcifikációjához. A mineralizáció együtt jár az emelkedett alkalikus foszfatáz aktivitással és az oszteokalcin szintézis szignifikáns emelkedésével. Ezen túlmenően az etanol megemeli a *Cbfa-1* expresszióját, mely transzkripciós faktor a humán simaizomsejtek oszteoblasztos transzformációjának szabályozásában játszik szerepet.

A glutamát receptorok szerepet játszanak a csontreszorpcióban és kandidátusi szerepet töltenek be a megváltozott alkoholfogyasztásban. Ebben az állatkísérletes munkában a genom vizsgálatot az eddigi 5 kromoszómáról (1, 2, 3, 9 és 15) az összes autoszómális

kromoszómára kiterjesztettük, és megnöveltük az alkoholpreferencia tesztben szereplő b_5i_7 RQI törzs mintaszámát. Az együttes adatokat összetett intervallum térképezéssel (CIM),-mely többszörösen kapcsolt QTL-ek esetében jobb megjelenítést tesz lehetővé-, és többszörös intervallum térképezéssel (MIM) analizáltuk. A kísérleteink során az alkoholfogyasztás új QTL-jeit azonosítottuk a 6-os és 12-es kromoszómán lévő teljes genomra kiterjedő szignifikancia értékkel. Az Eac1 és az Eac6 a már korábban azonosított alkoholfogyasztást meghatározó QTL-ekkel fed át. A metabotropic glutamate receptor type 7 (mGlu7) gén egy ígéretes, mások által is igazolt kandidátus génként szolgál, melynek megváltozott alkoholfogyasztásban lehet szerepe. A kvázi-kongenikus RQI törzsek a kongenikus törzsek kandidátus szegmenseinek gyors meghatározásával, vagy alacsony genetikai háttérzajjal rendelkező szegregáló populációk létrehozásával a jövőbeli bizonyító erejű kísérletek hasznára lehetnek.

8. NOVEL FINDINGS

Ethanol enhances mineralization of human vascular smooth muscle cells provoked by inorganic phosphate

Ethanol fosters phenotype change and transition of human vascular smooth muscle cells into osteoblast like cells triggered by inorganic phosphate.

Ethanol promotes the activity of alkaline phosphatase in human vascular smooth muscle cells.

Ethanol increases the synthesis of osteocalcin, a calcium binding protein in human vascular smooth muscle cells.

Ethanol enhances the expression of osteoblast specific transcription factor *Cbfa-1* in human vascular smooth muscle cells.

Ethanol does not alter intracellular phosphate levels in human vascular smooth muscle cells.

Alcohol dehydrogenase 1 is not expressed in human vascular smooth muscle cells, and acetaldehyde is not a contributing factor to mineralization and osteoblastic phenotype transition.

We identified new QTLs for alcohol consumption with genome-wide significance on chrs. 6 and 12 Eac1 and Eac6 overlap previously reported QTLs for alcohol preference.
Metabotropic glutamate receptor type 7 gene was shown to serve a promising candidate that might be implicated in altered alcohol preference.

9. REFERENCES

1. Renaud, S. and M. de Lorgeril, *Wine, alcohol, platelets, and the French paradox for coronary heart disease.* Lancet, 1992. **339**(8808): p. 1523-6.
2. Corrao, G., et al., *Alcohol and coronary heart disease: a meta-analysis.* Addiction, 2000. **95**(10): p. 1505-23.
3. Ronksley, P.E., et al., *Association of alcohol consumption with selected cardiovascular disease outcomes: a systematic review and meta-analysis.* BMJ, 2011. **342**: p. d671.
4. McClelland, R.L., et al., *Alcohol and coronary artery calcium prevalence, incidence, and progression: results from the Multi-Ethnic Study of Atherosclerosis (MESA).* Am J Clin Nutr, 2008. **88**(6): p. 1593-601.
5. Giachelli, C.M., *Vascular calcification: in vitro evidence for the role of inorganic phosphate.* J Am Soc Nephrol, 2003. **14**(9 Suppl 4): p. S300-4.
6. Mukamal, K.J., et al., *Binge drinking and mortality after acute myocardial infarction.* Circulation, 2005. **112**(25): p. 3839-45.
7. Tunstall-Pedoe, H., et al., *Contribution of trends in survival and coronary-event rates to changes in coronary heart disease mortality: 10-year results from 37 WHO MONICA project populations. Monitoring trends and determinants in cardiovascular disease.* Lancet, 1999. **353**(9164): p. 1547-57.
8. Ruidavets, J.B., et al., *Patterns of alcohol consumption and ischaemic heart disease in culturally divergent countries: the Prospective Epidemiological Study of Myocardial Infarction (PRIME).* BMJ, 2010. **341**: p. c6077.
9. Lim, S.P., K. Batta, and B.B. Tan, *Calciphylaxis in a patient with alcoholic liver disease in the absence of renal failure.* Clin Exp Dermatol, 2003. **28**(1): p. 34-6.
10. Goli, A.K., et al., *Calciphylaxis: a rare association with alcoholic cirrhosis. Are deficiencies in protein C and S the cause?* South Med J, 2005. **98**(7): p. 736-9.
11. Ferreres, J.R., et al., *Calciphylaxis associated with alcoholic cirrhosis.* J Eur Acad Dermatol Venereol, 2006. **20**(5): p. 599-601.
12. Almafragi, A., J. Vandorpe, and K. Dujardin, *Calciphylaxis in a cardiac patient without renal disease.* Acta Cardiol, 2009. **64**(1): p. 91-3.

13. Cahill, P.A. and E.M. Redmond, *Alcohol and cardiovascular disease--modulation of vascular cell function.* Nutrients, 2012. **4**(4): p. 297-318.
14. Persy, V. and P. D'Haese, *Vascular calcification and bone disease: the calcification paradox.* Trends Mol Med, 2009. **15**(9): p. 405-16.
15. Stary, H.C., et al., *A definition of advanced types of atherosclerotic lesions and a histological classification of atherosclerosis. A report from the Committee on Vascular Lesions of the Council on Arteriosclerosis, American Heart Association.* Circulation, 1995. **92**(5): p. 1355-74.
16. Block, G.A. and F.K. Port, *Re-evaluation of risks associated with hyperphosphatemia and hyperparathyroidism in dialysis patients: recommendations for a change in management.* Am J Kidney Dis, 2000. **35**(6): p. 1226-37.
17. Rumberger, J.A., et al., *Coronary artery calcium area by electron-beam computed tomography and coronary atherosclerotic plaque area. A histopathologic correlative study.* Circulation, 1995. **92**(8): p. 2157-62.
18. Sangiorgi, G., et al., *Arterial calcification and not lumen stenosis is highly correlated with atherosclerotic plaque burden in humans: a histologic study of 723 coronary artery segments using nondecalcifying methodology.* J Am Coll Cardiol, 1998. **31**(1): p. 126-33.
19. Beadenkopf, W.G., A.S. Daoud, and B.M. Love, *Calcification in the Coronary Arteries and Its Relationship to Arteriosclerosis and Myocardial Infarction.* Am J Roentgenol Radium Ther Nucl Med, 1964. **92**: p. 865-71.
20. Loecker, T.H., et al., *Fluoroscopic coronary artery calcification and associated coronary disease in asymptomatic young men.* J Am Coll Cardiol, 1992. **19**(6): p. 1167-72.
21. Lehto, S., et al., *Medial artery calcification. A neglected harbinger of cardiovascular complications in non-insulin-dependent diabetes mellitus.* Arterioscler Thromb Vasc Biol, 1996. **16**(8): p. 978-83.
22. Olson, J.C., et al., *Coronary calcium in adults with type 1 diabetes: a stronger correlate of clinical coronary artery disease in men than in women.* Diabetes, 2000. **49**(9): p. 1571-8.

23. Fitzgerald, P.J., T.A. Ports, and P.G. Yock, *Contribution of localized calcium deposits to dissection after angioplasty. An observational study using intravascular ultrasound.* Circulation, 1992. **86**(1): p. 64-70.
24. Niskanen, L.K., et al., *Aortic and lower limb artery calcification in type 2 (non-insulin-dependent) diabetic patients and non-diabetic control subjects. A five year follow-up study.* Atherosclerosis, 1990. **84**(1): p. 61-71.
25. Taylor, A.J., et al., *A comparison of the Framingham risk index, coronary artery calcification, and culprit plaque morphology in sudden cardiac death.* Circulation, 2000. **101**(11): p. 1243-8.
26. Burke, A.P., et al., *Coronary calcification: insights from sudden coronary death victims.* Z Kardiol, 2000. **89 Suppl 2**: p. 49-53.
27. Baldwin, C., et al., *Multi-intervention management of calciphylaxis: a report of 7 cases.* Am J Kidney Dis, 2011. **58**(6): p. 988-91.
28. Selye, H., G. Gentile, and P. Prioreschi, *Cutaneous molt induced by calciphylaxis in the rat.* Science, 1961. **134**(3493): p. 1876-7.
29. Giachelli, C.M., et al., *Vascular calcification and inorganic phosphate.* Am J Kidney Dis, 2001. **38**(4 Suppl 1): p. S34-7.
30. Shioi, A., et al., *Beta-glycerophosphate accelerates calcification in cultured bovine vascular smooth muscle cells.* Arterioscler Thromb Vasc Biol, 1995. **15**(11): p. 2003-9.
31. Jono, S., et al., *Phosphate regulation of vascular smooth muscle cell calcification.* Circ Res, 2000. **87**(7): p. E10-7.
32. Lomashvili, K.A., et al., *Phosphate-induced vascular calcification: role of pyrophosphate and osteopontin.* J Am Soc Nephrol, 2004. **15**(6): p. 1392-401.
33. Raggi, P., et al., *Cardiac calcification in adult hemodialysis patients. A link between end-stage renal disease and cardiovascular disease?* J Am Coll Cardiol, 2002. **39**(4): p. 695-701.
34. Block, G.A., et al., *Association of serum phosphorus and calcium x phosphate product with mortality risk in chronic hemodialysis patients: a national study.* Am J Kidney Dis, 1998. **31**(4): p. 607-17.
35. Guerin, A.P., et al., *Impact of aortic stiffness attenuation on survival of patients in end-stage renal failure.* Circulation, 2001. **103**(7): p. 987-92.

36. Blacher, J., et al., *Arterial calcifications, arterial stiffness, and cardiovascular risk in end-stage renal disease.* Hypertension, 2001. **38**(4): p. 938-42.

37. London, G.M., et al., *Arterial wave reflections and survival in end-stage renal failure.* Hypertension, 2001. **38**(3): p. 434-8.

38. McEniery, C.M., et al., *Aortic calcification is associated with aortic stiffness and isolated systolic hypertension in healthy individuals.* Hypertension, 2009. **53**(3): p. 524-31.

39. Jono, S., et al., *Vascular calcification in chronic kidney disease.* J Bone Miner Metab, 2006. **24**(2): p. 176-81.

40. Garcia-Sanchez, A., et al., *Effect of acute alcohol ingestion on mineral metabolism and osteoblastic function.* Alcohol Alcohol, 1995. **30**(4): p. 449-53.

41. Steitz, S.A., et al., *Smooth muscle cell phenotypic transition associated with calcification: upregulation of Cbfa1 and downregulation of smooth muscle lineage markers.* Circ Res, 2001. **89**(12): p. 1147-54.

42. Li, X., H.Y. Yang, and C.M. Giachelli, *Role of the sodium-dependent phosphate cotransporter, Pit-1, in vascular smooth muscle cell calcification.* Circ Res, 2006. **98**(7): p. 905-12.

43. Ducy, P., et al., *A Cbfa1-dependent genetic pathway controls bone formation beyond embryonic development.* Genes Dev, 1999. **13**(8): p. 1025-36.

44. Komori, T., *A fundamental transcription factor for bone and cartilage.* Biochem Biophys Res Commun, 2000. **276**(3): p. 813-6.

45. Inada, M., et al., *Maturational disturbance of chondrocytes in Cbfa1-deficient mice.* Dev Dyn, 1999. **214**(4): p. 279-90.

46. Komori, T., et al., *Targeted disruption of Cbfa1 results in a complete lack of bone formation owing to maturational arrest of osteoblasts.* Cell, 1997. **89**(5): p. 755-64.

47. Otto, F., et al., *Cbfa1, a candidate gene for cleidocranial dysplasia syndrome, is essential for osteoblast differentiation and bone development.* Cell, 1997. **89**(5): p. 765-71.

48. Shioi, A., et al., *Induction of bone-type alkaline phosphatase in human vascular smooth muscle cells: roles of tumor necrosis factor-alpha and oncostatin M derived from macrophages.* Circ Res, 2002. **91**(1): p. 9-16.

49. Jono, S., et al., *1,25-Dihydroxyvitamin D3 increases in vitro vascular calcification by modulating secretion of endogenous parathyroid hormone-related peptide.* Circulation, 1998. **98**(13): p. 1302-6.

50. Price, P.A. and S.K. Nishimoto, *Radioimmunoassay for the vitamin K-dependent protein of bone and its discovery in plasma.* Proc Natl Acad Sci U S A, 1980. **77**(4): p. 2234-8.

51. Poser, J.W., et al., *Isolation and sequence of the vitamin K-dependent protein from human bone. Undercarboxylation of the first glutamic acid residue.* J Biol Chem, 1980. **255**(18): p. 8685-91.

52. Deyl, Z., et al., *The presence of gamma-carboxyglutamic acid-containing protein in atheromatous aortae.* Biochim Biophys Acta, 1979. **581**(2): p. 307-15.

53. Levy, R.J., C. Gundberg, and R. Scheinman, *The identification of the vitamin K-dependent bone protein osteocalcin as one of the gamma-carboxyglutamic acid containing proteins present in calcified atherosclerotic plaque and mineralized heart valves.* Atherosclerosis, 1983. **46**(1): p. 49-56.

54. Cederbaum, A.I., *Microsomal generation of reactive oxygen species and their possible role in alcohol hepatotoxicity.* Alcohol Alcohol Suppl, 1991. **1**: p. 291-6.

55. Kukielka, E., E. Dicker, and A.I. Cederbaum, *Increased production of reactive oxygen species by rat liver mitochondria after chronic ethanol treatment.* Arch Biochem Biophys, 1994. **309**(2): p. 377-86.

56. Mantle, D. and V.R. Preedy, *Free radicals as mediators of alcohol toxicity.* Adverse Drug React Toxicol Rev, 1999. **18**(4): p. 235-52.

57. Sergent, O., et al., *[Alcohol and oxidative stress].* Pathol Biol (Paris), 2001. **49**(9): p. 689-95.

58. Cunningham, C.C. and S.M. Bailey, *Ethanol consumption and liver mitochondria function.* Biol Signals Recept, 2001. **10**(3-4): p. 271-82.

59. Salmela, K.S., et al., *Respective roles of human cytochrome P-4502E1, 1A2, and 3A4 in the hepatic microsomal ethanol oxidizing system.* Alcohol Clin Exp Res, 1998. **22**(9): p. 2125-32.

60. Lieber, C.S., E. Rubin, and L.M. DeCarli, *Hepatic microsomal ethanol oxidizing system (MEOS): differentiation from alcohol dehydrogenase and NADPH oxidase.* Biochem Biophys Res Commun, 1970. **40**(4): p. 858-65.

61. Kim, W., et al., *A porcine model of ischemic heart failure produced by intracoronary injection of ethyl alcohol.* Heart Vessels, 2011. **26**(3): p. 342-8.
62. Szczesniak, A.M., et al., *Mechanical loading modulates glutamate receptor subunit expression in bone.* Bone, 2005. **37**(1): p. 63-73.
63. McClearn, G.E. and D.A. Rodgers, *Differences in alcohol preference among inbred strains of mice.* Q. J. Stud. Alcohol, 1959. **20**: p. 691-659.
64. McClearn, G.E., *Genotype and Mouse Activity.* Journal of Comparative & Physiological Psychology, 1960. **54**: p. 674-676.
65. Belknap, J.K. and A.L. Atkins, *The replicability of QTLs for murine alcohol preference drinking behavior across eight independent studies.* Mamm Genome, 2001. **12**(12): p. 893-9.
66. Treadwell, J.A., K.B. Pagniello, and S.M. Singh, *Genetic segregation of brain gene expression identifies retinaldehyde binding protein 1 and syntaxin 12 as potential contributors to ethanol preference in mice.* Behav Genet, 2004. **34**(4): p. 425-39.
67. Treadwell, J.A., *Integrative strategies to identify candidate genes in rodent models of human alcoholism.* Genome, 2006. **49**(1): p. 1-7.
68. Fehr, C., et al., *The syntaxin binding protein 1 gene (Stxbp1) is a candidate for an ethanol preference drinking locus on mouse chromosome 2.* Alcohol Clin Exp Res, 2005. **29**(5): p. 708-20.
69. DuBose, C.S., et al., *Use of the expanded panel of BXD mice narrow QTL regions in ethanol-induced locomotor activation and motor incoordination.* Alcohol Clin Exp Res, 2013. **37**(1): p. 170-83.
70. Wang, X., et al., *A promoter polymorphism in the Per3 gene is associated with alcohol and stress response.* Transl Psychiatry, 2012. **2**: p. e73.
71. Gill, K., et al., *Alcohol preference in AXB/BXA recombinant inbred mice: gender differences and gender-specific quantitative trait loci.* Mamm Genome, 1998. **9**(12): p. 929-35.
72. Gill, K. and A.E. Boyle, *Genetic analysis of alcohol intake in recombinant inbred and congenic strains derived from A/J and C57BL/6J progenitors.* Mamm Genome, 2005. **16**(5): p. 319-31.

73. Bachmanov, A.A., et al., *Voluntary ethanol consumption by mice: genome-wide analysis of quantitative trait loci and their interactions in a C57BL/6ByJ x 129P3/J F2 intercross.* Genome Res, 2002. **12**(8): p. 1257-68.

74. Grahame, N.J., T.K. Li, and L. Lumeng, *Selective breeding for high and low alcohol preference in mice.* Behav Genet, 1999. **29**(1): p. 47-57.

75. Bice, P.J., et al., *Identification of QTLs influencing alcohol preference in the High Alcohol Preferring (HAP) and Low Alcohol Preferring (LAP) mouse lines.* Behav Genet, 2006. **36**(2): p. 248-60.

76. McClearn, G.E., *Behavioral genetics.* Annu Rev Genet, 1970. **4**: p. 437-68.

77. Bice, P.J., et al., *Fine mapping quantitative trait loci that influence alcohol preference behavior in the High and Low Alcohol Preferring (HAP and LAP) mice.* Behav Genet, 2011. **41**(4): p. 565-70.

78. Vadasz, C., et al., *Scanning of five chromosomes for alcohol consumption loci.* Alcohol, 2000. **22**(1): p. 25-34.

79. Vadasz, C., et al., *Self-administration of ethanol: towards the location of predisposing polygenes in quasi-congenic animal models.* Alcohol, 1996. **13**(6): p. 617-20.

80. Vadasz, C., et al., *Mapping of quantitative trait loci for ethanol preference in quasi-congenic strains.* Alcohol, 2000. **20**(2): p. 161-71.

81. Vadasz, C., et al., *Transfer of brain dopamine system-specific quantitative trait loci onto a C57BL/6ByJ background.* Mamm Genome, 1994. **5**(11): p. 735-7.

82. Vadasz, C., et al., *Genomic characterization of two introgression strains (B6.Cb4i5) for the analysis of QTLs.* Mamm Genome, 1996. **7**(7): p. 545-8.

83. Abiola, O., et al., *The nature and identification of quantitative trait loci: a community's view.* Nat Rev Genet, 2003. **4**(11): p. 911-6.

84. Vadasz, C., et al., *Analysis of the mesotelencephalic dopamine system by quantitative-trait locus introgression.* Neurochem Res, 1998. **23**(11): p. 1337-54.

85. Kovacs, K.M., et al., *Decreased oral self-administration of alcohol in kappa-opioid receptor knock-out mice.* Alcohol Clin Exp Res, 2005. **29**(5): p. 730-8.

86. Saito, M., et al., *Variants of kappa-opioid receptor gene and mRNA in alcohol-preferring and alcohol-avoiding mice.* Alcohol, 2003. **29**(1): p. 39-49.

87. Zarjou, A., et al., *Ferritin prevents calcification and osteoblastic differentiation of vascular smooth muscle cells.* J Am Soc Nephrol, 2009. **20**(6): p. 1254-63.

88. Balla, J., et al., *Endothelial-cell heme uptake from heme proteins: induction of sensitization and desensitization to oxidant damage.* Proc Natl Acad Sci U S A, 1993. **90**(20): p. 9285-9.

89. Bailey, D.W., *Recombinant-inbred strains. An aid to finding identity, linkage, and function of histocompatibility and other genes.* Transplantation, 1971. **11**(3): p. 325-7.

90. Vadasz, C., et al., *Genetic determination of mesencephalic tyrosine hydroxylase activity in the mouse.* J Neurogenet, 1987. **4**(5): p. 241-52.

91. Miller, S.A., D.D. Dykes, and H.F. Polesky, *A simple salting out procedure for extracting DNA from human nucleated cells.* Nucleic Acids Res, 1988. **16**(3): p. 1215.

92. Churchill, G.A. and R.W. Doerge, *Empirical threshold values for quantitative trait mapping.* Genetics, 1994. **138**(3): p. 963-71.

93. Kao, C.H., Z.B. Zeng, and R.D. Teasdale, *Multiple interval mapping for quantitative trait loci.* Genetics, 1999. **152**(3): p. 1203-16.

94. Kao, C.H. and Z.B. Zeng, *General formulas for obtaining the MLEs and the asymptotic variance-covariance matrix in mapping quantitative trait loci when using the EM algorithm.* Biometrics, 1997. **53**(2): p. 653-65.

95. Toyoda, T. and A. Wada, *Omic space: coordinate-based integration and analysis of genomic phenomic interactions.* Bioinformatics, 2004. **20**(11): p. 1759-65.

96. Belknap, J.K., J.C. Crabbe, and E.R. Young, *Voluntary consumption of ethanol in 15 inbred mouse strains.* Psychopharmacology (Berl), 1993. **112**(4): p. 503-10.

97. Downing, C., et al., *Genetic analysis of the psychomotor stimulant effect of ethanol.* Genes Brain Behav, 2003. **2**(3): p. 140-51.

98. Kelly, M.A., et al., *The mapping of quantitative trait loci underlying strain differences in locomotor activity between 129S6 and C57BL/6J mice.* Mamm Genome, 2003. **14**(10): p. 692-702.

99. Le Roy, I., J. Pager, and P.L. Roubertoux, *Genetic dissection of gustatory sensitivity to bitterness (sucrose octaacetate) in mice.* C R Acad Sci III, 1999. **322**(10): p. 831-6.

100. Risinger, F.O. and C.L. Cunningham, *Ethanol-induced conditioned taste aversion in BXD recombinant inbred mice.* Alcohol Clin Exp Res, 1998. **22**(6): p. 1234-44.

101. Harder, D.B. and G. Whitney, *A common polygenic basis for quinine and PROP avoidance in mice.* Chem Senses, 1998. **23**(3): p. 327-32.

102. Lush, I.E., *The genetics of tasting in mice. III. Quinine.* Genet Res, 1984. **44**(2): p. 151-60.

103. Singer, J.B., et al., *Mapping quantitative trait loci for anxiety in chromosome substitution strains of mice.* Genetics, 2005. **169**(2): p. 855-62.

104. Nelson, T.M., S.D. Munger, and J.D. Boughter, Jr., *Haplotypes at the Tas2r locus on distal chromosome 6 vary with quinine taste sensitivity in inbred mice.* BMC Genet, 2005. **6**(1): p. 32.

105. Primo-Parmo, S.L., et al., *The human serum paraoxonase/arylesterase gene (PON1) is one member of a multigene family.* Genomics, 1996. **33**(3): p. 498-507.

106. Bachmanov, A.A., et al., *High-resolution genetic mapping of the sucrose octaacetate taste aversion (Soa) locus on mouse Chromosome 6.* Mamm Genome, 2001. **12**(9): p. 695-9.

107. Palmer, A.A., et al., *Gene expression differences in mice divergently selected for methamphetamine sensitivity.* Mamm Genome, 2005. **16**(5): p. 291-305.

108. Sedelis, M., et al., *Chromosomal loci influencing the susceptibility to the parkinsonian neurotoxin 1-methyl-4-phenyl-1,2,3,6-tetrahydropyridine.* J Neurosci, 2003. **23**(23): p. 8247-53.

109. Boyle, A.E. and K. Gill, *Sensitivity of AXB/BXA recombinant inbred lines of mice to the locomotor activating effects of cocaine: a quantitative trait loci analysis.* Pharmacogenetics, 2001. **11**(3): p. 255-64.

110. Jones, B.C., et al., *Quantitative-trait loci analysis of cocaine-related behaviours and neurochemistry.* Pharmacogenetics, 1999. **9**(5): p. 607-17.

111. Fernandez, J.R., et al., *Sex-exclusive quantitative trait loci influences in alcohol-related phenotypes.* Am J Med Genet, 1999. **88**(6): p. 647-52.

112. Lin, T.C., et al., *Mechanical response of a calcified plaque model to fluid shear force.* Ann Biomed Eng, 2006. **34**(10): p. 1535-41.

113. Hoshino, T., et al., *Mechanical stress analysis of a rigid inclusion in distensible material: a model of atherosclerotic calcification and plaque vulnerability.* Am J Physiol Heart Circ Physiol, 2009. **297**(2): p. H802-10.

114. Guerin, A.P., et al., *Arterial stiffening and vascular calcifications in end-stage renal disease.* Nephrol Dial Transplant, 2000. **15**(7): p. 1014-21.

115. O'Rourke, M., *Mechanical principles in arterial disease.* Hypertension, 1995. **26**(1): p. 2-9.

116. Ross, E.A., *Evolution of treatment strategies for calciphylaxis.* Am J Nephrol, 2011. **34**(5): p. 460-7.

117. Mukamal, K.J., et al., *Roles of drinking pattern and type of alcohol consumed in coronary heart disease in men.* N Engl J Med, 2003. **348**(2): p. 109-18.

118. Mukamal, K.J., et al., *Alcohol consumption and risk of coronary heart disease in older adults: the Cardiovascular Health Study.* J Am Geriatr Soc, 2006. **54**(1): p. 30-7.

119. Kabagambe, E.K., et al., *Alcohol intake, drinking patterns, and risk of nonfatal acute myocardial infarction in Costa Rica.* Am J Clin Nutr, 2005. **82**(6): p. 1336-45.

120. Yuan, J.M., et al., *Follow up study of moderate alcohol intake and mortality among middle aged men in Shanghai, China.* BMJ, 1997. **314**(7073): p. 18-23.

121. Block, G.A., *Prevalence and clinical consequences of elevated Ca x P product in hemodialysis patients.* Clin Nephrol, 2000. **54**(4): p. 318-24.

122. Burke, S.K., *Phosphate is a uremic toxin.* J Ren Nutr, 2008. **18**(1): p. 27-32.

123. Block, G.A., et al., *Mineral metabolism, mortality, and morbidity in maintenance hemodialysis.* J Am Soc Nephrol, 2004. **15**(8): p. 2208-18.

124. Giachelli, C.M., *Ectopic calcification: gathering hard facts about soft tissue mineralization.* Am J Pathol, 1999. **154**(3): p. 671-5.

125. Li, W., et al., *Alcohol-induced apoptosis of canine cerebral vascular smooth muscle cells: role of extracellular and intracellular calcium ions.* Neurosci Lett, 2004. **354**(3): p. 221-4.

126. Clarke, M. and M. Bennett, *The emerging role of vascular smooth muscle cell apoptosis in atherosclerosis and plaque stability.* Am J Nephrol, 2006. **26**(6): p. 531-5.

127. Proudfoot, D., et al., *Apoptosis regulates human vascular calcification in vitro: evidence for initiation of vascular calcification by apoptotic bodies.* Circ Res, 2000. **87**(11): p. 1055-62.

128. Proudfoot, D., et al., *Acetylated low-density lipoprotein stimulates human vascular smooth muscle cell calcification by promoting osteoblastic differentiation and inhibiting phagocytosis.* Circulation, 2002. **106**(24): p. 3044-50.

129. Speer, M.Y., et al., *Runx2/Cbfa1, but not loss of myocardin, is required for smooth muscle cell lineage reprogramming toward osteochondrogenesis.* J Cell Biochem, 2010. **110**(4): p. 935-47.

130. Kugaya, A. and G. Sanacora, *Beyond monoamines: glutamatergic function in mood disorders.* CNS Spectr, 2005. **10**(10): p. 808-19.

131. Nelson, T.M., S.D. Munger, and J.D. Boughter, Jr., *Haplotypes at the Tas2r locus on distal chromosome 6 vary with quinine taste sensitivity in inbred mice.* BMC Genet, 2005. **6**: p. 32.

132. Bachmanov, A.A., et al., *Chemosensory factors influencing alcohol perception, preferences, and consumption.* Alcohol Clin Exp Res, 2003. **27**(2): p. 220-31.

133. Tarantino, L.M., et al., *Confirmation of quantitative trait loci for alcohol preference in mice.* Alcohol Clin Exp Res, 1998. **22**(5): p. 1099-105.

134. Sayegh, J.F., et al., *Effects of social isolation and the time of day on testosterone levels in plasma of C57BL/6By and BALB/cBy mice.* Steroids, 1990. **55**(2): p. 79-82.

135. Acuna-Goycolea, C., Y. Li, and A.N. Van Den Pol, *Group III metabotropic glutamate receptors maintain tonic inhibition of excitatory synaptic input to hypocretin/orexin neurons.* J Neurosci, 2004. **24**(12): p. 3013-22.

136. Gyetvai, B., et al., *mGluR7 genetics and alcohol: intersection yields clues for addiction.* Neurochem Res, 2011. **36**(6): p. 1087-100.

137. Guilfoyle, D.N., S. Gerum, and C. Vadasz, *In vivo Proton NMR spectroscopy of genetic mouse models BALB/cJ and C57BL/6By: variation in hippocampal glutamate level and the metabotropic glutamate receptor, subtype 7 (Grm7) gene.* J Mol Neurosci, 2014. **53**(1): p. 135-41.

10. KEY WORDS/ TÁRGYSZAVAK

Vascular calcification/ Vaszkuláris kalcifikáció

Smooth muscle cells/ Simaizomsejtek

Osteoblastic differentiation/ Oszteoblasztos transzformáció

Ethanol/ Etanol

Phosphate/ Foszfát

Calcium/ Kalcium

Hydroxyapatite/ Hidroxiapatit

Alkaline phosphatase / Alkalikus foszfatáz

Osteocalcin/ Oszteokalcin

Cbfa-1/ Cbfa-1

QTL mapping/ QTL térképezés

RQI strains/ RQI törzsek

Grm7/ Grm7

11. ACKNOWLEDGEMENTS

I am grateful to my consulent, Professor László Nagy. His support, wealth of knowledge and mentorship were invaluable during my training. I am also grateful to my outer consulent, Professor Csaba Vadász at the NKI, Orangeburg in the field of QTL mapping. He provided me the opportunity to enjoy science but also served as a role model to be a good researcher.

I am also grateful to Professor László Fésüs for giving me the opportunity to improve my knowledge at his academic institute, at the Biochemistry and Molecular Biology Department, University of Debrecen. Special thanks to Attila Szántó; Ibolya Fürtös for technical assistance and all the members of the Nuclear Receptor Laboratory.

I am grateful to Professor Ábel Lajtha at the NKI, Orangeburg to improve the Hungarian young scientists giving them the opportunity to train them on the field of the up-to-date science.

My special thanks also go to Professor Gábor Méhes and to Zoltán Hendrik for their help of histochemistry at the Department of Pathology, University of Debrecen.

I would also like to thank Erzsébet Zavaczki, Gergely Becs, and all the colleagues of the Vascular Biology Research Laboratory.

I am also grateful to Mariko Saito, Beatrix Gyetvai, István Szakáll, Réka Tóth, Ágota Ádám, János Piturca and all the members of the Neurochemistry laboratory, NKI, Orangeburg for their help in scientific work.

The work/publication is supported by the TÁMOP-4.2.2/B-10/1-2010-0024 and TÁMOP 4.2.2./A-11/1/KONV-2012-0045 project. The project is co-financed by the European Union and the European Social Fund.

12. APPENDIX

DEENK www.lib.unideb.hu
UNIVERSITY AND NATIONAL LIBRARY UNIVERSITY OF DEBRECEN
KENÉZY LIFE SCIENCES LIBRARY

Register Number: DEENKÉTK/285/2013.
Item Number:
Subject: Ph.D. List of Publications

Candidate: Melinda Oros
Neptun ID: N00W7Y
Doctoral School: Doctoral School of Molecular Cell and Immune Biology

List of publications related to the dissertation

1. **Oros, M.**, Zavaczki, E., Vadász, C., Jeney, V., Tósaki, Á., Lekli, I., Balla, G., Nagy, L., Balla, J.: Ethanol increases phosphate-mediated mineralization and osteoblastic transformation of vascular smooth muscle cells.
J. Cell. Mol. Med. 16 (9), 2219-2226, 2012.
DOI: http://dx.doi.org/10.1111/j.1582-4934.2012.01533.x
IF:4.753

2. Vadász, C., Saito, M., Gyetvai, B., **Oros, M.**, Szakáll, I., Kovács, K.M., Prasad, V.V.T.S., Morahan, G., Tóth, R.: Mapping of QTLs for oral alcohol self-administration in B6.C and B6.I quasi-congenic RQI strains.
Neurochem. Res. 32 (7), 1099-1112, 2007.
DOI: http://dx.doi.org/10.1007/s11064-006-9234-4
IF:1.811

3. Vadász, C., Saito, M., Gyetvai, B.M., **Oros, M.**, Szakáll, I., Kovács, K.M., Prasad, V.V.T.S., Tóth, R.: Glutamate receptor metabotropic 7 is cis-regulated in the mouse brain and modulates alcohol drinking?
Genomics. 90 (6), 690-702, 2007.
DOI: http://dx.doi.org/10.1016/j.ygeno.2007.08.006
IF:3.613

H-4032 Debrecen, Egyetem tér 1. e-mail: publikaciok@lib.unideb.hu

List of other publications

4. Gyetvai, B., Simonyi, Á., **Oros, M.**, Saito, M., Smiley, J., Vadász, C.: mGluR7 genetics and alcohol: Intersection yields clues for addiction.
Neurochem. Res. 36 (6), 1087-1100, 2011.
DOI: http://dx.doi.org/10.1007/s11064-011-0452-z
IF:2.24

5. Zavaczki, E., Jeney, V., Agarwal, A., Zarjou, A., **Oros, M.**, Katkó, M., Varga, Z., Balla, G., Balla, J.: Hydrogen sulfide inhibits the calcification and osteoblastic differentation of vascular smooth muscle cells.
Kidney Int. 80 (7), 731-739, 2011.
DOI: http://dx.doi.org/10.1038/ki.2011.212
IF:6.606

6. Szántó, A., Bálint, B.L., Nagy, Z., Barta, E., Dezső, B., Pap, A., Széles, L., Póliska, S., **Oros, M.**, Evans, R.M., Barak, Y., Schwabe, J., Nagy, L.: STAT6 Transcription Factor Is a Facilitator of the Nuclear Receptor PPAR?-Regulated Gene Expression in Macrophages and Dendritic Cells.
Immunity. 3 (5), 699-712, 2010.
DOI: http://dx.doi.org/10.1016/j.immuni.2010.11.009
IF:24.221

7. Vadász, C., Smiley, J., Figarsky, K., Saito, M., Tóth, R., Gyetvai, B., **Oros, M.**, Kovács, K.K., Mohan, P., Wang, R.: Mesencephalic dopamine neuron number and tyrosine hydroxylase content: Genetic control and candidate genes.
Neuroscience. 149 (3), 561-572, 2007.
DOI: http://dx.doi.org/10.1016/j.neuroscience.2007.06.049
IF:3.352

8. Saito, M., Szakáll, I., Tóth, R., Kovács, K.M., **Oros, M.**, Prasad, V.V.T.S., Blumenberg, M., Vadász, C.: Mouse striatal transcriptome analysis: Effects of oral self-administration of alcohol.
Alcohol. 32 (3), 223-241, 2004.
DOI: http://dx.doi.org/10.1016/j.alcohol.2004.02.005
IF:1.874

9. Saito, M., Ehringer, M.A., Tóth, R., **Oros, M.**, Szakáll, I., Sikela, J.M., Vadász, C.: Variants of kappa-opioid receptor gene and mRNA in alcohol-preferring and alcohol-avoiding mice.
Alcohol. 29 (1), 39-49, 2003.
DOI: http://dx.doi.org/10.1016/S0741-8329(02)00322-1
IF:1.585

Total IF: 50.055

Total IF (publications related to the dissertation): 10.177

The Candidate's publication data submitted to the Publication Database of the University of Debrecen have been validated by Kenezy Life Sciences Library on the basis of Web of Science, Scopus and Journal Citation Report (Impact Factor) databases.

27 August, 2013

ATTACHMENT

Inserted according to the reviewers' suggestions.

4. MATERIALS AND METHODS

4.7. Western Blot and Osteocalcin assay – on page 26

for Osteocalcin ELISA

Cells grown on 6-well plates were treated for 7 days. Extracellular matrix was dissolved in 200 µL of EDTA (0.5 mol/L, pH 6.9) for 30 minutes, then 25 µL of the dissolved extracellular matrix was added to sample wells and incubated at room temperature for 2 hours on a microplate shaker at 400 rpm. After emptying the wells 400 µL of Wash Buffer was added to the wells and washed 3 times. After washing 100 µL of TMB Substrate Solution was added to the wells and incubated for 10 minutes at room temperature avoiding direct exposure to intense light. The enzyme reaction was stopped by quickly adding 100 µL of Stop Solution into the wells, then the absorbance was measured on a spectrophotometer using 450 nm. The osteocalcin concentrations of the samples were calculated from the Standard curve.

4.17. QTL mapping – on page 31

Quantitative Trait Locus analysis is a statistical method that determines a relationship between the phenotypic (trait measurements) and the genotypic data (microsatellite markers) so as to study the genetic basis of variation in complex traits (*Falconer & Mackay, 1996; Kearsey, 1998; Lynch & Walsh, 1998; Cecilia M. Miles & Marta Wayne*).

Composite Interval Mapping (CIM) method combines interval mapping with multiple regression analysis, while Multiple Interval Mapping (MIM) method combines QTL mapping with the analysis of genetic architecture of quantitative traits.

5. DISCUSSION – on page 69

To the end of the 2nd paragraph

Melroy,W.E., Vadasz, C., McQueen, M.B., Corley, R.P., Stallings, M.C., Crowley,T.J., Hopfer, C.J., Krauter, K.S., Hewitt, J.K., Ehringer, M.A. (2012) Variation in GRM7 is associated with alcohol consumption in a family based analysis. 35th Annual Meeting of the Research Society on Alcoholism June 23-27 -- San Francisco, California. Alcoholism: Clinical and Experimental Research, Volume 36, Issue Supplement s1, pp. 253A, #0972.